University of Washington
Department of Civil and Environmental Engineering

PREDICTABILITY OF RUNOFF IN THE MISSISSIPPI RIVER BASIN

EDWIN P. MAURER

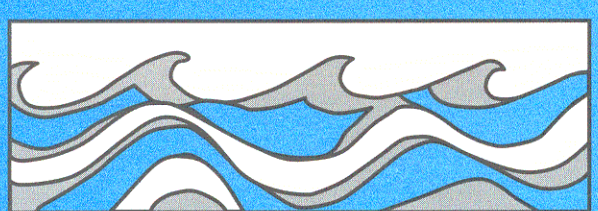

Water Resources Series
Technical Report No.172
OCTOBER, 2002

Seattle, Washington
98195

Department of Civil and Environmental Engineering
University of Washington
Box 352700
Seattle, Washington 98195-2700

PREDICTABILITY OF RUNOFF IN THE MISSISSIPPI RIVER BASIN

By

Edwin P. Maurer

Water Resources Series
Technical Report No. 172

October, 2002

ABSTRACT

Prediction of streamflow is the essential challenge of hydrology. The large and growing economic costs associated with flood and drought events provide the motivation for this study: to investigate opportunities for improving long-lead (monthly to seasonal) runoff prediction over large continental areas; and to evaluate the potential impacts of these improvements on water resources management. Potential runoff predictability as used in this study derives from climate signals and from initial conditions -- soil moisture and snow water equivalent at the beginning of the forecast period. Because long-term spatially distributed observations of soil moisture and snow water do not exist, a 50-year, hydrologically consistent data set of observed and derived surface energy and moisture fluxes and state variables was derived for the continental U.S. This data set provided the basis for investigating relative influences of initial states of the climate signal, snow water content, and soil moisture on long-lead predictability of runoff across the Mississippi River basin. The potential value of runoff predictability for water management was investigated using a simulation model of the Missouri River main stem reservoirs. In the Mississippi basin, climate indicators provide a small but significant source of winter runoff predictability through a lead time of three months. Soil moisture provides the dominant source of runoff predictability at lead times of one to two months over most of the Mississippi basin, except in the snow dominated mountainous areas of the west. For smaller sub-areas, runoff predictive skill exists through a lead of two seasons, longer than is currently used in operational forecasting. There was a very small difference in Missouri River system hydropower benefits associated with perfect forecast skill, due primarily to the system's large storage capacity relative to inflow. An investigation of the effect of prediction skill relative to reservoir size found a generally inverse relationship, which is which is consistent with various previous studies. A hypothetical reduced-volume system showed greater sensitivity to runoff predictability; with knowledge of the climate state, and snow and soil moisture initial states providing an increase of $6.8 million in annual hydropower benefits, about two percent of total annual hydropower revenues.

TABLE OF CONTENTS

List of Figures iii

List of Tables v

CHAPTER I: INTRODUCTION 1

CHAPTER II: MODEL-DERIVED DATA OF LAND SURFACE STATES AND FLUXES 5

Introduction 5

Hydrologic Model Description 9

Model Input Data Sets 10
Land Surface Characteristics 10
Meteorological and Radiative Forcings 11

Preliminary Analysis 14
Comparison of routed VIC runoff with observed streamflow 15
Comparison with Illinois soil moisture 19
Comparison of Diurnal Cycle of Surface Fluxes with Observations 21
Derived Soil Moisture Persistence 23
Observed and Simulated Snow Extent 24

Data Format and Availability 25

Conclusions 27

CHAPTER III: LONG-LEAD HYDROLOGIC PREDICTABILITY IN THE MISSISSIPPI RIVER BASIN 29

Introduction 29

Methods and Data 31
Evaluation of Predictability 34
Climate Signals 37
Snow 41
Soil Moisture 42

Runoff Data 43

Results and Discussion 44
Seasonal runoff magnitude 44
Total runoff predictability 44
Runoff predictability due to climate 46
Runoff predictability due to snow state 48
Runoff predictability due to soil moisture state 51
Importance of predictability due to defined sources 53

Conclusions 57

CHAPTER IV: POTENTIAL EFFECTS OF LONG-LEAD HYDROLOGIC PREDICTABILITY 59

Introduction 59

Study Site Description 61

Methods 63
Predictability for each contributing area 63
MOSIM Missouri River mainstem system model 65
Forecasted inflows representing predictability levels 70
The value of added predictability 71

Results and discussion 73
Current system configuration 73
Modified system configuration 75
Seasonal distribution of predictability 78

Conclusions 79

CHAPTER V: CONCLUSIONS 82

BIBLIOGRAPHY 86

APPENDIX: DEVELOPMENT OF FORECAST RESERVOIR INFLOWS 96

LIST OF FIGURES

Figure 2.1 - LDAS Domain with modeling sub-areas *10*
Figure 2.2 - Comparison of effect of stochastic disaggregation of daily precipitation totals versus constant precipitation rate on simulated runoff and evapotranspiration. Columns in the figure are for different variables, and rows are for each of four seasons. *14*
Figure 2.3 - Comparison of routed simulated runoff (dashed lines) with observed (or naturalized) streamflows (solid lines). Shaded areas are the contributing regions to each identified point. Ordinate values are runoff in m^3s^{-1}, abcissa is a ten year period, the beginning of which varies by basin depending on observed flow availability. *16*
Figure 2.4 - Average flows by month for each of the 12 basins shown in Figure 2.3. Ordinate values are m^3s^{-1}, solid lines are observed or naturalized flows, and dashed lines are routed simulated runoff. *17*
Figure 2.5 - Taylor diagram for simulated monthly runoff routed to basin outlet points. The plotted numbers identify the basin, using the same numbering system as used in Figures 2.3 and 2.4, and are shown in font sizes scaled by the cube root of the observed flow. See text for details. *18*
Figure 2.6 - Comparison of observed soil moistures in Illinois from 1981-1996 with simulated values for the same period. a) average soil moisture in the top 1 meter of soil for each month; b) average soil moisture tendency for each month; c) coefficient of variation of monthly soil moisture anomalies; d) autocorrelation of soil moisture anomalies. *20*
Figure 2.7 - Comparison of observed (thick lines) and simulated (thin lines) downward solar radiation and net radiation at four SURFRAD sites. Data is average for June, July and August, 1996-1999, with the observations aggregated temporally to 3-hours for comparison. *22*
Figure 2.8 - Comparison of observed (thick lines) and simulated (thin lines) surface fluxes at the FIFE site; averaged June, July and August values over 1987-1989. ..... *23*
Figure 2.9 - Autocorrelation of soil moisture anomalies at lags of 3, 6, and 9 months. Shaded regions include correlations significant at a 0.05 level. *26*
Figure 2.10 - Comparison of simulated snow water equivalent and the observed snow extent for 1971-1995. Countour line indicates the extent of observed snow cover 80% of the time on the specified date. Shaded areas are those showing simulated snow water equivalent in excess of 5 mm 80% of the time on the indicated dates. *27*
Figure 3.1 - Location of the Mississippi River basin in North America. The basin boundary is shown in white, as is a north-south line at longitude 100 west. *32*
Figure 3.2 - Example of initialization dates for forecasting the DJF runoff at lead times of 0 through 4 seasons. *33*
Figure 3.3 - Schematic of the predictable and unpredictable influences on seasonal runoff considered in this study. Note that for this study the interactions are one-way; feedback from the land surface to climate is not considered -- only the initial conditions of the climate indicators are included. *34*
Figure 3.4 - Predictability of seasonal runoff due to SOI, expressed as the fractional variance, r^2, of seasonal runoff explained by SOI, using a) a simple persistence model, and b) the ENSO-CLIPER model. Countour intervals of r^2 values are every 0.1, and shading indicates locations where the r^2 is statistically significant. In the lower right corner of each panel is the fraction of the total basin area with significant correlation. *39*
Figure 3.5 - Average seasonal runoff for the Mississippi River basin, divided by the seasonal basin-wide average. *44*
Figure 3.6 - Predictability of seasonal runoff for each season (columns) and each lead time (rows), using combined climatic and land surface predictors, SOI, AO, SM, and SWE. Predictability is defined as the fractional runoff variance explained by the predictors, r^2, in a multiple linear regression. Contour interval is 0.1, with locally significant r^2 values shaded. The number in the lower right corner of each panel indicates the fraction of the basin exhibiting local statistical significance; this number is used in comparison with the field significance thresholds in Table 3.1. ..... *45*
Figure 3.7 - Same as for Figure 3.6, but including only climatic indicators, SOI and AO as predictors. *47*

Figure 3.8 - For each season, the correlation coefficient between the seasonal average SM and seasonal average SWE. 49
Figure 3.9 - As for Figure 3.6, but showing the predictability due to SWE alone. 50
Figure 3.10 - As for Figure 3.6, but showing the predictability of seasonal runoff due to SM alone. 52
Figure 3.11 - Unitless variable representing the importance of predictability. The variable is defined as the fraction of the runoff explained by the climate or land surface indicators (defined in the left panel for each row) times the unitless runoff (Figure 3.5), for a lead of 0 seasons. 55
Figure 3.12 - - Same as for Figure 3.11, but for a lead of 2 seasons. 56
Figure 4.1 - Missouri River main stem dams. Size of circle at each point is scaled according to the ratio of the active storage volume to the river flow at that point. 60
Figure 4.2 - a) Monthly mean inflow to upper three reservoirs in the Missouri River main stem system; b) Standard deviation of the monthly inflows; c) Coefficient of Variation. 62
Figure 4.3 - Monthly simulated and historic Missouri River main stem system volumes, 1968-1997. 69
Figure 4.4 - Monthly energy generation of Missouri River main stem dams, historic and simulated. a) Time series of monthly values; b) average annual cycle for the 50-year period, 1968-1997. 69
Figure 4.5 - Accumulated inflow to Ft. Peck dam for a 12-month forecast period under conditions of perfect and zero predictability. 70
Figure 4.6 – Monthly historic and simulated main stem system storage, as in Figure 4.3, but including the system operation under the flexible rule curve adopted in this study to adapt operations to different levels of predictability. MOSIM – no forecast component corresponds to the MOSIM model plotted in Figure 4.3 72
Figure 4.7 - Ratio of system volume to annual system inflow versus the percent difference between perfect and no forecast skill for past studies and the current study. Symbols drawn with dotted pen indicate sensitivity studies for reduced volume systems (see discussion in text). 74
Figure 4.8 - Reliability of system for meeting environmental release targets at Ft. Peck and Garrison dams, measured as the fraction of time that the releases are met, and the average magnitude of each shortfall expressed as a fraction of the target release. 76
Figure 4.9 - Benefits above a zero predictability scenario with the specified level of predictability in the current month, and no predictability in other months. 78

LIST OF TABLES

Table 2.1 - Simulated and observed streamflow comparison statistics. 15
Table 2.2 - Variables Included in Data Archive. 28
Table 3.1 - Fractional area thresholds (expressed as percentages of entire Mississippi River basin area exhibiting local significance) that must be exceeded to achieve statistical field significance at a 95% confidence level. 36
Table 3.2 - Summary of relative importance of predictors in forecasting seasonal runoff. Values are computed by multiplying at each grid cell the runoff variance explained by the predictors by the local unitless seasonal runoff, and summing these values over the Mississippi basin. Higher values indicate greater basin-wide predictability of seasonal runoff volume attributable to the predictor(s). Bold indicates the most influential factor for each season and lead. 53
Table 3.3 - Summary of relative importance of predictors, as for Table 3.2 but only for regions west of longitude 100 West. 54
Table 3.4 - Summary of relative importance of predictors, as for Table 3.2 but only for regions east of longitude 100 West. 54
Table 4.1 - Ratio of the total volume and active volume for each dam (the reservoir volume minus the permanent pool storage) to the average annual flow at each site. 62
Table 4.2 - Seasonal weighted average C_p values for the contributing area to Fort Peck dam, derived from Maurer and Lettenmaier (2002b) for the cases of different predictors (see text). Leads indicate the number of intervening seasons between the forecast date and the forecasted seasonal average runoff. Seasons are winter (DJF), spring (MAM), summer (JJA) and fall (SON). 65
Table 4.3 - Dam release constraints and key elevations for U.S. Army Corps of Engineers main stem Missouri River project used in the MOSIM model. 67
Table 4.4 - Total system storage category definitions and navigation flow targets, adapted from COE (1994a) and Jorgensen (1996). 68
Table 4.5 - Energy and capacity values used in this study 71
Table 4.6 - - Data related to the sensitivity study with resizing of the main-stem Missouri River system reservoirs. 75
Table 4.7 - Total system hydropower benefits for reduced-volume Missouri River main stem dams under different levels of predictive skill. 76

ACKNOWLEDGEMENTS

This technical report is based on the doctoral dissertation of Edwin P. Maurer. The author gratefully acknowledges the technical direction and support provided by his advisor, Professor Dennis P. Lettenmaier at the University of Washington, and the valuable input and advice of Professors Stephen J. Burges, Richard N. Palmer, Nathan Mantua of the University of Washington, and Professor John O. Roads of Scripps Institution of Oceanography, who generously participated as supervisory committee members. The research presented in this dissertation was supported by a NASA Earth System Science Fellowship. Research was also supported in part by the Joint Institute for the Study of the Atmosphere and Ocean (JISAO) at the University of Washington, funded under NOAA Cooperative Agreement NA17RJ11232, as part of the GEWEX Continental-Scale International Project (GCIP). This work also benefited from the generous assistance and insights of fellow graduate students in the Surface Water Hydrology group in the Civil and Environmental Engineering Department at the University of Washington.

CHAPTER I: INTRODUCTION

"Those who have knowledge do not predict. Those who predict do not have knowledge."
Lao Tzu

Extreme hydrologic events such as floods and droughts exact a large economic toll on society. While estimates are approximate and vary with the period analyzed and technique used, floods are the most costly natural disasters in the United States, with average damages of $5 billion per year in the 1990s (Pielke and Downton, 2000). Droughts, although less visible than floods, have economic costs nearly as large. The most costly natural disaster in the U.S. was the 1987-89 drought, which had $39 billion in total damages and affected 70% of the U.S. population (Riebsame et al., 1991). Costs due to both floods and drought have been rising, with flood damages increasing by a factor of five (in constant dollars) between the 1940s and 1990s (Pielke and Downton, 2000) and drought by a factor of two from 1975 to 1994 (Mileti, 1999). Furthermore, global climate change is expected to increase the magnitude and frequency of these events in some areas (National Assessment Synthesis Team, 2001). Clearly, effective management of water resources is critical to the mitigation of flood and drought losses. While some drought damages are not directly associated with water management (e.g., in the case of unirrigated crops), greater than half of the market value of U.S. agricultural crops is from irrigated land (U.S. Department of Agriculture, 1997). These large and growing costs could translate into substantial societal benefits to the extent that hydrologic extremes are predictable, and that forecast information is usable in mitigation and adaptation.

The economic importance of flood and drought prediction helped inspire the recommendations of the National Research Council (NRC) for research "increasing the extent to which such events can be predicted" (NRC, 2002) and "determining [the predictions'] usefulness for water management. (NRC, 2001) These recommendations provide a two-fold motivation for this study:

to investigate the opportunities for improving long-lead (monthly to seasonal) runoff prediction; and to evaluate the potential impacts of these improvements on water resources management.

Characterization of the land surface moisture state (especially soil moisture and snow) has long been recognized as a crucial component in hydrologic forecasting. Typically, long-lead (monthly to seasonal) streamflow forecasts rely on regression-based methods (Soil Conservation Service, 1988; Garen, 1992), or use hydrologic simulation models to capture the hydrologic memory reflected in soil moisture and snow storage, with climatological average conditions assumed during the forecast period. (Twedt et al., 1977). Comprehensive, accurate observations of soil moisture and snow water equivalent could result in improved runoff forecasts. Although improved characterization of soil moisture and snow conditions over large areas is evolving through better satellite information (e.g. Koike et al., 2000; Kelly, et al, 2001) and macroscale modeling (e.g., the North American Land Data Assimilation (LDAS) experiment (Mitchell, et al, 1999)), comprehensive, long term, validated data sets of these products sufficient for this study are not currently available. However, we now have the capability to produce model-derived products, which in the absence of observations can act as surrogates, in much the same way that reanalysis products are used in atmospheric studies.

Improved knowledge of climate dynamics and teleconnections, as manifested by ocean-atmosphere phenomena such as El Niño-Southern Oscillation (ENSO) (Rasmussen and Wallace, 1983), the Pacific Decadal Oscillation (Mantua et al., 1997), and the Arctic Oscillation (Thompson and Wallace, 2000), have resulted in improvements in long-lead (months to as much as a year) forecasts of sea surface temperature (SST), and some general climate anomalies (seasonal precipitation and temperature departures from normal), based on coupled ocean-atmosphere-land models (e.g., Barnston et al., 1999).

ENSO is the largest predictable climate signal at seasonal to interannual scales (Gershunov and Barnett, 1998), and its phase is correlated with a discernable response of regional climate (Goddard et al., 2001). This has resulted in a focus on coupled models' ability to predict ENSO phase (Barnston, et al., 1999), and hence provide predictive skill for regional hydrology in teleconnected areas. However, the factors influencing the development of each El Niño event, and ultimately its predictability, are case-specific (Philander, 1999; Fedorov, 2002), resulting in dependence of model-based forecast skill on the ability of a given coupled model to simulate the

particular features of the developing SST patterns associated with a given El Niño event. Furthermore, the nature of the land surface manifestations vary significantly from one El Niño event to another, and there is great spatial variability in the strength and character of the regional effects at the land surface (e.g., Kahya and Dracup, 1993). These difficulties notwithstanding, incorporation of climate forecasts in long-lead streamflow forecasts has been demonstrated in some settings (e.g. Wood et al, 2002; Baldwin, 2001; Hamlet et al., 2002).

Improved land surface moisture state determination combined with improved knowledge of the climate teleconnections has the potential to yield better predictability of streamflow to the extent that contributing runoff is influenced by these factors. This study identifies, over a large continental region, the relative importance to runoff predictability of hydrologic initial conditions and climate signals, as encoded in teleconnection patterns. Subsequently, the value of the resulting runoff predictability to management of water resources within the Missouri River basin is assessed.

In the context of water resources management, streamflow forecast information is only of value when there are physical and institutional structures that can respond to the information. These challenges of assessing the level and importance of long lead hydrologic predictability are summarized by two questions, which form the core of this study:

1. What is the predictability of continental scale runoff attributable to climate teleconnections, surface, and subsurface moisture storage, given perfect land surface moisture knowledge, across the Mississippi River basin at seasonal to annual lead times?

2. What are the potential benefits of improved runoff predictability to the operation of the major reservoirs of the Missouri River basin?

The approach for addressing these questions is summarized in the following three chapters. Chapter 2 is a paper, accepted for publication in the *Journal of Climate* (Maurer et al., 2002a) that describes the long-term derived data set that forms the basis for my investigations. Due to the lack of comprehensive, long-term observational data sets of soil moisture and snow water content, a hydrologic model was used to create a 50-year data set of surrogate observations over the continental U.S. and portions of Canada and Mexico. The data set is composed of gridded observations of precipitation and temperature, with surface meteorological forcing variables

derived directly from the observations, and other land surface states and fluxes derived indirectly via a land surface model. Chapter 3, which has been accepted for publication by the *Journal of Geophysical Research* (Maurer and Lettenmaier, 2002a), characterizes the potential predictability of land surface runoff due to knowledge of the climate and land surface initial states, focusing on the Mississippi River basin. Chapter 4, submitted to *Journal of Climate* (Maurer and Lettenmaier, 2002b), uses the predictability results from Chapter 3 in conjunction with a simplified system model of the Missouri River mainstem reservoirs to quantify the possible influence of increased predictability on the operation of a large water resource system, and the additional hydropower benefits that could be derived with added knowledge of climate state and initial land surface moisture conditions.

CHAPTER II: MODEL-DERIVED DATA OF LAND SURFACE STATES AND FLUXES

"It is a capital mistake to theorize before one has data. Insensibly one begins to twist facts to suit theories, instead of theories to suit facts."
Sir Arthur Conan Doyle

This chapter has been accepted for publication in Journal of Climate in April 2002 in its current form: Maurer, E.P., A.W. Wood, J.C. Adam, D.P. Lettenmaier, and B. Nijssen, 2002, A Long-Term Hydrologically-Based Data Set of Land Surface Fluxes and States for the Conterminous United States, *J. Climate* (in press).

INTRODUCTION

Early evidence of the importance of the land surface as a boundary condition in climate modeling (Namias, 1952, 1962) helped inspire the incorporation of land surface representations in coupled atmospheric models (Manabe, 1969). As computational capabilities have improved, the representations of the land surface included in these coupled models have become more detailed (e.g., Mahrt and Pan, 1984). Investigations using coupled land-atmosphere models have shown significant sensitivity of precipitation forecasts for lead times of several days to initial land surface states such as soil moisture (Beljaars et al. 1996; Betts et al., 1996a), and of long-lead (months or more) forecasts of surface air temperature (Huang et al, 1996). These sensitivities, of course, vary regionally and seasonally. For example, Brubaker et al. (1993) argue that precipitation forecasts should be most sensitive to land surface conditions where local feedbacks exist through recycling of moisture via evapotranspiration, which in general suggests that sensitivities should be highest in mid-continental areas in summer. This has been confirmed recently in experiments by Koster et al. (2000), where soil moisture memory was shown to be a dominant source of long-term weather predictability for some midlatitude continental regions.

The greatest difficulty in assessing the performance of coupled (and uncoupled) land-atmosphere parameterizations is the absence of comprehensive land surface observations against which simulations can be compared at the spatial and temporal resolutions at which the models operate.

The Atmospheric Model Intercomparison Project (Gates, 1992) included global climate simulations using 31 different coupled models, producing output including land surface variables of soil moisture, snow, and latent and sensible heat fluxes. In the validation stage, Gates et al. (1999) compare modeled precipitation to a gridded global data set based on both gauge and satellite estimates (Xie and Arkin, 1997), while most remaining surface variables were only intercompared, due to the limited quality and coverage of observations. Several methods have been used to evaluate the land surface representations in coupled models in so-called off-line experiments, i.e., where surface forcings to the models (precipitation, surface air temperature, as well as other surface meteorological variables and radiative forcings) are prescribed. These include comparisons of model-predicted evapotranspiration with those derived from an atmospheric water balance (Lohmann et al., 1998a), comparison of model-predicted energy and radiative fluxes with tower measurements during periods of intensive observations (Betts et al., 1996b), comparison of model-predicted runoff with observed streamflow (Koster et al., 1999), and comparison of model predictions of soil moisture with spatial averages over large regions of point observations of soil moisture (Robock et al., 1998). While these approaches have provided useful model diagnostic information, the observation-based products used in the comparisons in all cases have some inconsistency with the model variables with which they are compared – e.g., observations are for points or areas much smaller than the model spatial resolution (in the case of tower observations), comparisons are restricted to temporal averages rather than time step evolution of predicted variables (in the case of soil moisture), or the spatial scale is large compared to that resolved by the model (in the case of estimates of evapotranspiration based on atmospheric budget analysis). Furthermore, none of the data sets available at present allows an evaluation of the interaction of the water balance components over large regions for long periods.

A recent report of the U.S. Global Change Research Program (Hornberger et al., 2001) on global water cycle research identified as one of its three “pillar initiatives” determination of “whether or not the global water cycle is intensifying and to what degree human activities are responsible.” A key element in any attempt to identify possible ongoing changes in the land surface component of the global water cycle is the use of long records to determine the variability of land surface moisture fluxes and storages. The lack of long-term, continent-wide observations of many of the component variables of the water cycle greatly complicates the direct determination of changes in most of these variables (Ziegler et al., 2001)

Global reanalyses, such as those produced using global forecast models of the U.S. National Centers for Environmental Prediction (NCEP) (Kalnay et al., 1996) and the European Centre for Medium-Range Weather Forecasts (Gibson et al., 1997) provide one means of diagnosing model predictions of moisture and energy fluxes in the atmosphere and at the land surface. The reanalyses are produced by implementing a fixed or "frozen" version of a weather forecast model retrospectively, using the best available data in the analysis cycle, and archiving the model analysis output, which forms a consistent space-time field of all fluxes and state variables simulated by the model. The initial reanalysis produced using the NCEP model (produced in cooperation with the National Center for Atmospheric Research (NCAR), and usually referred to as the NCEP/NCAR reanalysis) is termed NRA1, to distinguish it from a more recent reanalysis, referred to here as NRA2, that uses the same forecast model (Ebisuzaki et al., 1998; Kanamitsu et al., 2000). NRA1 has been widely used for moisture and energy budget studies, model diagnosis, and many other purposes where temporally and spatially continuous-discrete fields are needed. Kalnay (personal communication) and her colleagues estimate that over 3000 journal articles have made use of NRA1 directly or indirectly in the 5 years since the data (now periodically updated to cover the 50+ year period from 1949 to within approximately one month of current time) were first made publicly available. Reanalyses like NRA1 and NRA2 can provide an excellent resource for studies examining variables that are closely linked to assimilated variables (mostly atmospheric profiles of moisture, temperature, and wind), and in fact Kalnay et al. (1996) provide a classification of the quality of NRA1 variables which is largely based on how closely related an archived variable is to assimilated observations. Under this scheme, variables related to the land surface water budget are assigned to Class C, meaning there are no observations directly affecting the variables, which are completely determined by the model, and may have considerable biases. For example, large biases have been identified in NRA1 precipitation (Higgins et al., 1996; Janowiak et al, 1998; Trenberth and Guillemot, 1998), evapotranspiration (Lenters et al., 2000), runoff (Roads and Betts, 2000; Coe, 2000), snow and soil moisture (Lenters et al, 2000; Maurer et al., 2001), although interannual variability of some variables, such as precipitation and runoff have been found to be better simulated (Roads and Betts, 2000). The follow-up NRA2 reduces NRA1 land surface water budget biases, though some biases remain (Maurer et al., 2001), and NRA2 covers a much shorter period, covering the "satellite" era of 1979-2000.

A major cause of problems with land surface variables in both NRA1 and NRA2 is the use of soil moisture "nudging" (or adjustment in the case of NRA2), which results in nonclosure of the surface water budget. Maurer et al (2001) showed that the nonclosure term can be of the same order as other terms (e.g., runoff) in the surface water cycle. Although nudging in a reanalysis is designed to bring the model state (especially atmospheric moisture variables) closer to observations, this is done at the expense of other components of the water budget, and complicates studies focused on the interaction and variability of water budget components at the land surface (see, e.g. Maurer et al. (2001) for an assessment of the effect of soil moisture nudging on runoff in NRA1). For these reasons, reanalysis data can be inappropriate for diagnosis of land surface moisture and energy flux and state variable simulations, by either uncoupled or coupled land-atmosphere models (Maurer et al., 2000), especially where the relationships between the budget components and their variability are of interest.

As argued by Maurer et al. (2000; 2001), better data for diagnosis of land surface water budget simulations can be produced through use of a physically based land surface model forced with quality controlled surface variables, and whose predicted surface runoff, when routed to correspond to streamflow measurements at the outlet of large river basins, matches observations. The effective degrees of freedom in a land surface scheme can be greatly reduced by prescribing, rather than predicting, model forcing variables at the land surface. For consistency of results, land surface schemes should, by construct, close the surface water and energy budgets (Pitman et al., 1999), and given the closure of these budgets by design, the variability and interaction of other "internal" variables can be expected to be much more realistic than those produced by reanalyses (or for that matter, any coupled model) that include some type of updating of model states.

We describe in this paper a consistent set of observation-based land surface forcings, and derived surface fluxes and state variables for a 50-year period that is more or less consistent with that available from NRA1. Like the reanalyses, the derived data are based on use of a consistent model for the entire simulation period and model domain. The time step is sub-daily (3-hours), and the model (and hence derived data) spatial resolution is 1/8 degree. The domain covers all of the conterminous U.S. plus a bounding area that covers parts of Canada and Mexico (specifically longitudes 67°W to 125°W and latitudes 25°N to 53°N), and is consistent with the domain and resolution of the Land Data Assimilation System (LDAS) – North America project (see Mitchell

et al., 1999). By construct, the surface energy and water budgets close at each time step; no assimilation of land surface state observations is performed.

HYDROLOGIC MODEL DESCRIPTION

The hydrologic model used in this study is the variable infiltration capacity (VIC) model (Liang et al. 1994; 1996). VIC is a macroscale hydrologic model that balances both surface energy and water over a grid mesh, typically at resolutions ranging from a fraction of a degree to several degrees latitude by longitude. Macroscale in this context refers to areas above a critical scale at which subgrid hydrologic variability can be captured statistically (e.g., Wood et al., 1988) – typically taken to be around 10 km. The controls of vegetation on land-atmosphere moisture and energy fluxes within VIC can be considered to constitute a soil-vegetation-atmosphere transfer scheme (SVAT). One distinguishing characteristic of the VIC model is its use of a subgrid parameterization of the effects of spatial variability in soils, topography, and vegetation that allows it to represent the observed nonlinear soil moisture dependence of the partitioning of precipitation into direct runoff and infiltration. It also features a nonlinear mechanism for simulating slow (baseflow) runoff response, and explicit treatment of vegetation effects on the surface energy balance.

In contrast with most SVATs, the VIC model generally (based e.g. on results of PILPS experiments; Lohmann et al., 1998a) does a better job of reproducing observed runoff characteristics, whereas compared with other hydrologic models, it includes a full energy balance formulation absent from most hydrologic, or rainfall-runoff models. The VIC model has been successfully applied to many large global rivers (e.g., Abdulla et al., 1996; Lohmann et al., 1998b; Nijssen et al., 1997; Wood et al., 1997; Nijssen et al., 2001). For this study, the model was run at a 1/8-degree resolution from January 1950 through July 2000 (with 1949 used for a 1-year spin-up to remove the effects of initial moisture storages).

Prior to conducting the archived simulations described below, simulations of more limited length were conducted for sub-areas of the domain shown in Figure 2.1. The simulated runoff was routed through the grid cell network to strategic outlet points, where it was compared to observed, or, where available, naturalized (water management effects removed) runoff. The simulated runoff was calibrated by adjustment of soil parameters describing soil depth, baseflow drainage

and infiltration capacity of the soil layers, which is described in greater detail by Maurer et al. (2001), with the resulting "pseudo-observations" used to compare various coupled models.

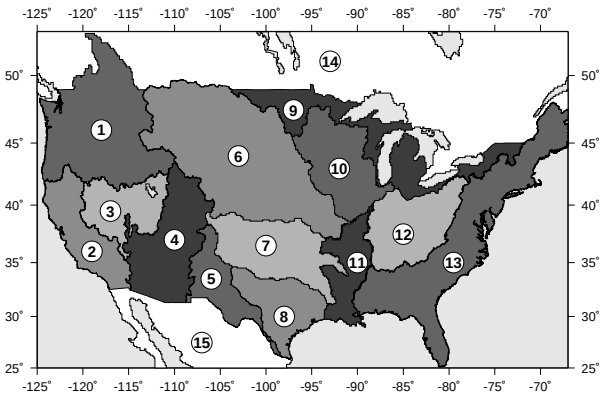

1 Northwest	6 Missouri	11 Lower Mississippi
2 California	7 Arkansas-Red	12 Ohio
3 Great Basin	8 Gulf	13 East Coast
4 Colorado	9 Great Lakes	14 Canada
5 Rio Grande	10 Upper Mississippi	15 Mexico

Figure 2.1 - LDAS Domain with modeling sub-areas

MODEL INPUT DATA SETS

Land Surface Characteristics

The soil characteristics used were taken from gridded 1/8° data sets developed as part of the LDAS (Mitchell et al., 1999) project. Within the conterminous U.S., these data sets are based on the 1-km resolution data set produced by Pennsylvania State University (Miller and White, 1998). For areas in Canada and Mexico, the LDAS soil data are derived from the 5-minute Food and Agriculture Organization data set (FAO, 1998). Soil texture in the LDAS data set is divided into 16 classes for each of 11 layers, inferring specific soil characteristics (e.g., field capacity, wilting point, saturated hydraulic conductivity) based on the work of Cosby et al. (1984) and Rawls et al. (1998), and Reynolds et al. (2000). These LDAS data sets were used to specify the relevant soil parameters required by the VIC model directly. For remaining soil characteristics (e.g., soil quartz content), values were specified using the soil textures from the 1-km database, which were then indexed to published parameter values (the primary source was Rawls et al. (1993)), and aggregated to the 1/8° model resolution. The VIC model as applied in this study uses a three-layer soil column, with depths of each layer specified for each grid cell as derived during sub-area calibration.

Land cover characterization was based on the University of Maryland global vegetation classifications described by Hansen et al. (2000), which has a spatial resolution of 1 km, and a total of 14 different land cover classes. From these global data we identified the land cover types present in each 1/8° grid cell in the model domain and the proportion of the grid cell occupied by each, as described by Maurer et al. (2001). The primary characteristic of the land cover that affects the hydrologic fluxes simulated by the VIC model is leaf area index (LAI). LAI is derived from the gridded (1/4°) monthly global LAI database of Myneni et al. (1997), which is inverted using the Hansen et al. land cover classification to derive monthly mean LAIs for each vegetation class for each grid cell. The LAI values do not change from year to year in this implementation of VIC, hence interannual variations in vegetation characteristics are ignored. Furthermore, the Myneni et al. LAI values to which the method is tied are based on averages over the period 1981-1994 which may not be representative of the entire simulation period. Rooting depth is specified for each land use type so that shorter crops and grasses draw moisture from the upper soil layers, and tree roots from the deeper layer (e.g. Jackson et al., 1996). Additional parameters for each vegetation type were assembled based on several sources, including roughness length and displacement height (Calder, 1993), architectural resistance (Ducoudré et al., 1993), and minimum stomatal resistance (DeFries and Townshend, 1994).

Meteorological and Radiative Forcings

The VIC model is forced with observed surface meteorological data, which include precipitation, temperature, wind, vapor pressure, incoming longwave and shortwave radiation, and air pressure. Because only temperature and precipitation are measured routinely at a reasonably large number of locations within the domain, we use established relationships relating these other meteorological and radiation variables (excluding wind) to precipitation, daily temperature and temperature range. For example, dew point temperature is calculated using the method of Kimball et al. (1997), which relates the dew point to the daily minimum temperature and precipitation, and downward shortwave radiation is calculated based on daily temperature range and dew point temperature using a method described by Thornton and Running (1999). Because surface observations of wind speed are sparse and are biased toward certain geographical settings (e.g., airports), daily 10-m wind fields were obtained from the NCEP/NCAR reanalysis (Kalnay

et al., 1996), and regridded from the T62 Gaussian grid (approximately 1.9° square) to the 1/8° grid using linear interpolation.

Within the conterminous U.S., precipitation data consist of daily totals from the National Oceanic and Atmospheric Administration (NOAA) Cooperative Observer (Co-op) stations, the average density of which is about one station per 700 km^2. Daily precipitation totals were assigned to each day based on the time of observation for the gauge. For example, a gauge reporting precipitation accumulation at 7 am would have 7/24 of the daily total assigned to the reporting day, and the remainder to the previous day. The precipitation gauge data were gridded to the 1/8° resolution using the SYMAP algorithm of Shepard (1984) as implemented by Widmann and Bretherton (2000). The gridded daily precipitation data were then scaled to match the long-term average of the parameter-elevation regressions on independent slopes model (PRISM) precipitation climatology (Daly et al., 1994, 1997), which is a comprehensive data set of twelve monthly means for 1961-1990 that is statistically adjusted to capture local variations due to complex terrain. This was done by generating twelve scale factors for each grid cell, one for each month, where each scale factor was the ratio of the PRISM mean monthly precipitation for 1961-1990 to the mean monthly gridded, unscaled co-op station precipitation for 1961-1990. Although the PRISM data do account for the lower station density in more complex terrain, they do not include an adjustment for precipitation gauge undercatch, which can be significant especially for snowfall measurements (Goodison et al., 1998). For this reason, some underestimate of precipitation may still be present in snow-dominated areas. The minimum and maximum daily temperature data, also obtained from Co-op stations (approximately one station per 1000 km^2 on average), were gridded using the same algorithm as for precipitation, and were lapsed (at –6.5°C/km) to the grid cell mean elevation. Temperatures at each time step were interpolated by fitting an asymmetric spline through the daily maxima and minima.

For Canadian portions of the study area, the daily gridded precipitation and temperature data are generally of lower quality than in the U.S. part of the domain, due to lower station density and the need to include some less reliable sources to obtain a complete record. For the years 1949 through 1999 (excluding British Columbia for 1999), observed daily temperature and precipitation station data (Environment Canada, 1999) were used in the same manner as were such observations over the U.S. Precipitation is measured at more than 2500 Environment

Canada meteorological stations, resulting in an average station density of one station per 4,000 km^2 in the region of Canada included in this study (Metcalf et al., 1997). Additional sources of data were used to complete the precipitation and temperature forcings for British Columbia for 1999 and for all of Canada for 2000. For precipitation, the Global Precipitation Climatology Project (GPCP) gridded one-degree precipitation product (Huffman et al., 2001) was used. The GPCP daily product, available from 1997 on, is derived from gauge data merged with satellite estimates of precipitation. The gauge data in the GPCP product include monthly precipitation reported via the World Weather Watch Global Telecommunication System, which are observations at a lower station density than the Environment Canada meteorological stations. For temperature, the NCEP/NCAR reanalysis product (Kalnay et al., 1996) daily minimum and maximum 2-meter air temperatures were used. At present, the PRISM data do not include Canada or Mexico, with the exception of the Canadian portion of the Columbia River basin, hence no rescaling of precipitation was performed for the portions of Canada or Mexico without PRISM data.

As for the Canadian portions of the study area, the Mexican portion also has a relatively low station density, and uses data sources that are generally less reliable than those used within the U.S. to obtain a complete record. For the years 1949 through 1997, observed daily temperature and precipitation station data were used. Daily precipitation and temperature measurements were available from 1949-1997 at 132 stations in the Mexican region of the domain (Servicio Meteorológico Nacional, 2000), for an average station density of one station per 6,000 km^2. For 1998-2000, the GPCP precipitation and the NCEP/NCAR reanalysis air temperatures were used.

Daily precipitation totals were apportioned evenly over each three-hour model time step. To evaluate the sensitivity of the diurnal cycle of model-predicted fluxes to this assumption, we developed a simple algorithm for disaggregating daily precipitation. From NCDC Co-op stations reporting hourly data, we derived the probabilities of time-of-occurrence and number of hours of precipitation, and created cumulative distribution functions of these for each season for five ranges of daily total precipitation at each co-op station. Using these relationships, we stochastically disaggregated the gridded daily precipitation and ran the VIC model, with both disaggregated and non-disaggregated (evenly distributed through the day) daily precipitation. A comparison of the mean diurnal cycle of precipitation, runoff, and evapotranspiration from these

two simulations, run over the lower Mississippi River basin for 1996-1999, is shown in Figure 2.2. Even in the summer, when the diurnal cycle of precipitation is strongest, the assumption of uniform diurnal precipitation rate does not substantially affect the mean diurnal cycle of the partitioning of precipitation into evapotranspiration and runoff. The same is true for the mean diurnal cycle of the energy balance. The use of a constant daily precipitation rate does result in slightly increased runoff and decreased evapotranspiration. However, it should be noted that the model parameters were estimated based on a constant diurnal cycle of precipitation, and the results for disaggregated precipitation may be slightly biased as the model was not recalibrated to the disaggregated precipitation. Nonetheless, the results show that the assumption of a constant diurnal cycle has minimal effect on the model-derived moisture and energy fluxes.

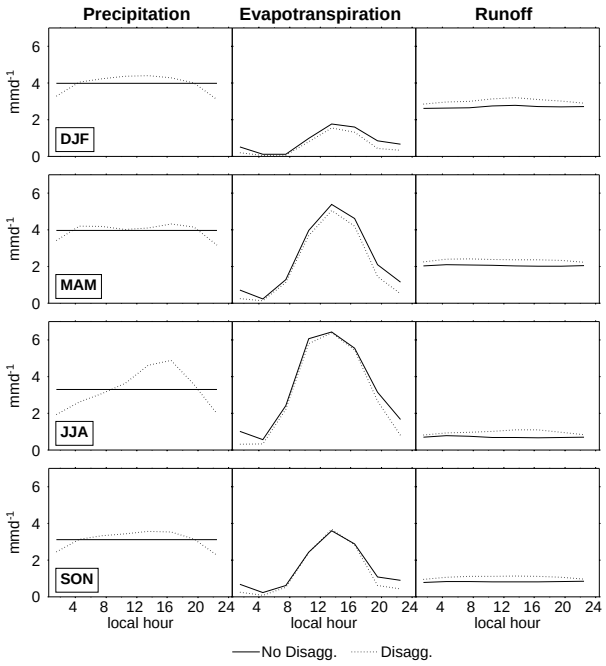

Figure 2.2 - Comparison of effect of stochastic disaggregation of daily precipitation totals versus constant precipitation rate on simulated runoff and evapotranspiration. Columns in the figure are for different variables, and rows are for each of four seasons.

PRELIMINARY ANALYSIS

The parameterized forcings and model-simulated variables were compared to selected sets of observations where available, in order to evaluate the quality of the model-simulated data. We

present five comparisons here, both to confirm the validity of the derived variables, and to illustrate some potential uses of the data set.

Comparison of routed VIC runoff with observed streamflow

As in previous applications of the VIC model, the runoff was routed from individual grid cells, through a defined channel network, to produce hydrographs at selected points. The routing algorithm is based on Lohmann et al. (1996), which uses daily runoff at each contributing grid cell. Although the routing model can be calibrated to improve timing of hydrographs, we performed no calibration of the routing model for this comparison. The resulting predicted hydrographs for 12 locations throughout the domain are shown in Figure 2.3. For comparison, observed flows at U.S. Geological Survey stream gauges are shown. In the case of the Columbia, Sacramento, Tuolumne, Colorado, Missouri, Alabama and Potomac Rivers, naturalized flows, that is, observed flows that have been adjusted for anthropogenic effects (e.g., irrigation diversions, reservoir storage, and evaporation) are shown. In general, the VIC model is quite successful in capturing the peak flows, the baseflow-dominated low flows, and the interannual variation of streamflows.

Table 2.1 - Simulated and observed streamflow comparison statistics.

River	RMSE[a] (%)	Relative Bias[b] (%)	Average Observed Flow (m^3s^{-1})
Columbia R.	44.0	9.0	5349
Sacramento R.	46.4	-0.4	239
Tuolumne R.	68.4	30.3	76
Colorado R.	45.7	26.7	580
Neches R.	61.4	29.5	44
Arkansas R.	56.3	35.0	1605
Missouri R.	38.8	-3.7	3119
Upper Mississippi R.	25.6	-13.8	3511
Ohio R.	21.3	-14.8	9760
Alabama R.	48.2	31.7	1113
Moose R.	71.8	-50.9	738
Potomac R.	47.9	0.5	424
Overall (weighted by Obs. Flow)	34.5	-3.1	

Figure 2.4 shows the average annual cycle of the simulated and observed flows for the 10 year time series in Figure 2.3. As with Figure 2.3, the range of flows represented varies widely

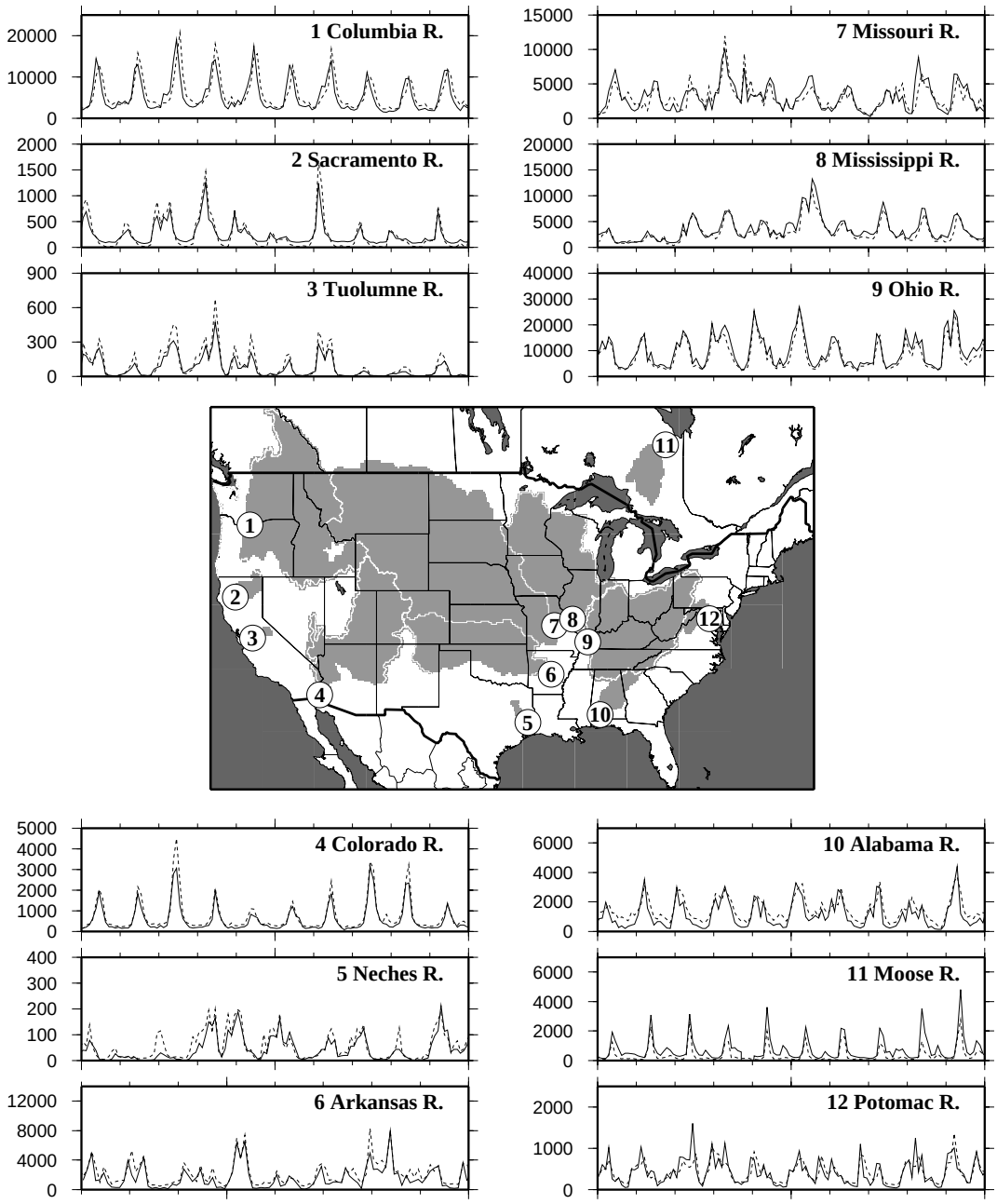

Figure 2.3 - Comparison of routed simulated runoff (dashed lines) with observed (or naturalized) streamflows (solid lines). Shaded areas are the contributing regions to each identified point. Ordinate values are runoff in m^3s^{-1}, abcissa is a ten year period, the beginning of which varies by basin depending on observed flow availability.

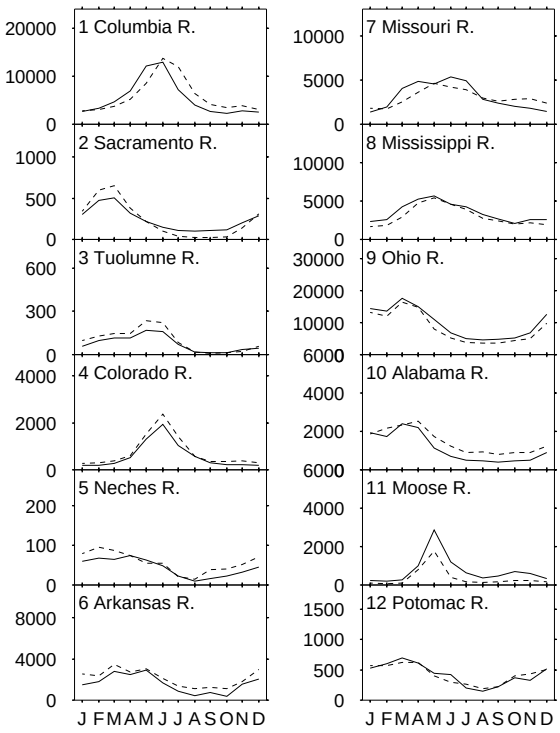

Figure 2.4 - Average flows by month for each of the 12 basins shown in Figure 2.3. Ordinate values are m^3s^{-1}, solid lines are observed or naturalized flows, and dashed lines are routed simulated runoff.

between basins. The root mean square error (RMSE) and relative bias for these 12 locations are summarized in Table 2.1. It should be noted that for the Arkansas River, significant withdrawals and diversions affect the observed flows, but unfortunately naturalized flows for this river are not available for the period analyzed. Therefore it is expected that the simulated flows, which do not consider water management effects and diversions, will exceed the observed flows, and in fact the VIC simulations generally exceed the USGS observations. Based on data for 1995 (Solley et al., 1998), the depletions are estimated to be 10-15% of the annual flow, thus the relative bias in Table 2.1 would be reduced accordingly, as would the RMSE. The bias over all areas, weighted by flow, is quite low; relative bias for the basins contributing the smallest amounts of flow tends to be larger than for the higher flow producing regions. RMSE, representing the average error in monthly flow simulation, shows the same pattern where RMSE tends to be smaller for the areas contributing greater flows. The Moose River in Ontario, Canada shows the highest bias and RMSE of the basins included in Table 2.1. This reflects the lower density of meteorological stations in Canada, hence greater uncertainty in the forcing data for the hydrologic model. In

addition, the undercatch of frozen precipitation, which is not corrected for in this study, would more important at higher latitudes. Further, no calibration to streamflow was performed for the portions of the domain in Canada (except the Canadian portion of the Columbia River basin, which was calibrated) or Mexico, for which soil parameters were transferred from the nearest calibrated basins in the U.S. For the Columbia River basin, the RMSE value is inflated due to the timing shift apparent in both Figures 2.3 and 2.4, which illustrates the sensitivity of the RMSE statistic when applied to timing errors in seasonal hydrographs. Although no calibration of the routing model was performed for this study, manually shifting the flows by two to three weeks reduces the RMSE by 50%. This shows that the simulated model output, when used with a customized routing for each basin, could produce simulated streamflows with lower RMSE than that shown in Table 2.1, although the bias would remain unchanged. It should be emphasized that the RMSE values shown in Table 2.1 are applicable to individual months and years; the errors associated with mean flows averaged over n years would scale with approximately $1/n^{1/2}$.

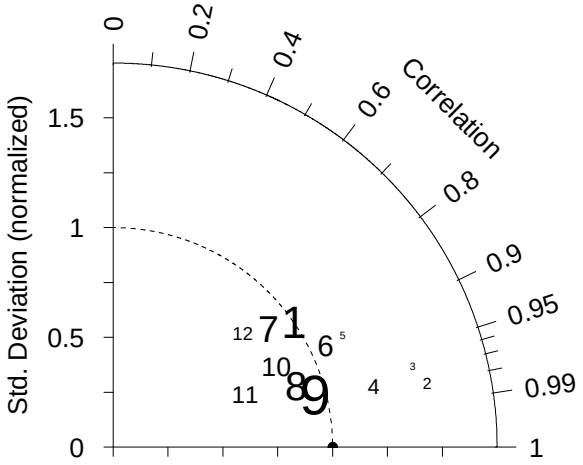

Figure 2.5 - Taylor diagram for simulated monthly runoff routed to basin outlet points. The plotted numbers identify the basin, using the same numbering system as used in Figures 2.3 and 2.4, and are shown in font sizes scaled by the cube root of the observed flow. See text for details.

Figure 2.5 illustrates three important characteristics of the simulated and observed monthly time series for each basin, using a Taylor diagram (Taylor, 2001). The numbers plotted correspond to the numbering of the basins in Figures 2.3 and 2.4, and the font size for each number is scaled by the cube root of the observed average flow. The radial distance from the origin to each number represents the ratio of the simulated to the observed standard deviation; the cosine of the azimuth angle represents the correlation of simulated streamflows with observations (after removal of the

mean); and the distance from the point where observations would plot, located at (1,0), is proportional to the RMSE. Figure 2.5 shows good correlation of simulated and observed flows, with all basins exceeding 0.8, and most above 0.9. The most prominent feature is that the basins with the largest runoff show the best correspondence with observed variance, plotting very close to the dashed line at the radial value of unity.

The overall success at reproducing runoff hydrographs, taken together with the use of observed precipitation, implies that, over time scales long enough for the change in surface storage to be small relative to the accumulated values for other variables in the water budget, ET is realistically estimated. In addition, due to the physically based representation of soil moisture and runoff generation processes within the model, simulations of other surface flux and state variables (e.g., ET, total soil moisture storage, and snow) should reasonably represent the true (but unobserved) variables. Although runoff can be validated against observed streamflow at many locations, validation of other model simulated variables, such as ET and soil moisture are more difficult due to the paucity of long-term observations over broad spatial domains. Ongoing validation of the data set presented here will identify areas where this approach performs best, and where improvements will be most valuable for future investigations. We report below comparisons for a few locations where long-term observations of variables other than runoff are available.

Comparison with Illinois soil moisture

There are few systematic measurements of soil moisture within the model domain that provide records of a length sufficient for comparison to the VIC model simulation. The soil moisture database described by Hollinger and Isard (1994), available from as early as 1981 through August 1996 through the Global Soil Moisture Data Bank (Robock et al., 2000), is unique in the length and detail of the measurements. Observations are available from 19 sites distributed more or less uniformly over the state. Soil moisture is reported at 11 different depths to a total of 2 m, with a sampling interval of approximately every 2 weeks on average (less frequently in the winter). For comparison with these 19 point measurements, we selected the 17 VIC 1/8-degree grid cells that

contain all of the observation locations. In addition, because the soil depths in the VIC grid cells vary between 1.0 and 2.3 meters, only the soil moisture from the top 1 meter from both the observations and the VIC model were used in the comparisons. Figure 2.6a compares the observed monthly average soil moisture for the top 1 m for 1981-1996 with the VIC model simulation for the same period. The climatological soil moisture level for the VIC simulation is low relative to the observations, but the average monthly flux, which affects the model's water

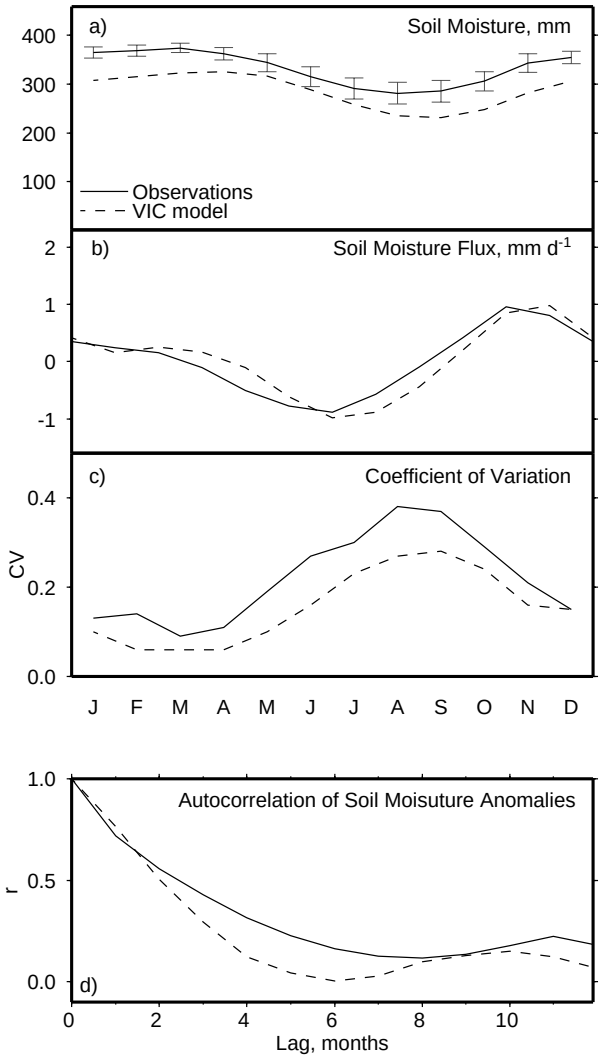

Figure 2.6 - Comparison of observed soil moistures in Illinois from 1981-1996 with simulated values for the same period. a) average soil moisture in the top 1 meter of soil for each month; b) average soil moisture tendency for each month; c) coefficient of variation of monthly soil moisture anomalies; d) autocorrelation of soil moisture anomalies.

balance, is simulated quite accurately (Figure 2.6b). This suggests that, at least in the Illinois area, the VIC simulation produces soil moisture storage changes that are consistent with observations.

Additionally, a monthly time series of average soil moisture in the top 1 meter was computed for both the Illinois observations and the VIC simulations. The coefficient of variation of each month, defined as the standard deviation divided by the mean, is a measure of the interannual variability of soil moisture. Figure 2.6c shows that the coefficient of variation for the VIC simulations slightly underestimates the seasonal variation of interannual variability seen in the observations. Finally, Figure 2.6d illustrates that the autocorrelation of soil moisture anomalies in the VIC model is similar to that of observed data, which suggests that the persistence of soil moisture anomalies is comparable in the model and observations.

Comparison of Diurnal Cycle of Surface Fluxes with Observations

To evaluate the simulated daily radiation, as well as the diurnal cycle, we use observations of selected sites in the continental U.S. established as part of the Surface Radiation Budget Network (SURFRAD) (Augustine et al., 2000). We chose the four sites with the longest records, beginning in 1994-1995, which are located in Mississippi, Montana, Illinois, and Colorado. Figure 2.7 shows the observed downward solar radiation and net (longwave plus shortwave) radiation fluxes at these four sites (aggregated from 3-minute to 3-hour, to match the VIC simulation time step), averaged for June, July, and August for 1996-1999, and the model simulated fluxes for the grid cells containing these points. Both the simulated average daily downward solar radiation and net radiation are within ten percent of the observations at all locations; averaged over all sites these are within two percent. There is a downward bias of the daily peak for these fluxes of between three and 15 percent, with an average of ten percent over all sites. In general, the comparisons indicate reasonable agreement of daily radiative fluxes, with some peak radiation underestimation, across a wide range of geographical settings.

The First International Satellite Land Surface Climatology Project (ISLSCP) Field Project (FIFE) included an intensive collection of land surface flux data at multiple locations within a 15 km x 15 km site near Manhattan, Kansas (centered at 39.05°N, 96.53°W). Intensive field campaigns

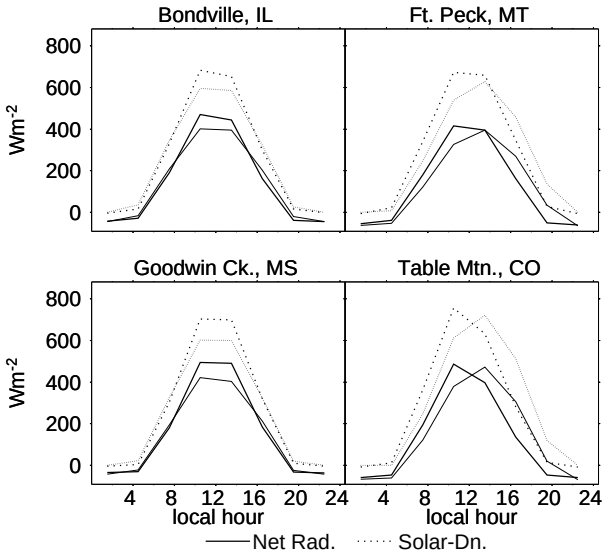

Figure 2.7 - Comparison of observed (thick lines) and simulated (thin lines) downward solar radiation and net radiation at four SURFRAD sites. Data is average for June, July and August, 1996-1999, with the observations aggregated temporally to 3-hours for comparison.

were conducted during the summers of 1987 and 1989, generally of length about 2-3 weeks each, with continuing observations with fewer stations during the remainder of the summers, and during the summer of 1988 (Sellers et al., 1992). The resulting tower flux observations were compiled and quality controlled by Betts and Ball (1998). The data set provides a multi-site average of surface fluxes, reported every 30-minutes, that allows examination of the VIC model output with an observed diurnal cycle for surface flux variables.

As an example, we compare the average diurnal cycle of surface fluxes for the VIC grid cell centered at 39.0625°N, 96.5625°N, which is comparable to the FIFE site in location and dimension, measuring 13.9 km north-south x 10.8 km east-west. Figure 2.8a compares the average diurnal cycle for this grid cell with the FIFE observations for June through August, averaged over 1987-1989. In general, the VIC-derived peak solar radiation is underestimated by 15 percent, while the daily average is underestimated by 7 percent. The net radiation is also underestimated relative to the observations, by 16 percent for the peak, and by 9 percent for the daily average. The average underestimate of the latent heat flux by VIC, for the averaged 1987-1989 period, is 21 W m^{-2}, or 19 percent, which is equivalent to 0.73 mm d^{-1} of evaporation. This

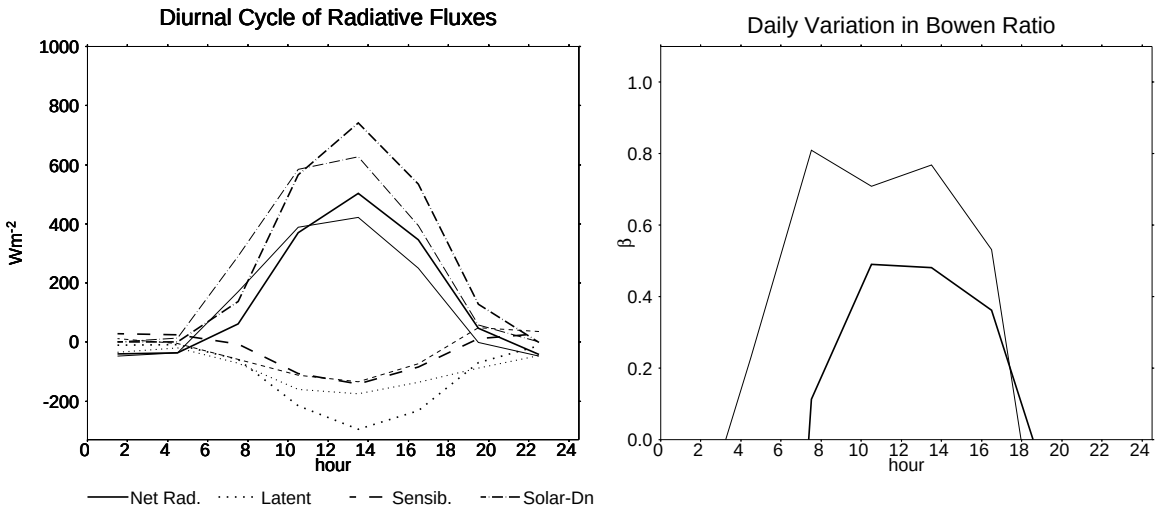

Figure 2.8 - Comparison of observed (thick lines) and simulated (thin lines) surface fluxes at the FIFE site; averaged June, July and August values over 1987-1989.

can be compared to estimates of the site-averaged non-closure of the water balance for the observations, which for the period May 29 – October 16, 1987 which vary from 20 mm (Duan et al., 1996) to 40 mm (Betts and Ball, 1998), or an average 0.14-0.28 mm d^{-1} over the observation period. As shown in Figure 2.8b, the partitioning of the net radiation into latent and sensible heat does follow the pattern seen in the observations. The average simulated sensible heat flux exceeds the observed by 5 Wm^{-2}, which is a 16 percent overestimation. The average Bowen ratio for daytime hours for the observations for this period is 0.36, and for VIC is 0.61. Although summer evapotranspiration for this grid cell shows some bias relative to the observations, since the model is forced with precipitation and reproduces observed runoff, evapotranspiration is correctly estimated over larger areas.

Derived Soil Moisture Persistence

Huang et al. (1996) produced a 63-year time series of monthly soil moisture for the conterminous U.S., using historical monthly average precipitation and temperature at 344 climate divisions. They developed a simple monthly water balance bucket-type soil model, where potential evapotranspiration was computed using a temperature index method, which was then scaled by the soil saturation level to estimate actual evapotranspiration. Surface runoff was calculated based on incident monthly

precipitation, scaled by a non-linear relation of saturation of the soil, and base flow discharge from the soil column was a function of soil moisture in the column. Using their derived soil moistures, they produced maps of the autocorrelation of soil moisture, as well as correlations of soil moisture with precipitation and temperature. Huang et al. apply uniform soil model parameters to the conterminous U.S., developed based on runoff data in Oklahoma and validated against soil moisture in Illinois. Figure 2.9 compares the autocorrelation of soil moisture anomalies at 3-, 6- and 9-month lags for the VIC model output. Panel 4d) is comparable to Figure 3 in Huang et al. (1996). There is a strong correspondence with the VIC-derived statistics and Huang et al. (1996). For instance, both sets of results show higher soil moisture persistence toward the western portions of the domain, and more moderate levels in the north-central U.S., though the VIC model correlations are generally lower than the Huang et al. values by 0.1 to 0.2. Focusing specifically on Illinois, at a 3-month lag the VIC model simulations show a monthly autocorrelation of soil moisture anomalies between May and August of approximately 0.25-0.3 (with an average of 0.28 over the Illinois area) while the Huang et al. model estimates approximately 0.35-0.5 for this region. By comparison, the Illinois soil moisture measurements show a 3-month autocorrelation of soil moisture anomalies for May/August of 0.27, again using the soil moisture observations discussed above. This suggests that, at least for Illinois, the more complex VIC model land surface representation reproduces observed soil moisture persistence somewhat better than does the more simplified model of Huang et al. Figure 2.9 also illustrates the decay of the autocorrelation with time. For instance, February soil moisture anomalies tend to dissipate more quickly than August anomalies, which have significant persistence over larger areas 9 months later.

Observed and Simulated Snow Extent

Northern hemisphere snow extent data are archived by the National Snow and Ice Data Center (1996) for the period 1971-95. These data were derived from digitized versions of manual interpretations of AVHRR, GOES and other visible band satellite data, and are

gridded to a spatial resolution of 25 km. For comparison with the gridded observations of snow extent, Figure 2.10 shows the areas that, in the hydrologic model simulation, contain greater than 5 mm of snow water equivalent on the selected dates at least 80% of the time during 1971-1995. The contour line on Figure 2.10 shows for each date the extent to which snow cover is observed 80% of the time during the same period. It should be noted that there is not direct, fixed correspondence between a specific snow water equivalent on the ground and snow extent detected by a satellite, but a qualitative assessment can be made on the basis of this comparison. Figure 2.10 illustrates three

features of the model simulated snow: the seasonal retreat of the snow line for the eastern half of the domain closely matches the observations; but the model underestimates snow extent in the northern great plains; and a slight overestimation of late season snow by the model relative to the observations is apparent in some areas of the mountainous western U.S. Cherkauer (2001, Appendix A) in a study focused on the Upper Mississippi River basin demonstrated the significant effect of correcting precipitation for undercatch of precipitation, especially frozen precipitation. The increase in winter (December, January February) precipitation was greatest in northern areas, and may account for some of the difference in observed snow extent and simulated snow water equivalent in the northern Great Plains.

DATA FORMAT AND AVAILABILITY

The data described in this paper are archived in netCDF format. Monthly summaries of model forcing variables, model output, and derived variables are available to the public via ftp from our web site (www.hydro.washington.edu). Arrangements are currently in progress to make the data set accessible via the University Corporation for Atmospheric Research (UCAR) Joint Office of Science Support. Details of access to the full dataset, which includes 3-hour output and daily summary data archived by variable by year, are also available from our web site. This site will also announce updates of the archive.

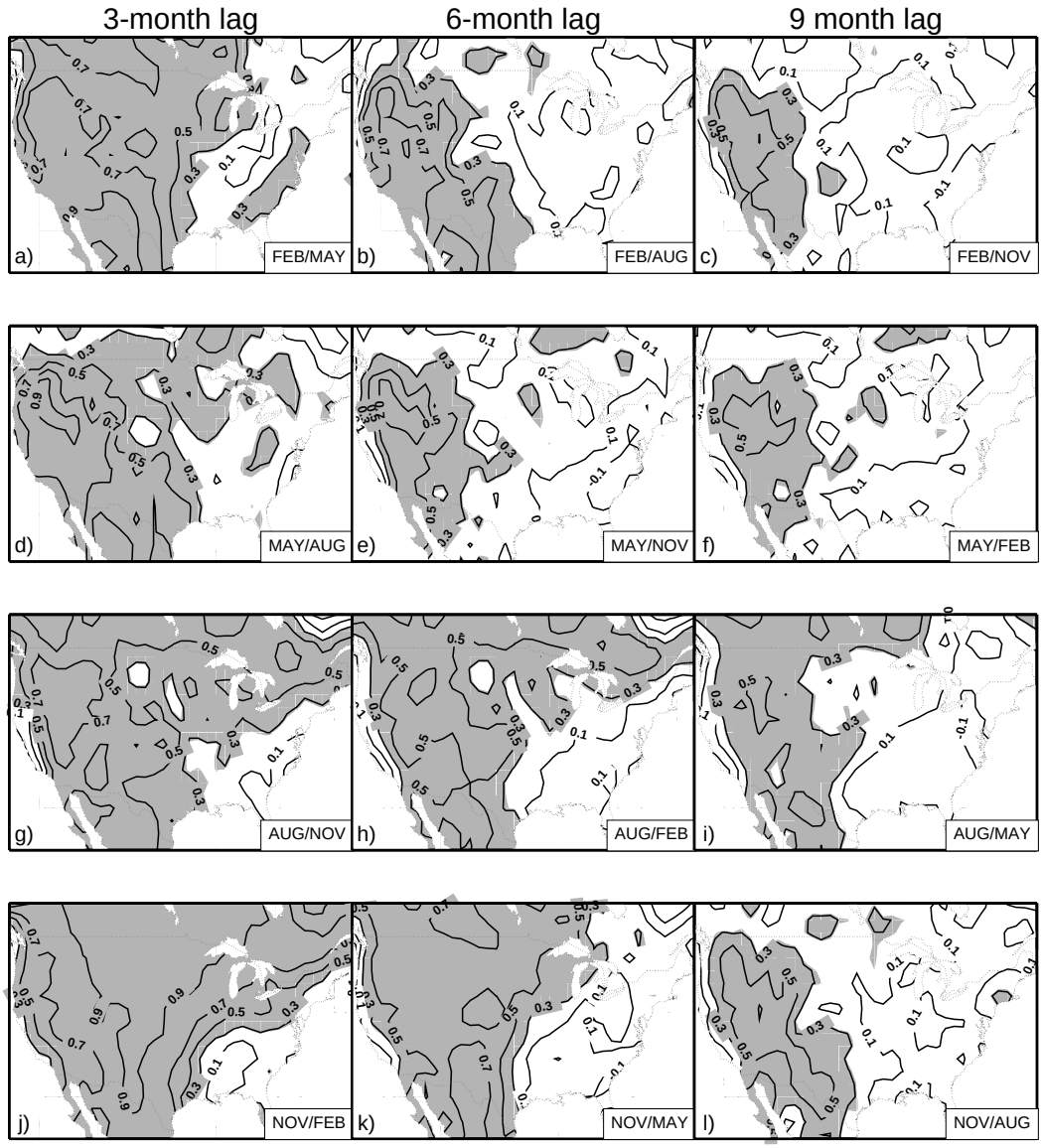

Figure 2.9 - Autocorrelation of soil moisture anomalies at lags of 3, 6, and 9 months. Shaded regions include correlations significant at a 0.05 level.

The variables included in the archive are listed in Table 2.2. For the 3-hourly data, flux variables (in units of either $kgm^{-2}s^{-1}$ or Wm^{-2}) reported at each time step are averages over the preceding 3 hours. State variables (kgm^{-2}) are reported at the end of the time step. For monthly and daily summary data, both flux and state variables are averages of the eight reported values during that day. In addition to the model forcing and output variables, there are derived monthly summary

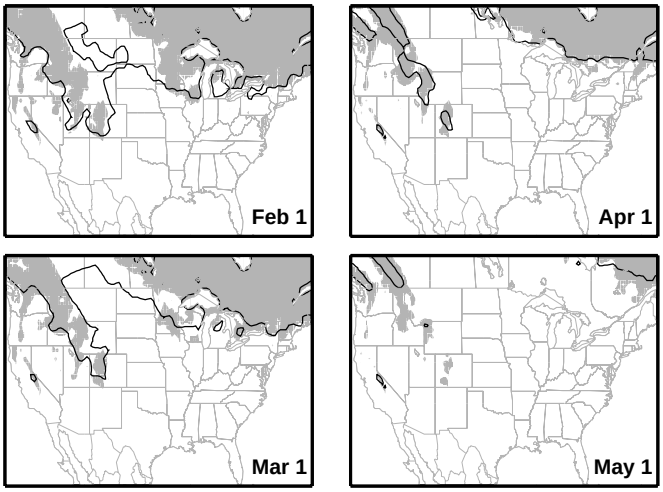

Figure 2.10 - Comparison of simulated snow water equivalent and the observed snow extent for 1971-1995. Countour line indicates the extent of observed snow cover 80% of the time on the specified date. Shaded areas are those showing simulated snow water equivalent in excess of 5 mm 80% of the time on the indicated dates.

data, including soil moisture and snow water fluxes averaged over each month. The variable names are generally consistent with the Assistance for Land Surface Modeling (ALMA) standards (Polcher et al., 2001). For variables not included in the ALMA list, variable naming conventions are based on the LDAS (Mitchell et al., 1999) common output standard.

CONCLUSIONS

We have described a derived data set of land surface states and fluxes for the LDAS domain, which comprises the conterminous United States, and portions of Canada and Mexico. The data set spans the period 1950-2000, and is at a resolution of 1/8 degree, or roughly 140 km^2 per grid cell on average. The data are distinct from reanalysis products in that both the water and energy budgets at the land surface balance at every time step. Furthermore, the surface forcings include observed precipitation, and the simulated runoff is shown to match observations quite well over large river basins, indicating that, over the long term, in order to balance precipitation and runoff, evapotransporation must also be realistic. Given the physically-based parameterizations in the model, we argue that over shorter timescales other terms in the surface water balance (e.g., soil moisture) are probably well represented, at least for the purposes of diagnostic studies such as those in which reanalysis products have been widely used. These characteristics give this data set promise for proving useful for a variety of studies, especially where ground observations are

lacking. As the data are extended through 2000 and 2001, the overlap of the data set with archived model results including assimilation of remotely sensed observations will provide more opportunities for study.

Table 2.2 - Variables Included in Data Archive.

Variables – 3-hour and Daily	Variable Name	Units
Precipitation	Prate	$kgm^{-2}s^{-1}$
Evapotranspiration	Evap	$kgm^{-2}s^{-1}$
Runoff (surface)	Qs	$kgm^{-2}s^{-1}$
Baseflow	Qsb	$kgm^{-2}s^{-1}$
Soil Moisture, Layer 1	Soilm1	kgm^{-2}
Soil Moisture, Layer 2	Soilm2	kgm^{-2}
Soil Moisture, Layer 3	Soilm3	kgm^{-2}
Snow Water Equivalent	SWE	kgm^{-2}
Net Shortwave Radiation at the Surface	SWnet	Wm^{-2}
Incoming (downward) Longwave Radiation	LWdown	Wm^{-2}
Net Radiation at the Surface	NetRad	Wm^{-2}
Latent Heat Flux	Qle	Wm^{-2}
Sensible Heat Flux	Qh	Wm^{-2}
Ground Heat Flux	Qg	Wm^{-2}
Albedo	Albedo	---
Surface (skin) Temperature	RadT	K
Relative Humidity	RH	%
Air Temperature	Tair2	K
Wind Speed	Wind	ms^{-1}

Variables – Derived Monthly	Variable Name	Units
Average Soil Moisture Tendency, Layer 1	DelSoilm1	$kgm^{-2}s^{-1}$
Average Soil Moisture Tendency, Layer 2	DelSoilm2	$kgm^{-2}s^{-1}$
Average Soil Moisture Tendency, Layer 3	DelSoilm3	$kgm^{-2}s^{-1}$
Average Snow Water Tendency	DelSWE	$kgm^{-2}s^{-1}$

CHAPTER III: LONG-LEAD HYDROLOGIC PREDICTABILITY IN THE MISSISSIPPI RIVER BASIN

"There is genius in persistence"
Orison Swett Marden

This chapter has been accepted for publication in Journal of Geophysical Research in its current form: Maurer, E.P and D.P. Lettenmaier, 2002, Predictability of seasonal runoff in the Mississippi River basin, *J. Geophys. Res.* (in press).

INTRODUCTION

The history of the United States, and especially its expansion westward, is inextricably tied to water. Beginning with the Homestead Act of 1862, the federal government actively promoted settlement of the arid and semi-arid west. Incentives were increased as the available lands became less fertile and more arid. The Reclamation Act of 1902 was transformed in the early 1930s into a major land and water development program, and the period of settlement that ended around 1900 was followed by a period of intense construction of increasingly large, multi-purpose water projects, which continued into the 1960s. As the better dam sites were developed and their economic feasibility came into question, and with a mounting environmental opposition, the emphasis in water policy shifted toward management of resources. (e.g. Plummer 1994; Beard, 1994; Marston, 1987) This last period, which continues today, arguably began with the Wild and Scenic Rivers Act of 1968. With population of the U.S. projected to rise by 20 percent by 2020 (U.S. Census Bureau, 2000) and the West, where water scarcity is greatest, by up to 30 percent (Western Water Policy Review Advisory Commission, 1998), water planners are being forced to look for new opportunities for better management of a resource that is now essentially fully developed. In addition, some have argued that climate change may increase water scarcity in areas of the U.S. where water supplies generally are not currently constrained (Intergovernmental Panel on Climate Change, 2001, Chap. 4; National Assessment Synthesis Team, 2001; Vörösmarty et al., 2000).

Aside from structural changes in water use (e.g., reallocation of water, such as from agriculture to municipal and industrial), perhaps the greatest potential for improving water management is through more accurate streamflow forecasting. Over the last decade, great strides have been made in two areas that offer considerable potential for improved streamflow forecasting. The first is better understanding of climate teleconnections as manifested by ocean-atmosphere phenomena such as El Niño-Southern Oscillation (ENSO), the Pacific Decadal Oscillation, and the Arctic Oscillation (AO). A second opportunity is use of remote sensing products for better initialization of the hydrologic system (e.g. Walker and Houser, 2001; Pauwels, 2001; Rango et al., 2000; Carroll, et al, 1999). These include snow cover extent, snow water equivalent, and surface skin temperature. All of these variables are observed, with various limitations, by existing sensors, the resolution and quality of which have improved with launch of Earth Observing System (EOS) Terra and Aqua platforms, and with planned soil moisture missions. (Hall et al., 2001; Ma et al., 2002; Njoku and Li, 1999; Kerr et al., 2001)

Improved knowledge of climate dynamics has resulted in demonstrable improvements in long-lead (to lead times as long as a year) climate forecasts, based on coupled ocean-atmosphere-land models (e.g., Goddard et al., 2001 and references therein). Teleconnections of climate signals, especially ENSO and also the AO, have been established for the U.S. for precipitation and temperature (Higgins et al., 2000; Livezey and Smith, 1999; Kumar and Hoerling, 1998; Gershunov, 1998; Wang et al., 1999), snowfall (Kunkel and Angel, 1999), and streamflow (Dracup and Kahya, 1994; Kahya and Dracup, 1993). Despite the presence of apparent predictability in the climate signal, and the teleconnections to land surface hydrologic variables, the incorporation of climate forecasts in forecasts of seasonal runoff (or streamflow) has thus far been largely limited to experimental settings (e.g. Wood et al, 2002; Baldwin, 2001; Garen, 1998; National Water and Climate Center, 1998). Monthly to seasonal streamflow forecasts widely used in the western U.S. more commonly rely on regression-based forecasts (Soil Conservation Service, 1988; Garen, 1992), or use hydrologic simulation models to capture the hydrologic memory, as reflected in soil moisture and snow storage, and then assume, explicitly or implicitly, climatological average conditions during the forecast period (e.g. Twedt et al., 1977). We contend that recent advances in climate prediction and remote sensing provide the capability to improve long-lead streamflow forecasts by utilizing climate forecasts, and by incorporating better

estimates of the state of the land surface at the time of forecast, a contention that we evaluate for the domain of the Mississippi River basin in the remainder of this chapter.

Hornberger et al. (2001), in their assessment of global water cycle research necessary to address critical water problems facing society, identified as one of their three key science questions the predictability of variations in the global and regional water cycle. The National Research Council (2002a) built on that assessment and raised the questions of whether accurate observation of initial land surface conditions increases hydrometeorological predictability, and when and where this predictability is likely to be most important. In this study, we address these questions by taking advantage of a recently developed hydrologically-based land surface data set (Maurer et al., 2002) to characterize hydrological predictability due to climatic persistence and persistence related to the initial state of the land surface. We focus on distributed runoff (e.g., spatial fields of runoff) rather than the space-time convolution of runoff (streamflow), in order to identify regional patterns and influences in runoff predictability. The primary questions we address are: 1) during which seasons is the predictability of runoff greatest? 2) how does the contribution of initial hydrologic conditions relative to climate predictability vary geographically? 3) where are potential improvements in seasonal runoff forecast accuracy due to improved observations (e.g. through remote sensing or in situ observations) of the land surface moisture state the greatest? We focus our attention on the Mississippi River basin (Figure 3.1), which coincides with the study area of the World Climate Research Programme's Global Energy and Water Cycle Experiment (GEWEX) Continental-scale International Project (GCIP), a project established with the long term goal of demonstrating skill in predicting changes in water resources on time scales up to seasonal, annual and interannual (World Meteorological Organization, 1992).

METHODS AND DATA

The gridded data set of land surface and climatic variables of Maurer et al. (2002) is used to determine the predictability of runoff throughout the Mississippi River basin from currently available, or potentially available information. Details of the data derivation and validation can be obtained in Maurer et al. (2002). To summarize briefly, the runoff data were produced using the

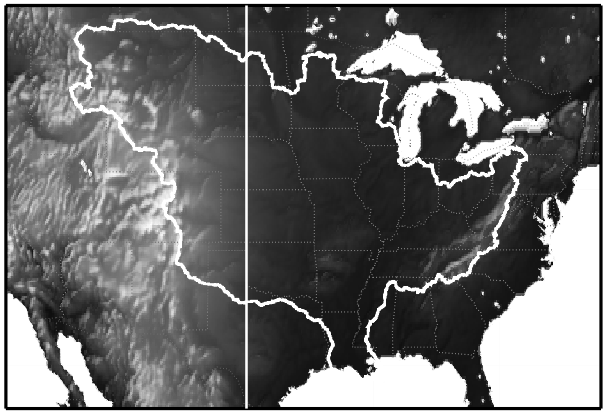

Figure 3.1 - Location of the Mississippi River basin in North America. The basin boundary is shown in white, as is a north-south line at longitude 100 west.

Variable Infiltration Capacity (VIC) hydrologic model driven by observed precipitation and temperature, and other derived surface radiative and meteorological forcings (see Liang et al., 1994, and Cherkauer et al., 2002 for details of the model structure). The model was run at a 3-hour time step for the period January 1950-July 2000, with a grid cell size of 1/8 degree (approximately 140 km^2 per grid cell). Throughout this paper, predictability is assessed for seasonal average runoff on a grid cell by grid cell basis for a range of lead times for hydrologic and climatic initial conditions extracted from the Maurer et al (2002) data set, as shown in Figure 3.2. Following the convention of Barnston (1994), the lead time is the number of seasons "skipped" between the predictor(s) and the predictand, so a lead-0 indicates a lead time of 1.5 months from the initialization to the mid-point of the predicted season. Seasons are defined as December-February (DJF), March-May (MAM), June-August (JJA), and September-November (SON). The date on which initial conditions are determined, i.e., the initialization date or date of forecast, is shown with vertical lines in Figure 3.2 for the example of predicting DJF runoff. Because we use climate and land surface variables on the initialization date to predict runoff in a future season, we do not include any runoff forecast skill obtainable through predictability of the evolution of these variables. For the case of climate initial conditions, this is discussed in more detail below.

Climate indicators (represented in this study by the Southern Oscillation Index, SOI and the Arctic Oscillation, AO, Index) and land surface state (snow water equivalent, SWE, and soil moisture, SM) influence seasonal runoff as indicated in Figure 3.3, which shows schematically

the effect of unpredictable weather noise in the climate system. Note that we ignore the possibility of an additional noise component between the soil moisture and snow states and runoff in this study. Because the runoff and land surface states in the Maurer et al (2002) data set are derived from the same model simulation, the only direct effect of noise on runoff in the data set is though the unpredictable weather component that drives the hydrologic model.

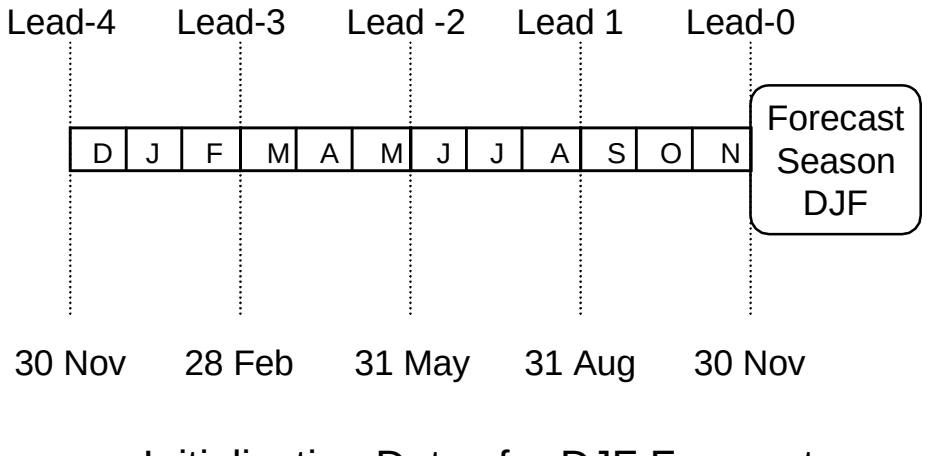

Figure 3.2 - Example of initialization dates for forecasting the DJF runoff at lead times of 0 through 4 seasons.

For this study, we consider only the initial conditions of the climate indicators and land surface moisture state as predictors of future runoff, so the process illustrated in Figure 3.3 is "one-way," in that no feedback from the initial land surface moisture state to climate evolution is included. Initial soil moisture, varying between extreme wet and dry initial states, has been shown to greatly change 30-day forecasts of precipitation averaged over regional to continental areas (Beljaars et al., 1996; Betts et al, 1996a), though the effects of initial soil moisture anomalies representative of typical interannual variability have been shown to have little impact on the evolving atmosphere (Oglesby et al., 2002). Because we include initial soil moisture explicitly as a predictor, any predictability due to feedback to the atmosphere, at least that which can be captured by the linear relationships used in this study, is attributed to knowledge of the initial moisture state rather than knowledge of climate evolution due to initial land surface state.

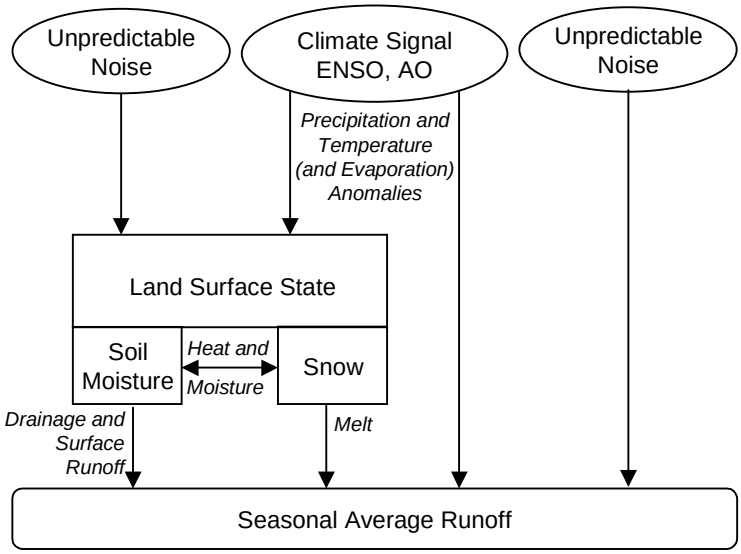

Figure 3.3 - Schematic of the predictable and unpredictable influences on seasonal runoff considered in this study. Note that for this study the interactions are one-way; feedback from the land surface to climate is not considered -- only the initial conditions of the climate indicators are included.

Evaluation of Predictability

To assess the predictability of seasonal average runoff, we used multiple linear regression, using as predictors various combinations of the SOI, AO, SM, and SWE at different lead times. The regressions were performed on a grid cell by grid cell basis across the domain. The multiple regression equations developed for the combinations of variables are not used as predictive models; only the variance explained by the regression is used. The values of the variance explained by the predictors, r^2 (where r is the correlation coefficient of the regression) were plotted spatially at the different lead times to illustrate their predictive capability of seasonal runoff by season and by lead time. The predictor variables are assigned to three tiers, where the climate indicators that are currently available for incorporation into forecasts, are assumed to be the best known variables, and SWE, which in practice is estimated by ground surveys and remote sensing, is less known, and SM is essentially unobserved, and hence is least well known. The variances explained by each tier are the incremental amounts over and above that already explained by better known variables. In this way, variances explained by two correlated variables are only counted once, and are attributed to the better known variable.

To test for significant correlations, the two step process outlined by Livezey and Chen (1983) was used. First, temporal autocorrelation was taken into account, and the effective number of temporal degrees of freedom was determined. As applied in this study, the time between independent samples was computed for each grid cell for each combination of predictors as (Livezey and Chen, 1983):

$$\tau_P = \left[1 + 2\sum_{i=1}^{N} C_P(i\Delta t) C_R(i\Delta t)\right]\Delta t \quad (1)$$

where C_P is the autocorrelation function for the selected combination of predictors (separated by season, e.g.. a 50 year sequence of DJF values of SOI), C_R is the autocorrelation function of the seasonal runoff, i is the sample number of N total samples, and Δt is the sampling time (one season for this study), so $i\Delta t$ represents a lag of i seasons. The effective number of degrees of freedom, n, was then determined by (Livezey and Chen, 1983):

$$n = \frac{N\Delta t}{\tau_P} \quad (2)$$

At each grid cell the computed value of the correlation coefficient r was compared against the 95% significance criterion for no correlation, which provided a determination of local significance.

The total amount of significant area was determined by counting the number of grid cells exhibiting locally significant correlation, with each grid cell weighted by the cosine of latitude to avoid biasing due to differences in grid cell area. If there were no spatial correlation and each grid cell (there are 1532 ½-degree grid cells in the Mississippi River basin) were an independent sample, we would expect 5% of the grid cells (77) to show significant correlation by chance 6% of the time, based on the binomial distribution. At lead times and seasons where greater than 6% of the area showed local significance, statistical field significance at the 95% confidence level would be claimed. Because there is spatial correlation between grid cells in the runoff fields (as well as in SM and snow fields), the actual number of spatial degrees of freedom is considerably less than 1532. As a first estimate, the number of empirical orthogonal functions needed to describe 95 percent of the variance in seasonal runoff varies from 35 in DJF to 39 in JJA, which

translates to 15.2-15.8% of the area that would show local significance by chance. As a practical matter, this suggests a need to use a Monte Carlo technique to assess spatial field significance.

Monte Carlo simulations were performed in a manner similar to that of Barnston (1994), in which the forecast to observation year correspondence was randomly shuffled over the entire domain, and the fractional area of the basin exhibiting significant correlation at a 95% level based on a t-test was computed. The process was repeated 500 times for each lead time, season, and set of predictors. For each season and lead time the area determined as significant by this Monte Carlo technique is the minimum for a result to achieve statistical field significance. Table 3.1 shows the results of these Monte Carlo simulations, and the minimum area with significant correlations for field significance. It should be noted that field significance is a basin-wide test in this study. If a particular (*a priori*) interest were exclusively in one sub-area of the basin, then local significance would still be pertinent, though basin-wide field significance of this may not. A separate set of Monte Carlo experiments for only the area of interest could be used to determine the area required for field significance of a sub-area.

Table 3.1 - Fractional area thresholds (expressed as percentages of entire Mississippi River basin area exhibiting local significance) that must be exceeded to achieve statistical field significance at a 95% confidence level.

	DJF					**MAM**				
	Lead					Lead				
Predictors	0	1	2	3	4	0	1	2	3	4
ALL	54	42	44	54	58	53	52	40	43	53
SOI AO	29	28	27	28	27	24	24	26	25	26
SWE	10	8	8	10	10	9	9	8	8	9
SM	10	8	8	9	9	9	8	8	8	9
	JJA					**SON**				
ALL	40	50	51	40	40	41	41	53	54	40
SOI AO	25	29	28	27	28	27	24	24	26	25
SWE	8	10	11	8	9	8	8	9	10	8
SM	8	10	8	8	9	9	9	8	8	8

Climate Signals

Given the established teleconnections of climate signals with hydrologic variables over the U.S. (see references above), our objective was to characterize the seasonal predictability of runoff, and the dominant sources of predictability. At seasonal to interannual scales, the El Nino/Southern Oscillation (ENSO) is the best known and most prominent predictable climate signal (Rasmussen and Wallace, 1983). One index used to quantify the phase of the ENSO signal is the SOI, which is based on the surface pressure difference across the South Pacific (Tahiti minus Darwin). The SOI has been related to various land surface effects in the continental U.S., including seasonal temperatures (Wolter, et al., 1999), precipitation (McCabe and Dettinger, 1999), and streamflow (Cayan et al., 1999). Because of this past use of the SOI in teleconnection studies we decided to use it in this study as well, and we obtained the monthly standardized difference index from the National Oceanic and Atmospheric Administration, National Centers for Environmental Prediction Climate Prediction Center (http://www.cpc.ncep.noaa.gov/data/indices/). Trenberth (1997) recommends smoothing of the monthly SOI index to remove the effect of high frequency, small scale phenomena. As in Ropelewski and Jones (1987), we applied a five-month moving average to the monthly SOI time series. Although the effect of this smoothing is to include some future information of SOI state in the value for the current month, we argue that that the smoothing, by removing high frequency fluctuations, makes the SOI more comparable to the more slowly-varying sea surface temperature (SST)-based ENSO indicators. For example, the unsmoothed SOI has a correlation with the SST index Niño 3.4, for the period 1950-1999 of –0.72, while 5-month smoothing of SOI produces a stronger correlation of –0.87. The smoothing therefore results in SOI values that more closely resemble the SST-based index that would be available at the time of forecast. These values can be used as an indicator of climate state that would be known at the initialization time, with the results of the predictability analysis being more robust, irrespective of the ENSO index chosen.

Shukla (1998) suggested that the evolution of ENSO events appears to be predictable 6 to 9 months in advance, and that SOI-based persistence forecasts may underestimate the predictability of sea surface temperature anomalies. Barnston et al. (1999) subsequently showed that both coupled GCMs and statistical models outperform simple persistence in forecasts of ENSO state at lead times of 3.5 to 9.5 months. Landsea and Knaff (2000) argued that a more reasonable baseline

of ENSO predictability than simple persistence is a simple statistical model such as the ENSO climatology and persistence (ENSO-CLIPER) model (Knaff and Landsea, 1997). Landsea and Knaff (2000) show that this simple regression-based model outperformed coupled GCMs and more complex statistical models for predicting the 1997-1998 El Niño event for lead times through two seasons, though for 3 and 4 season forecast lead times a modest improvement was achieved using a more sophisticated statistical model. The factors influencing the characteristics of an El Niño event, and ultimately its predictability, differ for each event (Philander, 1999; Fedorov, 2002). This implies that the predictability of an El Niño event achieved by any particular model will vary with each event, hence the relative skill attributed to coupled GCMs, statistical or persistence forecasts will change accordingly. Although the ENSO-CLIPER model will not outperform GCM forecasts for all historical El Niño events, we use the ENSO-CLIPER model to generate forecasts of SOI to estimate of the potential difference in runoff predictability between simple persistence and forecasted ENSO state.

Barnston et al. (1999) note that success in forecasting sea surface temperatures does not necessarily imply comparable success in forecasting impacts in teleconnected regions such as the continental U.S. The process of translating a predicted sea surface temperature anomaly into a remote land surface response introduces additional unpredictable noise, so that a marginal increase in prediction of ENSO will not necessarily result in measurable increase in predictability of the land surface effects associated with ENSO. In particular, the selection of an ENSO indicator used in persistence mode, or with a model to predict its evolution, may not result in substantially different land surface predictability.

To test whether, for predictions of seasonal runoff, there is any change in apparent potential skill between using the simple persistence of initial SOI relative to SOI forecasted by a statistical model, the ENSO-CLIPER model was obtained (from http://www.aoml.noaa.gov/hrd/Landsea/ensocliper/). It was run from 1951 (the earliest year for which required input data are available) through July 2000, with the climatological SOI values added for 1950 to make the record consistent with the period of record for the land surface variables included in this study. The SOI used for testing the simple persistence model was the smoothed SOI index discussed above.

a)

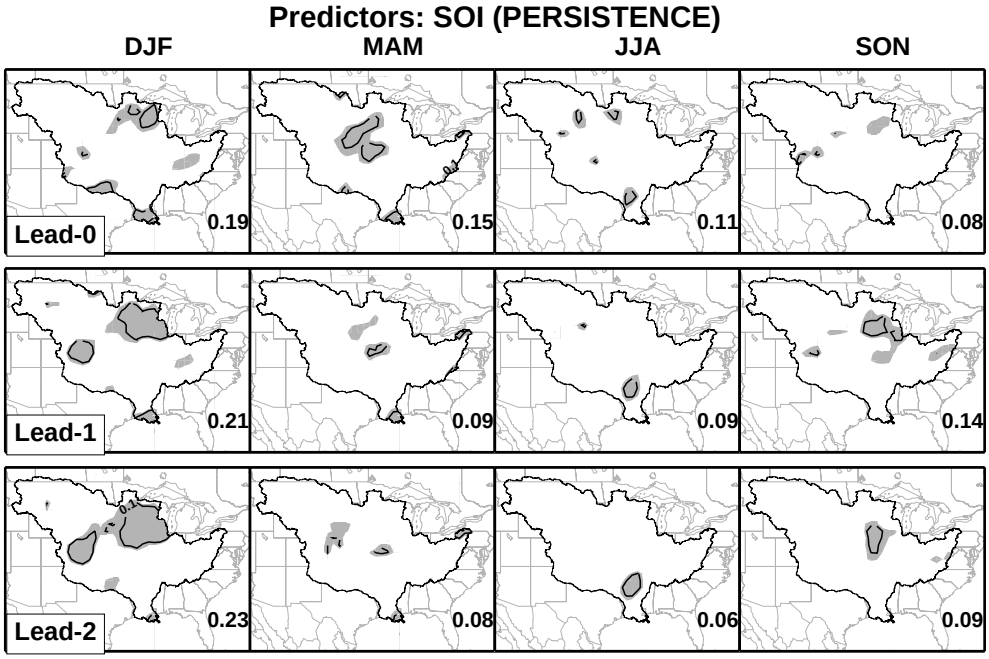

b)

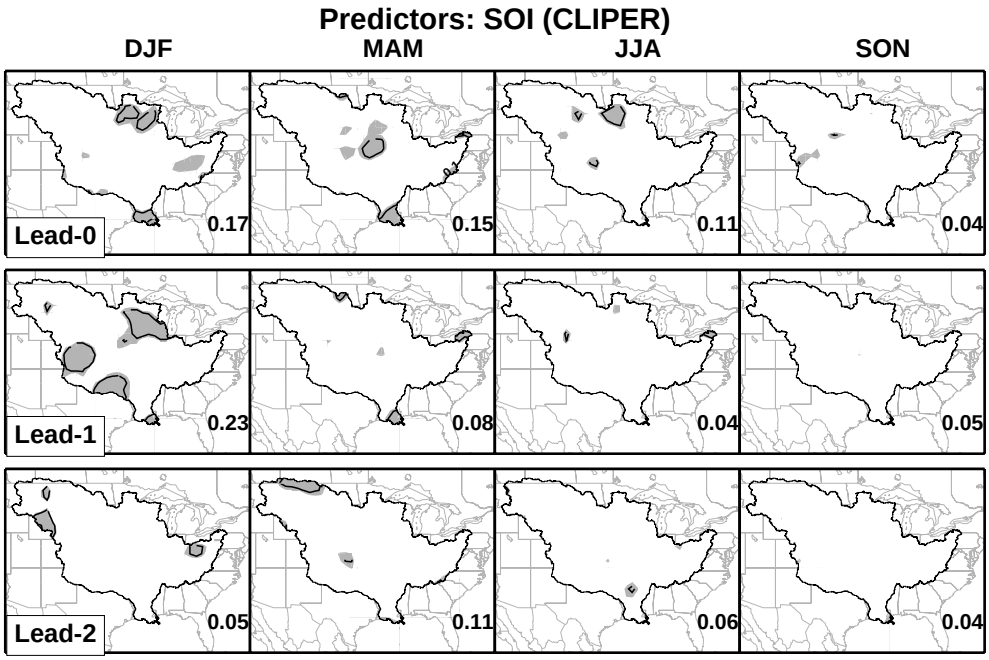

Figure 3.4 - Predictability of seasonal runoff due to SOI, expressed as the fractional variance, r^2, of seasonal runoff explained by SOI , using a) a simple persistence model, and b) the ENSO-CLIPER model. Countour intervals of r^2 values are every 0.1, and shading indicates locations where the r^2 is statistically significant. In the lower right corner of each panel is the fraction of the total basin area with significant correlation.

Seasonal average runoff values at each grid cell were regressed against the smoothed SOI values in a persistence mode – that is, against the SOI value for the appropriate initialization date for each season and lead times of 0, 1, and 2 seasons. Spatial plots of the variance explained by this SOI initialization (persistence mode) are shown in Figure 3.4a. For comparison, the seasonal runoff at each grid cell was also regressed against the ENSO-CLIPER forecasted SOI values. First, the ENSO-CLIPER model was initialized on the appropriate initialization date, after which seasonal average values of SOI were forecasted for each lead time. These forecasted SOI values were regressed against the seasonal average runoff for the same season. The runoff variance explained using ENSO-CLIPER forecasted SOI values is plotted in Figure 3.4b. The patterns exhibited in these two figures are in general very similar. This suggests that, although ENSO-CLIPER shows better sea surface temperature forecast skill (as measured by root mean square error, RMSE) than simple persistence (at least for the event studied by Landsea and Knaff, 2000), consistent with the discussion above, the marginal increase of ENSO predictability does not translate to a measurable increase in land surface predictability. We conclude that the use of the SOI forecasts produced by the ENSO-CLIPER model has a negligible effect on the skill of seasonal runoff predictability in the Mississippi River basin as compared to using SOI values in a persistence mode. Furthermore, because the RMSE of ENSO-CLIPER is shown by Landsea and Knaff (2000) to be 49-66% lower than the simple persistence model for leads of 0-2 seasons, with no measurable benefit for runoff forecasting, the additional improvement (reflected by a further RMSE reduction by 18-24%) of more sophisticated statistical models compared to ENSO-CLIPER at leads of 3-4 seasons would not be expected to provide additional predictability of seasonal runoff over the persistence model. We conclude, therefore, that for our purposes, treating SOI in a persistence manner (that is, discarding knowledge of the climatological evolution of ENSO events), produces results that are comparable to those achieved by using a more sophisticated statistical model.

Recent studies show that additional predictability of air temperature and precipitation, particularly in winter, can be obtained over portions of the U.S. by incorporating the modes of the AO, which encompasses the North Atlantic Oscillation (e.g. Higgins et al., 2000; Rohli et al., 1999; Lin and Derome, 1998). Operational seasonal climate predictions for the United States currently are capable of exploiting strong ENSO signals to improve forecast skill. It has been argued (Baldwin and Dunkerton, 2001; Higgins et al., 2000) that future forecast improvements will require the

ability to predict subtler changes in ENSO conditions, as well as the AO. For this reason, we use two indices to represent the predictability of seasonal runoff due to climate signals: the 5-month smoothed SOI index and the AO. Values of SOI for the initialization day were interpolated by averaging the two adjacent monthly values of the filtered SOI. To characterize the mode of the AO, an AO index was obtained (from http://www.atmos.colostate.edu/ao/Data/ao_index.html -- see Thompson and Wallace, 1998; 2000 for details). The AO index for the initialization day (date of forecast) was interpolated from adjacent monthly values, as for the SOI.

Snow

In areas where a substantial fraction of precipitation falls as snow, water stored in the snowpack can be released months later, providing a source of persistence that can be exploited in seasonal streamflow forecasting. In the U.S., seasonal streamflow forecasts have been based on estimates of the amount of water stored in the snowpack since at least 1900 (Church, 1937). Individual snow surveys (which, in automated form, remain at the heart of the streamflow forecasts produced by the National Resources Conservation Service (Soil Conservation Service, 1988) are (or were, prior to automated data collection) time consuming and cover relatively small areas. The need for a better spatial context for estimates of the snow state inspired early attempts to use panoramic photographs for forecasting runoff from snow melt (Potts, 1937). Because photographs provide a basis for estimating snow covered area (SCA) rather than the water equivalent of the snowpack, approaches based on SCA necessitated the development of methods to deduce snow water content from spatial coverage. In the satellite era, remotely sensed products have provided estimates of SCA, which have shown to be have value for runoff forecasting (e.g., Rango and Martinec, 1979). Although methods have been developed for direct estimation of the water content of the snowpack (or SWE) via remote sensing (e.g. Goodison and Walker, 1994; Shi and Dozier, 2000), and new sensors such as the Advanced Microwave Scanning Radiometer (launched in May 2002 on NASA's Aqua platform) hold promise for future SWE measurements, these methods have not been available operationally (Rango *et al.*, 2000), and cannot provide the length of record needed for this study of the variability of SWE in the context of runoff predictability.

Therefore, for assessing potential predictability due to knowledge of initial snow water storage, we use the derived snow water equivalent product in the Maurer et al (2002) data set. The snow

water equivalent used for prediction is the value for the last (3-hour) time step of the last day of the month prior to the beginning of the forecast season. We believe that this is a reasonable surrogate for the initial snow water equivalent condition that would be available at the forecast time, and therefore represents the maximum level of predictability obtainable through error-free observations of the water equivalent of the snowpack.

In order to avoid spurious correlations due to poorly conditioned probability distributions of SWE in areas that usually are snow-free, we apply a threshold to the SWE data at each grid cell. During the entire period of 51 years, we require for each season that during at least 10 of the years a minimum of 0.1 mm of SWE must be on the ground in order for SWE to be included as a candidate predictor.

Soil Moisture

In addition to the water stored as snow, the water stored in the soil column exhibits seasonal and interannual persistence that can be exploited in seasonal forecasts. It has been well known from the early days of hydrologic prediction that SM plays a key role in predicting the effect of a given precipitation pattern on the resulting runoff response of a watershed (e.g. Linsley and Ackerman, 1942). Despite its importance to hydrologic modeling and runoff forecasting, SM lacks a good observational database (Dirmeyer, 1995).

Given the expense and difficulty of collecting SM measurements, alternative techniques are being implemented that offer promise for better determination of SM state, and hence better definition of initial conditions for forecasting seasonal water supply. Two recent advances that offer the potential to provide more accurate estimates of SM conditions for runoff prediction are macroscale hydrologic modeling and remote sensing. The North American Land Data Assimilation (LDAS) experiment (Mitchell, et al, 1999) simulates SM fields in real-time over the continental U.S. using observations of precipitation and temperature to drive a suite of several land surface models. Shortcomings of SM estimates produced using this technique include errors in forcing data due to the inhomogeneity and low station density of near-real-time meteorological observing stations (Groisman and Legates, 1994), and the effects of model and parameter errors on the generated SM fields (Schaake et al., 2002).

The most promising method for estimating soil moisture via remote sensing is based on remote sensing using passive microwave instruments operating at long (in excess of 10 cm) wavelengths. A key technological constraint that has precluded spaceborne remote sensing of soil moisture to date is the tradeoff between the need for long wavelengths to penetrate soil to sufficient depths (which in any event are limited to a few cm) and to avoid obscuring the signal with vegetation water, and the requirement for large antennas to achieve adequate spatial resolution consistent with hydrological and atmospheric models (e.g., 10-25 km) at long wavelengths. The advanced scanning microwave radiometer (AMSR) instrument on board the EOS Aqua platform (launched May 4, 2002) has a 4.3 cm wavelength for one of its channels, which although not ideal for soil moisture sensing, provides some capabilities in regions of sparse vegetation cover. The current observations of SM, sparser and less consistent than observations of SWE, do not cover a time period or have a spatial resolution adequate for the investigation in this study.

Therefore, for this study we used an index of SM, specifically the total moisture in the soil column on the forecast initialization date from the derived data set of Maurer et al. (2002). Notwithstanding the inability at present to observe SM directly, the Maurer et al. (2002) data set can be considered to be a surrogate for the best information that may eventually be available through a combination of remote sensing and modeling. As such, it can be considered to provide an upper limit on the information content that would be available from high quality observations, and its use is consistent with our attempts to estimate potential runoff predictability.

Runoff Data

The runoff data used in this study were the derived product archived by Maurer et al. (2002). For this study we aggregated the 3-hourly runoff values to monthly and seasonal averages. Furthermore, we aggregated spatially from the 1/8 degree native spatial resolution of the data set to ½ degree spatial resolution, in order to reduce array sizes and produce a more computationally tractable data set. As shown by Maurer et al. (2002) the runoff, when routed through a channel network to basin outlet points, closely matches observed streamflows throughout the basin.

RESULTS AND DISCUSSION

Seasonal runoff magnitude

The magnitude of runoff in the Mississippi River basin varies considerably across the domain and throughout the year. Figure 3.5 shows the seasonal runoff, expressed as the average runoff at each grid cell divided by the basin-wide average runoff for each season. For example, most of the DJF runoff is produced in the southeastern part of the basin, and the highest JJA runoff is produced along the western edge of the basin, in the Rocky Mountains. Seasonal predictability is generally of greatest value where a) runoff volumes are high, as it indicates potential for forecast skill that could affect a relatively large part of the annual runoff, and/or b) in locations where infrastructure (such as large reservoirs) exists to allow water managers to respond to long lead forecast information.

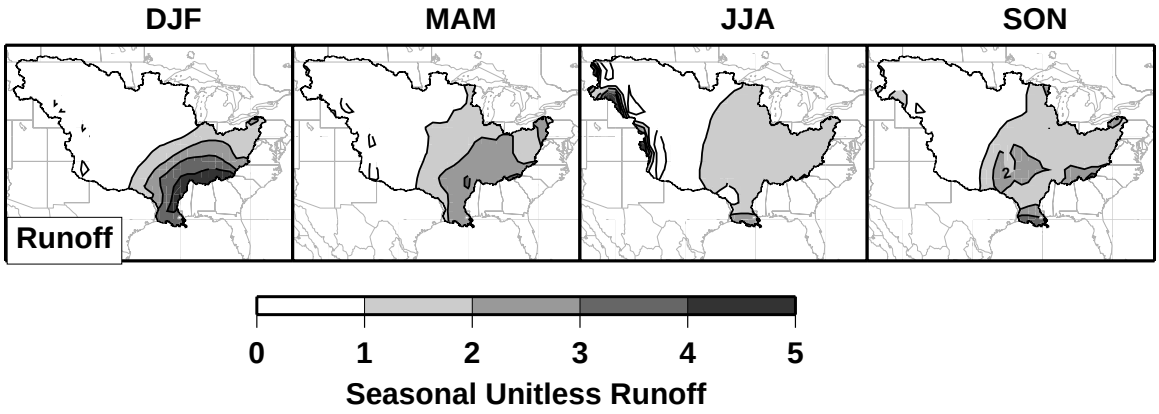

Figure 3.5 - Average seasonal runoff for the Mississippi River basin, divided by the seasonal basin-wide average.

Total runoff predictability

Figure 3.6 shows the total variance of seasonal runoff explained by the climatic and land surface predictors together. The shading highlights areas with locally statistically significant correlation. Shown on each plot are the fractions of the basin with significant local correlation, which were compared with the threshold values in Table 3.1 to test for field significance. Statistical field significance exists in DJF for leads up to and including 3 seasons, while MAM and SON runoff predictability shows field significance at leads through one season. The JJA season shows field significance through a lead of 1 season and also at a lead of 4 seasons.

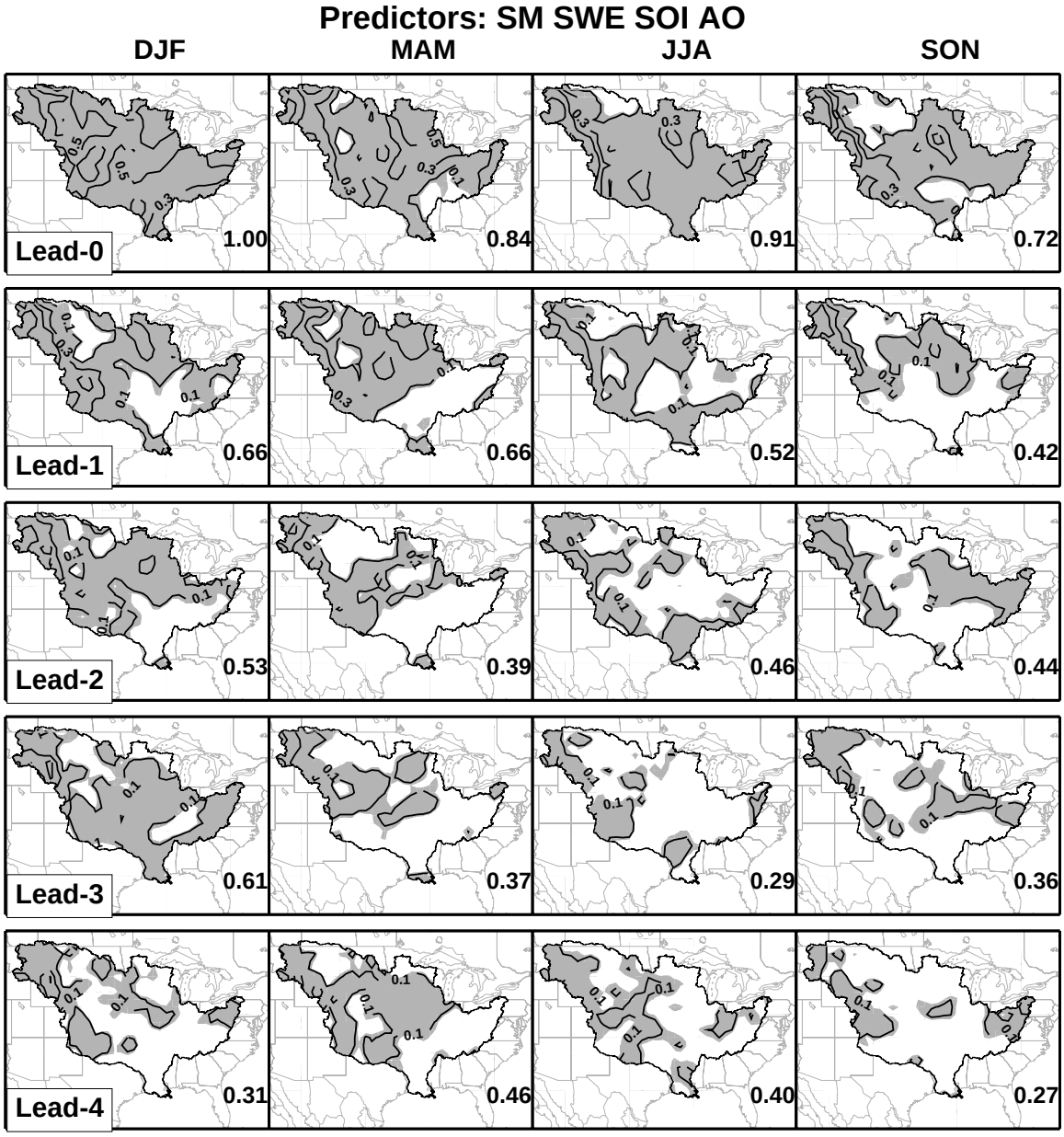

Figure 3.6 - Predictability of seasonal runoff for each season (columns) and each lead time (rows), using combined climatic and land surface predictors, SOI, AO, SM, and SWE. Predictability is defined as the fractional runoff variance explained by the predictors, r^2, in a multiple linear regression. Contour interval is 0.1, with locally significant r^2 values shaded. The number in the lower right corner of each panel indicates the fraction of the basin exhibiting local statistical significance; this number is used in comparison with the field significance thresholds in Table 3.1.

For DJF runoff predictability, a very large percentage (up to 70%) of the runoff variance at lead-0 is explained in the northern and western areas of the basin, while Figure 3.5 shows the greatest runoff occurs in the south and east. These very high levels of predictability in the western mountains are due to three combined effects: 1) precipitation is low during this season and snowmelt is limited, so direct surface runoff is low; 2) the runoff leaving each grid cell is drained from the lower soil layers, and 3) in the VIC model used to produce the data in Maurer et al. (2002), the rate of soil moisture drainage is controlled by the moisture level in the lowest soil layer. During MAM at lead-0, the variance explained by the predictors drops to 30-50% through most of the northern and western portions of the basin, with the lowest values tending to occur where runoff is highest. The JJA runoff variance explained by the predictors is more uniform throughout the basin, with a concentration of higher values along the mountainous western extreme of the basin, which coincides with the highest runoff values in Figure 3.5. JJA runoff predictability in this region is of particular importance, because it provides the water supply used to fill large reservoirs throughout the western part of the basin. It is this predictability that is exploited by streamflow forecasters in the west to anticipate available water supply. Typically this forecasting of MAM and JJA runoff begins in January. This figure shows that, using climatic indicators and knowledge of the land surface moisture state some measure of locally significant runoff predictability exists for the mountainous western area of the basin for lead times of 4 seasons, which would be a valuable extension of the current forecasts. By partitioning this predictability we will examine the sources of this total predictability during different seasons and at different lead times.

Runoff predictability due to climate

Figure 3.7 shows the runoff variance explained by the climatic predictors. Because these predictors (SOI and AO indices) are both available in near real-time, this represents a source of runoff predictability that is realistically achievable (discounting the effect of the 5-month smoothing of SOI). Applying the threshold values from Table 3.1, statistical field significance can be claimed for DJF at a lead of 0 seasons, and also at leads of 2 and 3 seasons. Runoff in MAM and JJA shows field significance through a 0 season lead, and SON shows no field significance for any leads.

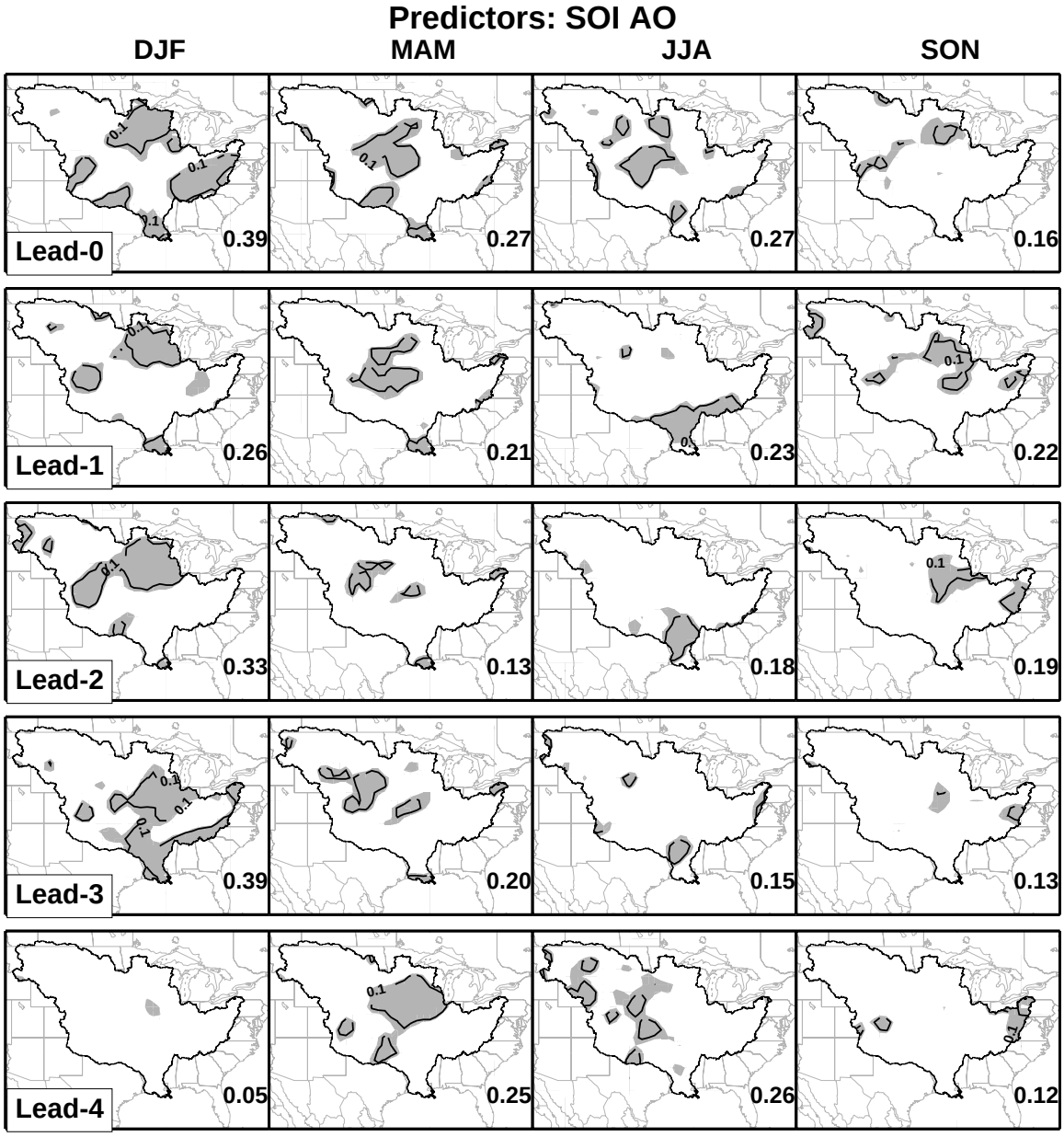

Figure 3.7 - Same as for Figure 3.6, but including only climatic indicators, SOI and AO as predictors.

This is consistent with the observation that ENSO (e.g. Kumar and Hoerling 1998) and AO (e.g. Higgins et al., 2000) signals typically exhibit their strongest signals in boreal winter. Although the runoff variance explained for DJF at a lead of three seasons is generally low (about 10%) its field significance and its overlap, at least partially, with areas of high runoff (Figure 3.5) suggest

that these climate indicators may be capable of providing valuable predictive information for runoff in the Mississippi River basin at leads of greater than 9 months. For the mountainous extreme western portion of the basin, even with relatively small areas showing significant amounts of JJA runoff variance explained at leads of two and three seasons, the relatively high runoff produced by these areas (Figure 3.5) during JJA implies a potential local benefit for including climatic indicators at these leads, despite the lack of field significance at a basin-wide level.

For DJF runoff, the coincidence of areas with high runoff with modest, but statistically significant, runoff predictability at long indicates that for prediction of DJF runoff, climatic indicators may be the most important source of long-lead predictability. This also illustrates a complication in using persistence of climate signals for prediction, as is done in this study. Specifically, noting the significant runoff predictability in the southeastern (Gulf) region of the basin at a lead of 3 seasons, this predictability vanishes at shorter leads of 1 and 2 seasons. Dracup and Kahya (1994) discuss one potential explanation for this phenomenon (in their case, it apparently occurs because observations of the La Niña phase of the ENSO cycle during winter and spring in the Gulf region of the United States are typically followed by anomalously wet conditions the next year). Although the results shown in Figure 3.7 include the effects of both ENSO and AO, this highlights the point that the predictability due to climate is not necessarily due to persistence of the climate signals, but may reflect a regionally specific response to climatic forcing. It should also be stressed that this analysis is based on a 50 year record, and individual events in each season may have differing sources and levels of predictability that do not match this general climatological predictability indicator.

Runoff predictability due to snow state

The climatic indicators we use as predictors are based on direct and readily available observations, whereas the soil and snow moisture states are based on perfect knowledge of the land surface moisture state. Because both SM and SWE are driven by the same climatic factors, and by their nature interact with one another, they can be highly correlated. Figure 3.8 shows the correlation coefficient between SWE and SM for each season. Not surprisingly, the two tend to be correlated most strongly in areas undergoing episodes of snow melt, thus MAM shows high

correlations over the northern and western areas, while the mountainous areas along the extreme west show very high correlation in JJA.

Due to the longer history of remote sensing of snow and the wider array of ground observations as compared to SM, for comparative purposes we first examine the portion of the runoff predictability due to land surface moisture that is attributable to knowledge of SWE. To do so, we subtract from the runoff variance explained by SOI, AO and SWE that explained by SOI and AO. In this way, runoff predictability due to SWE represents the incremental increase, above that due to climatic state, in explained runoff variance due to the knowledge of SWE alone. This is shown in Figure 3.9.

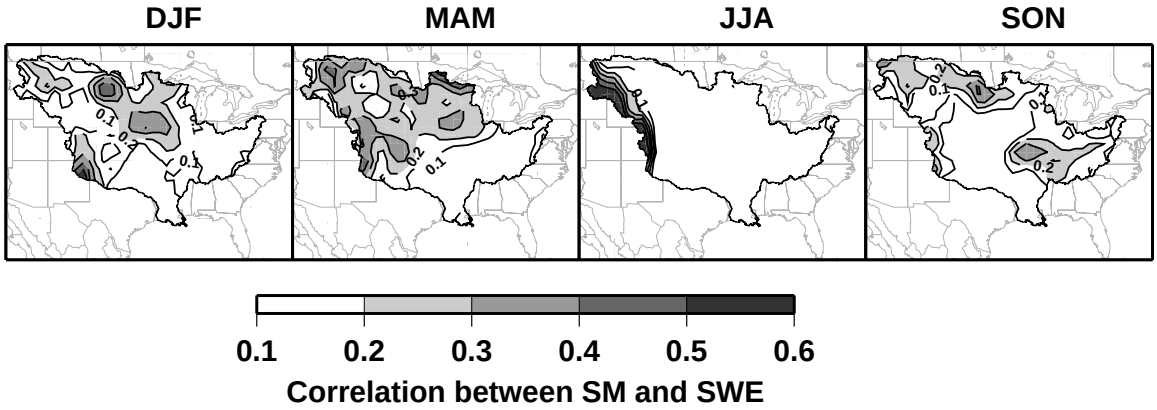

Figure 3.8 - For each season, the correlation coefficient between the seasonal average SM and seasonal average SWE.

As would be expected, SWE explains seasonal runoff variance most strongly where snow existing on the initialization date melts and forms runoff during the season being predicted. This can be seen most clearly at lead 0 in the northwestern portion of the basin. During DJF (at lead 0, using November 30 predictors) the correlations are strongest in the northwestern portion of the basin, while for MAM (February 28 predictors) the area of high correlation retreats toward the mountains and the northern central area, and during JJA (May 31 predictors) strong correlation is seen only in the Rocky mountains on the western boundary of the basin. Referring to Figure 3.5, the predictability due to SWE coincides closely with the areas of highest runoff production, which illustrates the importance of snow, and its current operational use, in forecasting late spring and summer streamflow in the rivers originating in the western Mississippi River basin.

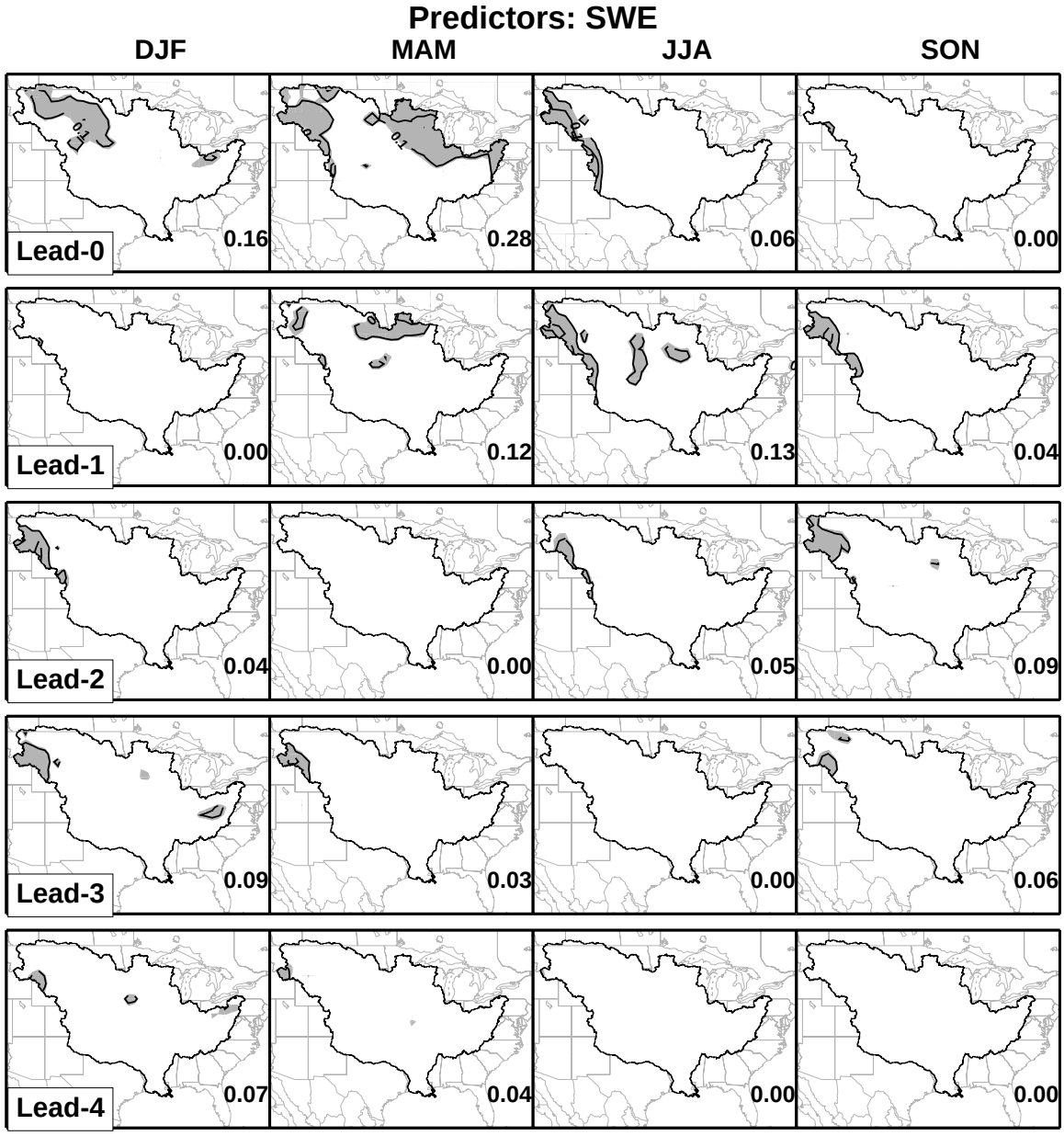

Figure 3.9 - As for Figure 3.6, but showing the predictability due to SWE alone.

At longer leads of two to three seasons, locally significant runoff predictability exists almost exclusively in isolated areas along the western boundary of the basin, which is again an anticipated result, as the snowpack disappears over virtually the entire basin each year, and deeper snowpacks that are capable of persisting longer than three seasons exist only in the highest mountains. JJA, which is the season with high runoff rates from the mountainous western areas of

the basin, shows areas with locally significant runoff variance explained at a lead of two seasons, that is, JJA runoff is partially predictable from SWE information on November 30. Although at the scale of the entire Mississippi basin this spatially limited response does not exhibit field significance, regional analyses could reveal useful predictability at a lead of two seasons. The current operational use of the snow state in spring-summer streamflow forecasts begins on January 1; however these results suggest that skillful forecasts could possibly begin at least one month earlier.

Runoff predictability due to soil moisture state

The predictability due to SM was computed using the combined variance explained by the climatic and land surface predictors, and subtracting the variance explained by the combination of SOI, AO and SWE, and is shown in Figure 3.10. By estimating the predictability of runoff due to SM in this way, Figure 3.10 displays the increase in predictability due to SM knowledge beyond that already explained by climate signals and the SWE. Field significance in Figure 3.10 can be claimed through a 4 season lead for DJF runoff prediction, and through 3 seasons for MAM and JJA runoff.

The most prominent feature in Figure 3.10 is the larger area of the basin, as compared to climate predictors (Figure 3.7) or SWE (Figure 3.9) that shows statistically significant runoff variance explained for all seasons at lead 0. Although SM explains considerably greater DJF runoff variance than SWE at leads of one to two seasons for the western regions, this area produces relatively little runoff during this period so the value of the added predictability is lessened. During the intense JJA runoff from the mountainous west, SM provides a small but significant increase in explained runoff variance in pockets of the mountainous western boundary in addition to that achievable due to knowledge of snow state, indicating that despite the high correlation of SWE and SM in this area, significant independent information is obtained from each source. The areas showing the greatest JJA runoff (Figure 3.5), however, are still more highly correlated with SWE (Figure 3.9) than with SM (Figure 3.10).

In general, for the western boundary of the Mississippi River basin, SM shows greater persistence than SWE, as indicated by higher levels of significant runoff variance explained at longer lead times. For example, SWE provides very little predictability of JJA runoff at a lead of three

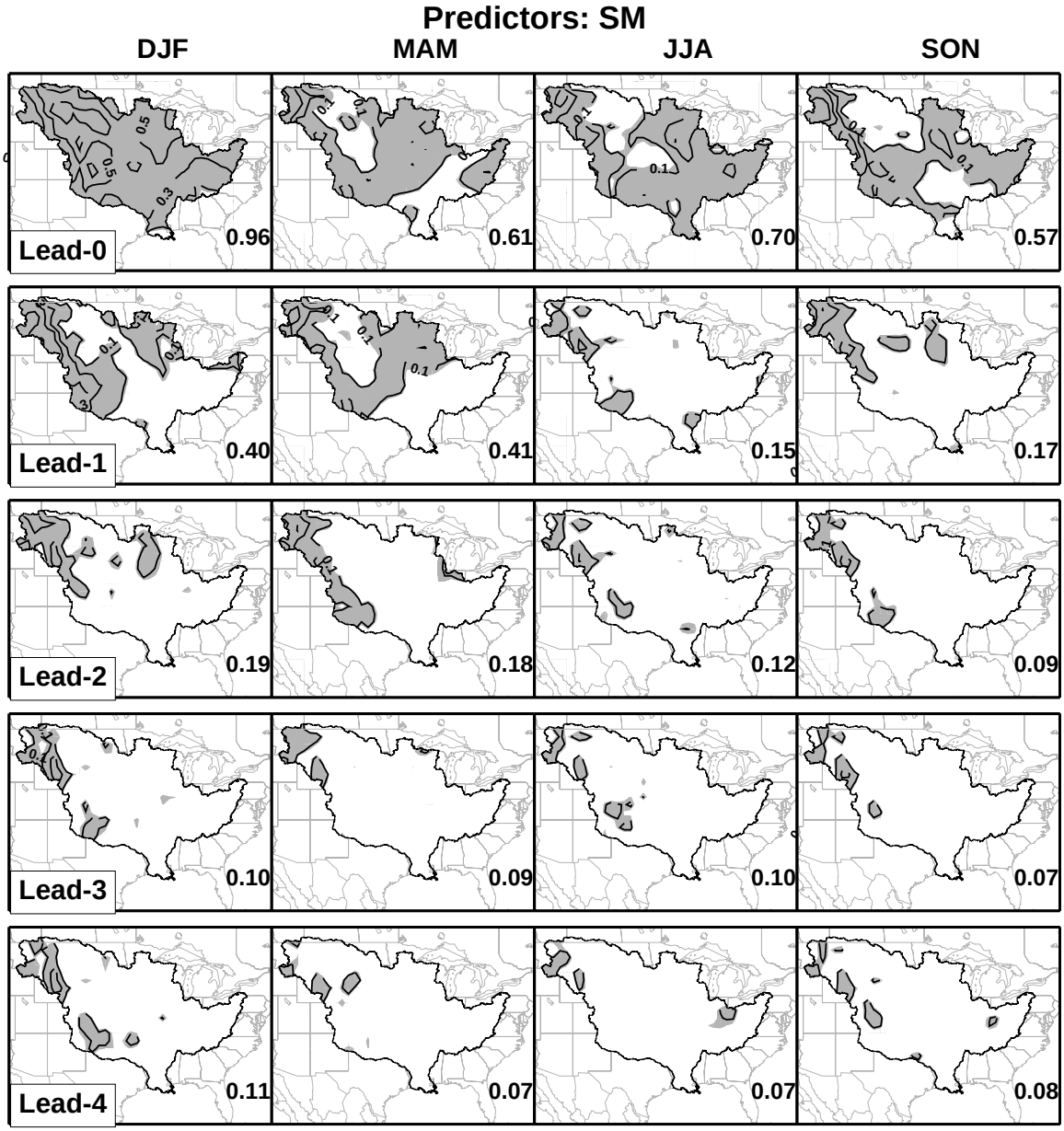

Figure 3.10 - As for Figure 3.6, but showing the predictability of seasonal runoff due to SM alone.

seasons, while significant SM influence is still seen. For an initialization date (date of forecast) of August 31 (i.e., lead-1 for DJF, lead-2 for MAM, lead-3 for JJA), snow is virtually absent from the basin, and can provide no forecast information, while SM shows significant explained runoff variance for DJF, MAM and JJA at leads through 3-4 seasons. This illustrates how knowledge of

the SM and snow states can complement each other in a forecast setting, providing considerable independent information despite their correlation with each other.

Importance of predictability due to defined sources

To quantify the importance of the climate indicators, SWE, and SM in forecasting runoff, a dimensionless variable is derived for each grid cell, and summed over the entire basin. The variable defined is the product of unitless runoff at each grid cell (Figure 3.5) and the variance explained by 1) SOI and AO (as in Figure 3.7); 2) SWE (Figure 3.9); and 3) SM (Figure 3.10) at each grid cell. Spatial plots of this variable are shown in Figures 3.11 and 3.12 for leads of 0 and 2 seasons, respectively. The basin-wide sum of this variable provides a snapshot of the relative importance of each source of predictive information in each season and at each lag. Table 3.2 presents these values for the entire Mississippi River basin. Most of our results (e.g., Figures 3.11, and 3.12) show distinct differences between the western and eastern portions of the basin Therefore, Tables 3.3 and 3.4 provide the same variable, summed over areas west and east, respectively, of longitude 100 West.

Table 3.2 - Summary of relative importance of predictors in forecasting seasonal runoff. Values are computed by multiplying at each grid cell the runoff variance explained by the predictors by the local unitless seasonal runoff, and summing these values over the Mississippi basin. Higher values indicate greater basin-wide predictability of seasonal runoff volume attributable to the predictor(s). Bold indicates the most influential factor for each season and lead.

	DJF					**MAM**				
	Lead					Lead				
Predictors	0	1	2	3	4	0	1	2	3	4
SOI AO	158	**95**	**75**	**157**	**27**	90	83	**55**	**60**	**81**
SWE	21	0	6	23	23	94	26	0	4	19
SM	**441**	75	44	26	26	**189**	**89**	45	39	27
	JJA					**SON**				
SOI AO	90	93	**82**	**70**	**85**	58	**69**	**76**	**64**	**56**
SWE	120	**102**	47	4	5	3	21	30	18	1
SM	**278**	53	49	36	37	**228**	48	35	34	38

Figure 3.11 shows the dominance of SM for runoff prediction at a lead of 0 seasons throughout the basin, which is also supported by Table 3.2. It is also obvious from Figure 3.11 that knowledge of SWE in the mountainous western extreme of the basin provides the most important information for predicting JJA runoff, as discussed above. It is interesting to note that the low

levels of predictability of MAM runoff due to SWE at lead-0 in Figure 3.9 are absent from Figure 3.11, since the predictability affects a very small amount of runoff. Figure 3.11 also illustrates that despite low levels of predictability (approximately 10-20% of runoff variance explained) by soil moisture in the southeast for JJA runoff at a lead of 0 seasons, the high levels of runoff in this region accentuates the importance of predictability attributable to soil moisture.

Table 3.3 - Summary of relative importance of predictors, as for Table 3.2 but only for regions west of longitude 100 West.

	DJF					**MAM**				
	Lead					Lead				
Predictors	0	1	2	3	4	0	1	2	3	4
SOI AO	2	2	3	3	2	6	4	4	**5**	3
SWE	1	0	**6**	**4**	2	11	5	0	4	3
SM	**30**	**20**	4	3	3	**20**	**20**	**13**	4	**4**
	JJA					**SON**				
SOI AO	25	23	25	**28**	**25**	6	8	5	5	**6**
SWE	**120**	**78**	**39**	4	5	3	**21**	**15**	**9**	1
SM	44	18	16	11	10	**61**	12	8	7	5

Table 3.4 - Summary of relative importance of predictors, as for Table 3.2 but only for regions east of longitude 100 West.

	DJF					**MAM**				
	Lead					Lead				
Predictors	0	1	2	3	4	0	1	2	3	4
SOI AO	156	**93**	**72**	**154**	**26**	84	**79**	**51**	**55**	**78**
SWE	20	0	0	19	21	84	21	0	0	16
SM	**411**	55	40	23	23	**169**	69	32	35	23
	JJA					**SON**				
SOI AO	65	**71**	**56**	**43**	**60**	52	**61**	**71**	**58**	**50**
SWE	0	23	8	0	0	0	0	14	9	0
SM	**234**	35	33	25	27	**168**	37	27	27	33

Table 3.2 indicates that the climate signal is dominant at leads of one season or more at the basin-wide scale for DJF and SON runoff, and at two seasons or more for MAM and JJA runoff. Examining the division of the basin in Tables 3.3 and 3.4, SWE provides the dominant source of JJA runoff predictability in the western portion of the basin through a lead of two seasons. SM provides the dominant influence on MAM runoff predictability in the west through a 2 season lead. The land surface signal, that is, SM and SWE combined, is a stronger predictor of runoff

than the climate signal in the western portion of the basin, except for JJA runoff at lead-3 and lead-4, though again these cases have limited practical significance. For the eastern portion of the basin (Table 3.4) the climate signal is the dominant source of important runoff predictability at lead times of 1 season or more.

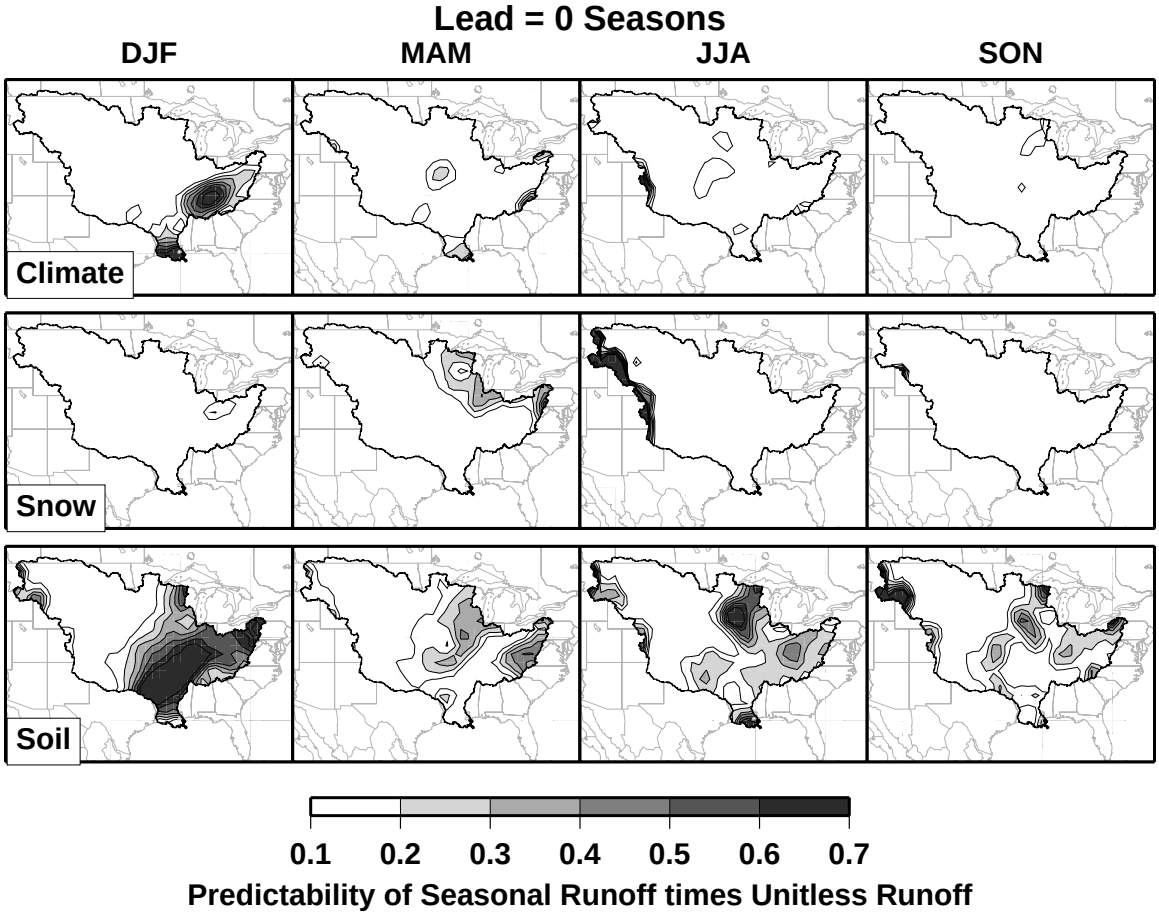

Figure 3.11 - Unitless variable representing the importance of predictability. The variable is defined as the fraction of the runoff explained by the climate or land surface indicators (defined in the left panel for each row) times the unitless runoff (Figure 3.5), for a lead of 0 seasons.

Figure 3.12 shows that this dominance of the climate signal in runoff predictability at a lead of 2 seasons is very limited spatially, and is accompanied by no important predictability from the land surface. It is evident from Figure 3.12 that the values in Tables 3.2, 3.3 and 3.4 at leads of two seasons (or more, though no Figure is shown) represent low predictability in spatially limited areas, with the SM and SWE generally only providing important predictability along the western edge of the basin, and climate information being focused in isolated pockets in the east and

southeast. Long lead runoff predictability is geographically limited, and is largely due to modest levels of predictability (Figures 3.7, 3.9 and 3.10) in areas with high levels of runoff.

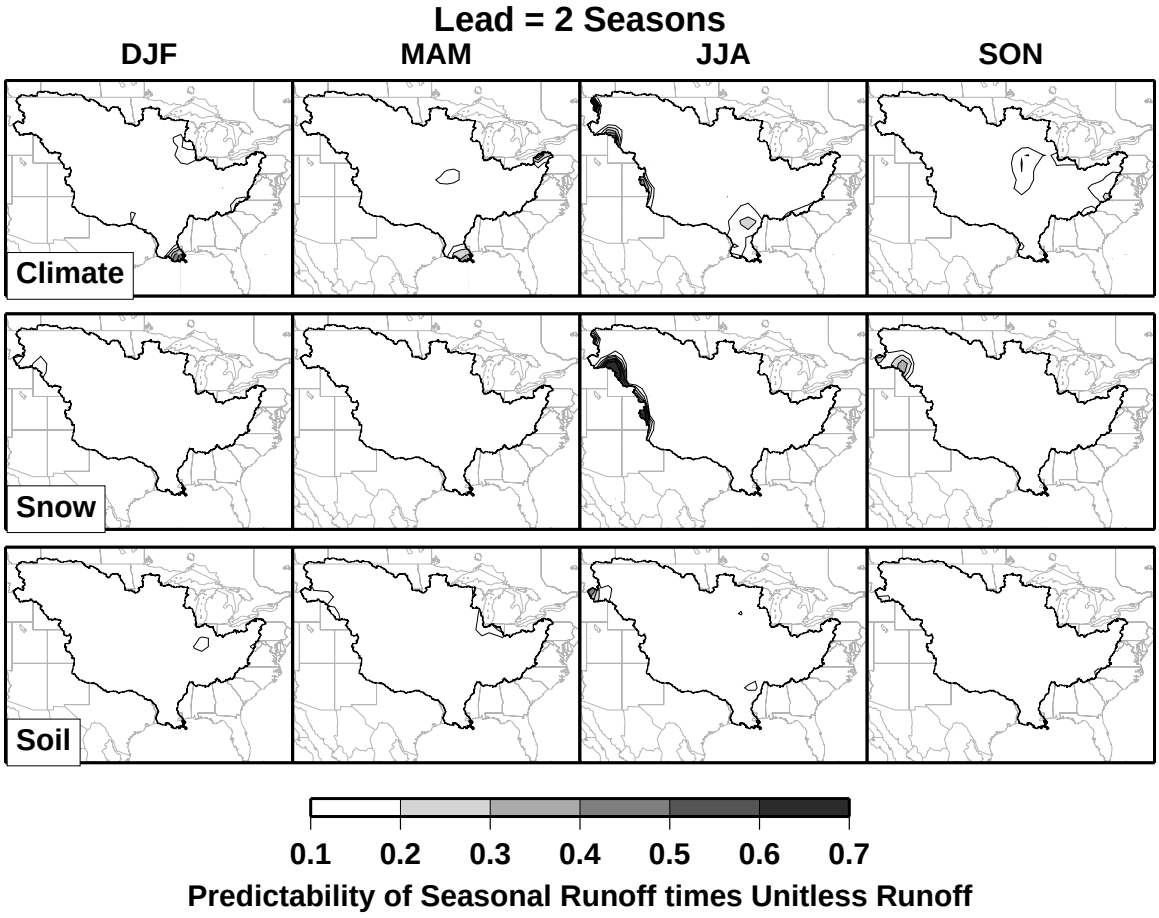

Figure 3.12 - - Same as for Figure 3.11, but for a lead of 2 seasons.

The field significance of the dimensionless variables plotted in each panel of Figures 3.11 and 3.12 correspond to those for Figures 3.7, 3.9, and 3.10; that is, for Figure 3.12, scaled predictability due to climate and soil moisture are field significant in all seasons, while snow is not field significant for seasons JJA or SON. For Figure 3.13, the scaled predictability due to climate is field significant only for the DJF season, that due to snow only for SON, and soil moisture passes the field significance test for all seasons. Figures 3.12 and 3.13 show that if the interest is related to a sub-area of the Mississippi River basin, as would be typical for a water manager concerned with runoff contributing to a reservoir, for example, the basin-wide field significance is too stringent a test. Failure to pass the basin-wide field significance test applied in

this study does not indicate that there is no important predictability in localized areas, however, a separate evaluation of the area of interest would be required.

CONCLUSIONS

The predictability of runoff throughout the Mississippi River basin has been evaluated both spatially, and by season and prediction lead time. As surrogates for climate predictability, we used the SOI and the AO. In general, SOI used in a simple persistence mode (ignoring climatological knowledge of ENSO event evolution) was found to provide comparable information for our purposes to a statistical forecast of SOI.

The climatic indicators provided a small but significant source of predictability for DJF runoff for leads of one through three seasons that exceeded that due to the land surface state, especially in the eastern portions of the Mississippi River basin. Because these climate indicators are readily available, this represents a source of predictability that can be exploited at present.

In general, SM is the dominant source of runoff predictability at lead 0 in all seasons. When the basin was divided at longitude 100 W into western and eastern portions, SM provided the dominant source of predictability at lead-0 (which represents an average lead time of 1.5 months) in both regions, except in JJA in the western mountainous region, where SWE was most important. For lead times of 1.5 months, then, a better determination of soil moisture state can provide valuable predictive capability of runoff throughout the basin. For areas west of longitude 100 W, the land surface state generally has a stronger predictive capability than the climate indicators; whereas climate indicators are more important for eastern areas of the Mississippi basin at leads of one season or greater. Although SM and SWE are correlated to varying extents during certain seasons in different parts of the basin, they nonetheless can provide a level of significant independent information and complement each other for runoff predictability.

Although modest (though statistically significant) DJF runoff predictability exists at a lead time of 3 seasons due to both climate and SM, much of this predictive capability is in areas producing little runoff, and is therefore of lessened practical importance. For JJA runoff in particular, locally significant runoff predictability, limited geographically to the western mountainous areas, at a lead of 2 seasons is coincident with high runoff producing areas. This information could be useful

to water managers in the western Mississippi River basin, since it suggests the potential to provide skillful forecast information at lead times earlier than are currently used operationally, and there are large storage facilities allowing managers to respond to long lead forecasts.

CHAPTER IV: POTENTIAL EFFECTS OF LONG-LEAD HYDROLOGIC PREDICTABILITY

"I must create a system, or be enslaved by another man's"
William Blake

This chapter was submitted for publication in Journal of Climate in August 2002 in its current form: Maurer, E.P and D.P. Lettenmaier, 2002, Potential effects of long-lead hydrologic predictability on Missouri River main-stem reservoirs, *J. Climate* (in review).

INTRODUCTION

Better understanding of the links between remote conditions, such as tropical sea surface temperatures, and climate over the continental U.S. has facilitated improved land surface hydrologic predictability, manifested especially in more accurate streamflow forecasts, especially for lead times longer than are achievable through traditional methods (Wood et al, 2002; Baldwin, 2001; Hamlet and Lettenmaier, 1999; Garen, 1998). In addition to these climate teleconnections, better definition of the land surface moisture state at the time of the forecast, through macroscale hydrologic modeling and remote sensing provides additional opportunities for improved hydrologic forecasting (e.g. Walker and Houser, 2001; Pauwels et al., 2001; Rango et al., 2000; Carroll et al, 1999).

Remote climate forcing signals and initial land surface states have been shown to provide a measure of predictability of runoff over the Mississippi River basin (Maurer and Lettenmaier, 2002b), with considerable spatial variability in the degree of predictability, its sources, and the lead times at which it is significant. Studies of the predictability of streamflow and/or of related climatic forcing variables, and implied benefits to water resources systems are numerous (e.g., Goddard et al., 2001; Hu and Feng, 2001; Fennessy and Shukla, 2000; Cayan et al., 1999; Dracup and Kahya, 1994; Kahya and Dracup, 1993). However, studies of the economic value of land surface hydrologic predictability are more rare (e.g., Hamlet et al., 2002; Yao and Georgakakos, 2001; Yeh, et al., 1982; Castruccio et al., 1980).

The National Research Council (2002a) identified the key to operational implementation of research findings related to hydrologic predictability as communication and strong linkages between research institutions and operational programs. However, an essential component of operational implementation of new techniques or data products (such as satellite-derived land surface characterizations) to improve predictability is a demonstration of the benefits the improved predictability may bring. Hornberger et al. (2001) assert that "Improved information systems and prediction methods can lead to large benefits for water, land, and biological resource management…" In this study we build on previous work by Maurer and Lettenmaier (2002b) that identified levels of predictability due to climate and land surface sources throughout the Mississippi River basin, and investigate how large an effect long-lead predictability can have on a water resource system, in comparison to that predictability already available.

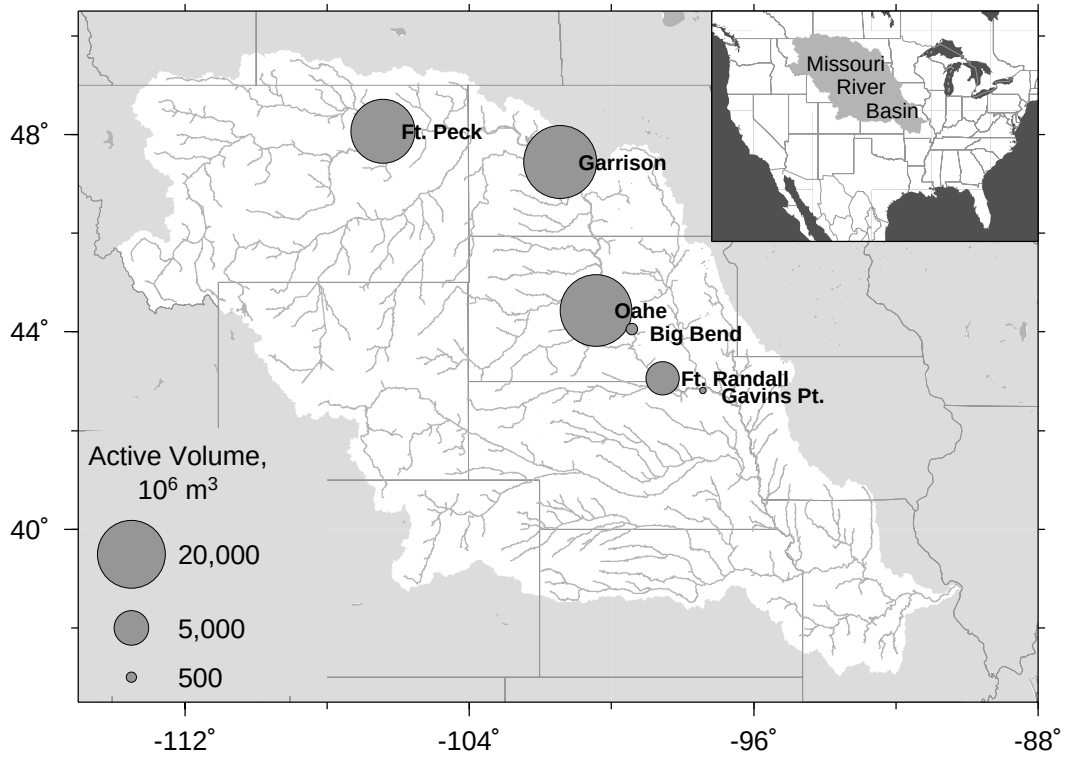

Figure 4.1 - Missouri River main stem dams. Size of circle at each point is scaled according to the ratio of the active storage volume to the river flow at that point.

Specifically, this study evaluates the impact of streamflow predictability at long lead times (months to a year) on reservoir operation in the main stem Missouri River system, which includes six dams managed by the U.S. Army Corps of Engineers (Figure 4.1). The Missouri River basin

was selected due to the demonstrable long-lead runoff predictability in the basin (Maurer and Lettenmaier, 2002b) and the extensive network of water management facilities that allow water managers to respond to monthly and seasonal forecast knowledge. We develop a simplified simulation model of the system of reservoirs, and use this reservoir simulation model to evaluate the bounding cases of perfect predictability and no predictability. We then use estimates of realistically achievable streamflow predictability determined by Maurer and Lettenmaier (2002b) to compute the value of predictive skill associated with knowledge of remote climate forcing impacts of Missouri River streamflow, as well as knowledge of initial snow water content and soil moisture over the basin.

STUDY SITE DESCRIPTION

The Missouri River is one of the largest rivers in North America, and in its virgin state exhibited highly variable flows. A combination of the Great Depression and the Dust Bowl of the early 1930's inspired the construction of Fort Peck dam, one of the largest modern structures on the planet (Reisner and Bates, 1990), completed on the upper main stem of the Missouri River in 1940. A sequence of three large floods in 1943 compelled the U.S. Army Corps of Engineers (COE) to draft plans for five additional large main stem dams, the last of which was completed in 1964 (Reisner, 1986). The motivation for drought and flood protection provided the extreme conditions reflected in the enormous system design volume, which is intended to provide protection against both a repeat of the 12-year 1930s drought (Lund and Ferreira, 1996) and the 1881 flood of record (COE, 1999). The system is operated to provide hydropower, flood control, navigation, water supply, recreation, and environmental mitigation benefits, although evacuating storage for spring runoff and releasing sufficient flow for downstream navigation largely drive the annual system operation. For example, the total annual requirements for irrigation, municipal, industrial, livestock and all water uses in tributary areas to the mainstem dams averages less than 200 m^3/s (COE, 1998), or about one third of the required release for navigation even in drought years.

The Missouri River basin and the six main stem dams are shown in Figure 4.1. The three upstream main stem reservoirs are significantly larger than the three downstream reservoirs. Table 4.1 shows the relative abilities of these reservoirs to regulate flow, expressed as the total active reservoir storage volume (excluding the permanent pool storage) divided by the average

annual main stem flow at the dam site. The upstream-most dam, Ft. Peck, has the largest ratio, with an active storage capacity of 1.8 times the average annual inflow. The overall dominance of the upper three dams for water management purposes at time scales greater than one month is clearly shown. For the system-wide total, the active reservoir capacity of all six reservoirs combined is approximately equal to the annual discharge at the mouth of the Missouri.

Table 4.1 - Ratio of the total volume and active volume for each dam (the reservoir volume minus the permanent pool storage) to the average annual flow at each site.

Dam	Total Vol./Avg. Annual Flow	Active Vol./Avg. Annual Flow
Ft. Peck	3.0	1.8
Garrison	1.6	1.0
Oahe	1.4	0.8
Big Bend	0.1	0.02
Ft. Randall	0.4	0.2
Gavins Pt.	0.03	0.01

Of the total annual flow at Gavins Point (23,300 million m^3), 89% is generated upstream of Oahe Dam, which highlights the importance of the upstream three reservoirs in regulating the annual flow variations. The downstream reservoirs provide additional hydropower generation and flow regulation over shorter time spans. With these large storage capacities, the Missouri River main stem system is capable of responding to long-lead forecasts by adapting water storage and release decisions to anticipated inflows months to a year in advance.

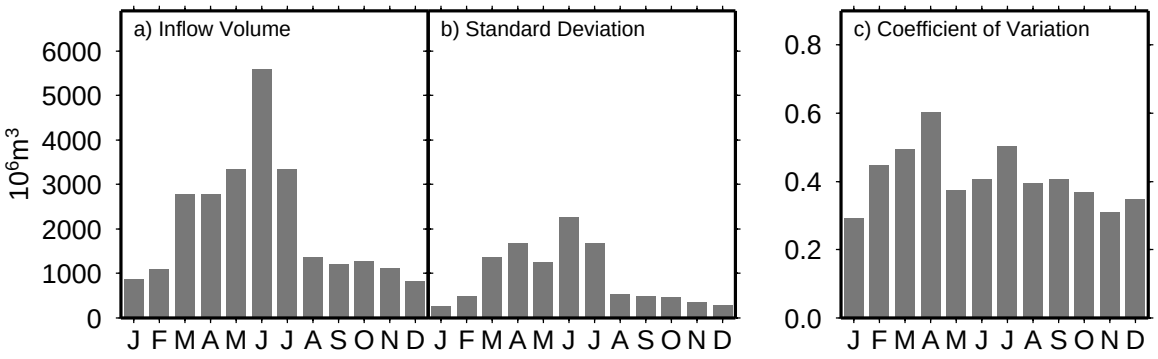

Figure 4.2 - a) Monthly mean inflow to upper three reservoirs in the Missouri River main stem system; b) Standard deviation of the monthly inflows; c) Coefficient of Variation.

Figure 4.2a shows the average annual cycle of inflow to the upper three reservoirs, which is dominated by snowmelt in the spring and early summer. The standard deviation of the flows is

shown in Figure 4.2b, which indicates that the variability is greatest in the spring and early summer. Figure 4.2c shows the coefficient of variation (standard deviation divided by the mean), and illustrates that, relative to the mean inflow, greatest variability in streamflow occurs in Spring. This means that predictability of spring and early summer flows can be expected to have the greatest impact on system operation, as it affects a substantial fraction of the annual inflow, during the time of year that it is most variable.

METHODS

The potential seasonal predictability of runoff identified by Maurer and Lettenmaier (2002b) for the Mississippi River basin implied an inherent benefit to water resources management. In order to quantify this benefit for the Missouri River main stem reservoir system, and to reveal the impact of increased predictability at long lead times on water resources management, a simulation model of the system of reservoirs was developed. The methods used in developing and applying the model are explained below.

Predictability for each contributing area

Maurer and Lettenmaier (2002b) computed for each season the r^2, representing predictability, associated with a multiple linear regression between selected initial conditions (i.e., different combinations of knowledge of climate or land surface conditions) and the seasonal average runoff at 1532 ½-degree grid cells in the Mississippi River basin. r^2 values were computed for seasons at leads of 0-4 seasons (where lead 0 would be a forecast of a season's runoff using initial conditions of the first day of the season, or an average of 1.5 month lead time). The r^2 associated with any correlation is numerically equal to the coefficient of prediction, C_p, defined in the Appendix, and this terminology will be used throughout.

For the present study, these C_p values (e.g., Figure 6 in Maurer and Lettenmaier, 2002b) are averaged over each of the contributing areas for the upstream three Missouri River reservoirs, weighting by the average runoff for each grid (Figure 5 in Maurer and Lettenmaier, 2002b). These values of weighted average C_p were developed for each season and each lead time of 0-4 seasons. A grid consisting of all values of 1 represents perfect predictability, and all 0 values indicates no predictability. In addition to these bounding conditions, C_p values were estimated for

three scenarios: 1) for the case of known climatic indicators; 2) for the case where perfect knowledge of snow water equivalent is added to the knowledge of climate signals; and 3) for the case where perfect soil moisture knowledge is also assumed, in addition to snow water content and climate signals. As discussed by Maurer and Lettenmaier (2002b), these three scenarios are arranged as "tiers" in accordance with how well defined the variables are with current technology. The climate indicators are best known, as they are available in real-time. Snow state is less well known, although ground surveys and remote sensing provide a basis for estimates that are available to water managers. Soil moisture is essentially unobserved, and hence is least well known. The difference between the C_p values for each scenario represents the incremental variance explained above that already achieved with better known variables, hence the variances explained by correlated variables (such as soil moisture and snow) are only counted once, and are attributed to the better known variable.

The climatic indicators used by Maurer and Lettenmaier (2002b) are the Southern Oscillation Index (SOI), which is an indicator of the state of the El Niño-Southern Oscillation, in combination with an Arctic Oscillation (AO) index. Both of these climate indicators are published monthly, and hence are currently available to water managers. Although the evolution of these indices through the forecast period is not considered, Maurer and Lettenmaier show that the predictability of runoff achieved using their states at the time of forecast are comparable to what is obtained by considering the evolution of climate state indicators in the Missouri and Mississippi River basins. The seasonal C_p values for Fort Peck are shown in Table 4.2 for each of the three cases. This indicates the runoff variance explained by each tier of variables, by correlating the seasonal average runoff with the initial state conditions of the indicated set of predictors for the corresponding lead time. For example, the C_p value associated with predicting DJF seasonal average runoff at lead-0 indicates the predictors were set on November 30. The table shows the general decrease in predictability with increasing lead time, the high levels of predictability identified by Maurer and Lettenmaier (2002b) for winter runoff at short lead times (attributable primarily to knowledge of soil moisture), and the important role of knowledge of snow water content for summer runoff predictability. Though not shown in the table, for the contributing areas to Garrison and Oahe dams, snow is of less importance for summer runoff prediction, and is of greater importance for spring runoff prediction, although only at lead times less than about three months.

These seasonal C_p values were interpolated to monthly values for lead times of 0-11 months, where a lead time of zero months indicates a forecast of a month's average runoff on the first day of the month. These monthly C_p values for each incremental area are represented by a 12 x 12 grid, with one row for each month for which flow is being predicted, and one column for each lead time from 0 to 11 months.

Table 4.2 - Seasonal weighted average C_p values for the contributing area to Fort Peck dam, derived from Maurer and Lettenmaier (2002b) for the cases of different predictors (see text). Leads indicate the number of intervening seasons between the forecast date and the forecasted seasonal average runoff. Seasons are winter (DJF), spring (MAM), summer (JJA) and fall (SON).

	Lead-0	Lead-1	Lead-2	Lead 3	Lead-4
Predictors: Climate Indicators					
DJF	0.046	0.041	0.065	0.076	0.04
MAM	0.039	0.044	0.038	0.049	0.04
JJA	0.064	0.075	0.08	0.083	0.096
SON	0.031	0.046	0.038	0.03	0.033
Predictors: Climate Indicators + Snow Water Content					
DJF	0.124	0.045	0.078	0.092	0.093
MAM	0.113	0.116	0.038	0.062	0.055
JJA	0.346	0.185	0.176	0.127	0.141
SON	0.048	0.06	0.059	0.067	0.034
Predictors: Climate Indicators + Snow Water Content + Soil Moisture					
DJF	0.672	0.311	0.187	0.145	0.148
MAM	0.276	0.271	0.099	0.091	0.089
JJA	0.393	0.203	0.196	0.14	0.15
SON	0.179	0.12	0.091	0.096	0.062

MOSIM Missouri River mainstem system model

The U.S. Army Corps of Engineers operates a series of six reservoirs along the main stem of the Missouri River. The operation of the reservoirs is governed by a master water control manual (COE, 1979), which has been under review for several years to adapt the management of the main stem system for ecological and other concerns (National Research Council, 2002b; COE, 2001).

As part of the review, extensive studies by the COE have been made on the operation of the system, using a system simulation model operating at a monthly time step, under different scenarios and constraints (COE, 1994a). In addition to COE efforts, other researchers have developed Missouri River main stem reservoir operation models for a variety of purposes. To investigate climate change effects, a daily Missouri River main stem system operation model was developed by Hotchkiss et al. (2000) based on work of Jorgensen (1996). Lund and Ferreira (1996) developed a monthly model using simulation software for the Missouri River basin. The COE monthly simulation model does not include an explicit ability to include forecast knowledge, nor does the Hotchkiss et al. model, which also does not consider hydropower generation. Although the Lund and Ferreira model did include hydropower, their optimized operating rules resulted in system operation very different from the historic (and current) operation.

For this study, our desire was to maintain the simplicity of a monthly model, to take advantage of the flexibility of simulation software, and to emulate the current operations relatively closely. To achieve this, we constructed a system model, MOSIM, using the Extend simulation software (Imagine That, Inc., 2001). MOSIM uses the physical reservoir data and minimum releases for hydropower and environmental constraints from the long-term study model described by the COE (1994a), which are shown in Table 4.3. We include the simplification used by Jorgensen (1996) and COE (1991) that combines local inflow to Big Bend and Ft. Randall reservoirs. This assumption is justified by the small contributing area between Big Bend and Oahe Dams.

The three upstream reservoirs contain about 90% of the total system storage, and therefore provide the majority of the capacity to operate the system by draining during the Fall and Winter and refilling during Spring. Therefore, in our system model the downstream three reservoirs are operated in a run-of-river mode, where for each month the inflow is equal to the outflow. The model determines the release from each reservoir at each time step in a two-step process. The first step consists of meeting the minimum and maximum flow release requirements in Table 4.3, and the release needed to evacuate reservoir storage in the winter to prepare for spring inflow volumes, which is set to match the current operational goal of draining each reservoir to the base of the multiple use zone by March 1 (COE, 1994a). Shortfalls in meeting environmental targets (required flows for Least Tern and Piping Plover habitat) up to 10% are permitted to occur in the

model when the total system storage is below the top of the carryover storage zone. This process is run from the upstream-most dam (Ft. Peck) downstream to Gavins Point. The second step involves checking the release at Gavins Point to see if the navigation target, which is a function of date and system storage (COE, 1994a) as shown in Table 4.4, has been met by the releases determined in the first step. If a supplemental release is needed to meet the navigation flow at

Table 4.3 - Dam release constraints and key elevations for U.S. Army Corps of Engineers main stem Missouri River project used in the MOSIM model.

	Ft. Peck Dam; Ft. Peck Lake	Garrison Dam; Lake Sakakawea	Oahe Dam; Lake Oahe	Big Bend Dam; Lake Sharpe	Ft. Randall Dam; Lake Francis Case	Gavins Pt. Dam; Lewis and Clarke Lake
Release, m^3/s						
Max. release[a]	708	1700	1925	2265	2265	2265
Max. winter release[b]	425	708	708	708	708	708
Max. hydropower	453	1189	1670	3115	1303	991
Min. hydropower[c]	85	227	28	0	28	142
Min. tern & plover[d]	241	566	0	0	793	821
Min. spawning, irrig., water supply[d]	85	453	170	0	142	170
Elevation, m						
Max. flood control	686.0	565.2	493.9	433.8	419.2	368.9
Max. multiple use	684.8	564.0	493.0	433.5	416.2	368.3
Max. carryover	681.1	560.2	490.1	432.9	411.6	367.2
Max. permanent pool	658.5	541.2	469.5	431.4	402.4	367.1
Avg. Tailwater	620.1	511.0	434.5	412.5	376.5	354.0
Volume at given elevation, 10^6 m^3						
Max. elev. flood control	23050	29380	28540	2290	6680	580
Max. elev. multiple use	21850	27550	27180	2220	5470	510
Max. elev. carryover[e]	18500	22340	23230	2070	3850	400
Max elev. permanent pool	5190	6140	6630	1740	1870	380

[a] *Values of 2265 indicate no defined maximum in the COE (1994a) Report.*
[b] *Maximum flows are reduced in winter (December through February) due to channel ice formation.*
[c] *Minimum hydropower is the sustained flow set to meet the MAPP requirements in the COE Long Range Study (LRS) model.*
[d] *Minimum flows (from both COE, 1994a and input files for the COE LRS model) applied May through August.*
[e] *As the base of the multiple use zone, this is the target volume for March 1 in COE (1994a).*

Gavins Point, this is allocated to the upper three reservoirs with the supplemental release drawn from each reservoir in proportion to its current volume. This helps to balance the levels of the upstream three reservoirs, which is an operational goal with the Missouri River main stem system, described by COE (1994a). These supplemental releases are passed through the system to determine the final releases at each dam.

Table 4.4 - Total system storage category definitions and navigation flow targets, adapted from COE (1994a) and Jorgensen (1996).

	High	Medium	Low
System Storage Definition, 10^6 m^3			
Dec-Feb	77710	71540	67840
Mar-Apr	67230	56740	49340
May	69080	59210	49340
Jun-Nov	72780	62290	49340
Service level flow (release target at Gavins Point) [a]**, m^3/s**			
Dec-Feb	708	425	255
Mar-Nov	991	821	566

[a] *Releases are based on the total system storage, as defined for the three categories of high, medium, and low. For system storages between the threshold values, flow targets are interpolated.*

Figure 4.3 compares the historic system-wide monthly storage for 1968-1997 with that simulated by the system model, MOSIM. The mean monthly bias is –557 million m^3, or 0.8% of the average historic system storage.. The root mean square error of monthly storage volumes is 3458 million m^3, or 4.8%, and the Pearson correlation coefficient of the historic and simulated monthly volumes is 0.92, which reflects the good correspondence between the model and historic system simulation seen in Figure 4.3.

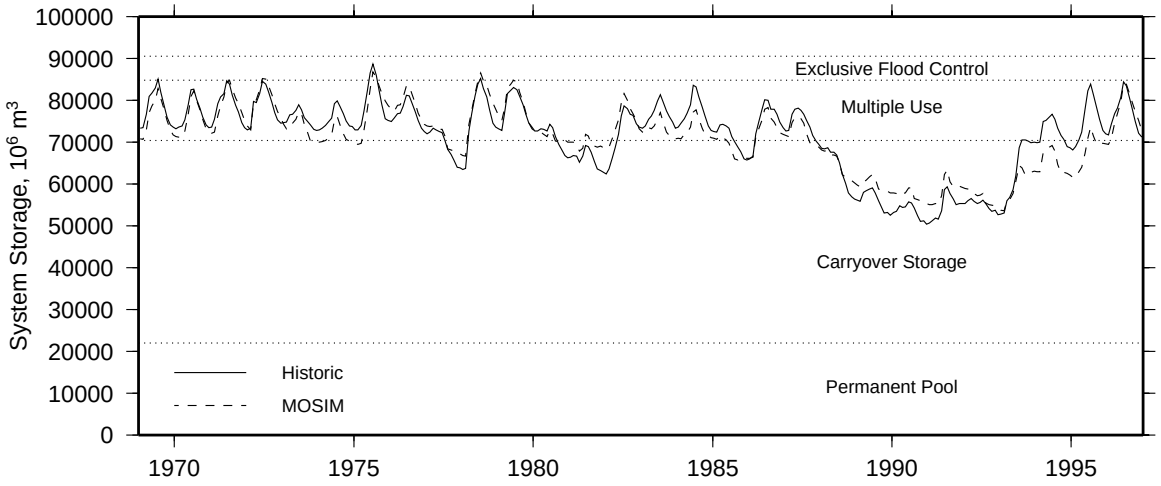

Figure 4.3 - Monthly simulated and historic Missouri River main stem system volumes, 1968-1997.

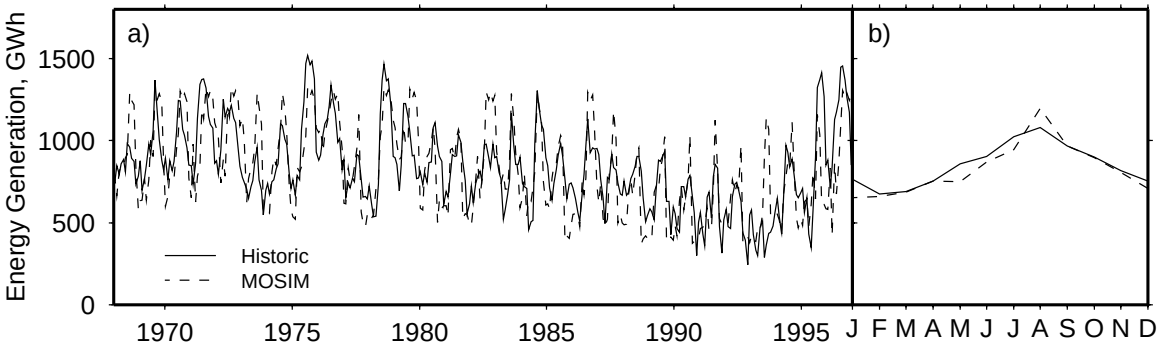

Figure 4.4 - Monthly energy generation of Missouri River main stem dams, historic and simulated. a) Time series of monthly values; b) average annual cycle for the 50-year period, 1968-1997.

MOSIM includes a computation of system hydropower generation and system energy capacity for each dam. System energy capacity is a function of reservoir elevation (tables relating elevation to capacity used in MOSIM are those used by COE 1994a), and is an indication of the ability of the system to generate peak power. Energy generation is a function of discharge and elevation at each reservoir. Historic and simulated energy generation in GWh for each month for 1968-1997 are shown in Figure 4.4. The annual average historic energy generation is 10,187 GWh, and the simulated value is nearly identical at 10,158. Although Figure 4.4a shows that MOSIM overpredicts the peak generation during the low system storage period during the late 1980s and early 1990s (when MOSIM has higher reservoir elevations than historic values), Figure 4.4b shows that the seasonal average cycle is captured accurately by the model.

Forecasted inflows representing predictability levels

To contrast the effects of different levels of predictability on the system operation, it was necessary to develop forecasted inflow sequences that reflect each predetermined level of predictability. This was accomplished by stochastically adding error to observed system inflow sequences, with larger errors reflecting lower levels of predictability, and perfect predictability resulting in forecasted flows equal to observed. The method used, based on Lettenmaier (1984), is outlined in Appendix A. To extend this analysis further into the past, we used as a surrogate for the historic record the 100-year reconstructed historic reservoir inflows developed by COE (1994a), which remove the effects of upstream water management and set a constant depletion level at the relatively low level present in 1949.

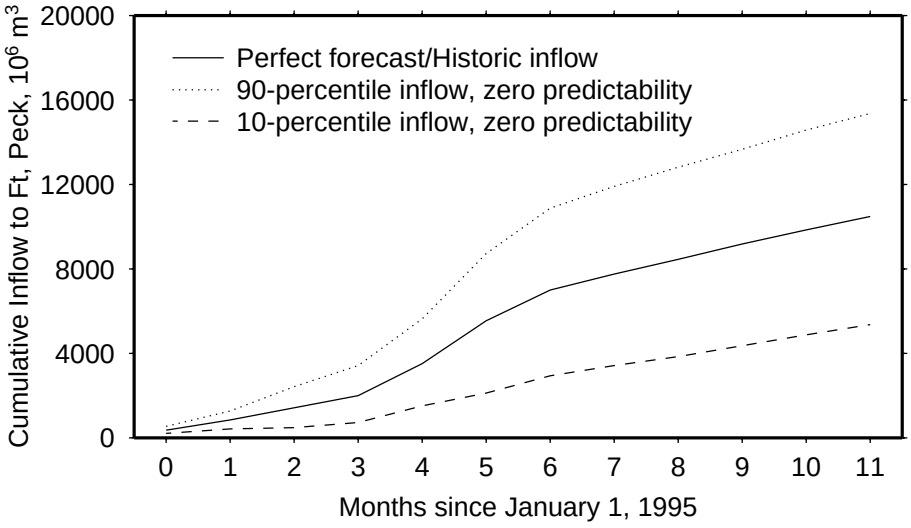

Figure 4.5 - Accumulated inflow to Ft. Peck dam for a 12-month forecast period under conditions of perfect and zero predictability.

For each month of the historic record for each contributing area, 500 synthetic forecasts were made for each of the following 12 months, reflecting the C_p values for the current month. From this sequence, the 90th percentile flow for each month was determined. These 90th percentile flows represent the assumed level of risk (10%) for this study (and the highest runoff conditions, or "upper decile," used in planning reservoir releases in COE, 1979), where operational decisions are based on these anticipated flow volumes for the following 12 months. An example of the generation of forecasted flow sequences is shown in Figure 4.5 for the case of no predictability

(all C_p values set to 0). This shows the widening band of uncertainty as the forecast lead time increases.

The value of added predictability

To compare the benefits associated with different levels of predictability quantitatively, it is convenient to compute system economic benefits under different alternatives. The current COE system operation produces many benefits, including flood control, navigation, hydropower, water supply and recreation. In addition, the system is operated to provide environmental mitigation benefits, including habitat protection for the Least Tern and Piping Plover populations that nest along the river. Among these benefits, hydropower dominates (COE, 1994a). For the MOSIM model developed for this study, the remaining purposes for the reservoir system were imposed as constraints, while differences in hydropower generation under different alternatives provided the metric for the value of the predictability.

Hydropower benefits were calculated for system capacity and energy production. COE (1994a) estimated that system capacity historically has generated roughly two thirds of the total hydropower benefits. The economic benefits of both capacity and energy vary through the year. A set of monthly capacity and energy benefits were derived based on COE (1994b), which are shown in Table 4.5.

Table 4.5 - Energy and capacity values used in this study

	Jan	Feb	Mar	Apr	May	Jun	Jul	Aug	Sep	Oct	Nov	Dec
Energy, mills/kWh	21.00	21.00	19.00	19.00	19.00	27.00	27.00	27.00	19.80	19.80	19.80	21.00
Capacity, $/kW/month	13.26	9.62	5.33	0	4.01	18.44	30.10	26.73	12.99	1.36	7.32	12.99

The annual operation in MOSIM was based on COE (1994a), which uses a target of draining all reservoirs (in the case of MOSIM, the three upper reservoirs only, as the lower three are run-of-river) to the target elevation corresponding to the base of the annual flood control zone (also referred to as the flood control and multiple use zone) by March 1. In order to permit the use of long-lead forecast information, this rule was altered to use two forecast volumes. First, rather than fix the March 1 level to the base of the multiple use zone, the level was set to allow storage of the forecasted volume of spring and summer inflow (defined as March through July) less the maximum amount that could be released through the turbines, in order to minimize spill. Second,

the forecasted inflow volume from the current month through March 1 was compared against the maximum volume that could be released through the turbines by March 1. This allowed a decision each month as to whether the evacuation needs to begin or not, and retained the reservoir at as high a level as possible until lowering of levels to meet the March 1 target must begin. Table 4.5 shows how maintaining higher water surface elevations, especially in December-February and June-August, can result in increased system benefits due to greater economic value of energy production and capacity. Additional predictability, and hence reduced uncertainty in anticipated flow volumes, allows the maintenance of higher reservoir levels, and provides a quantitative estimate of benefits due to additional predictive skill.

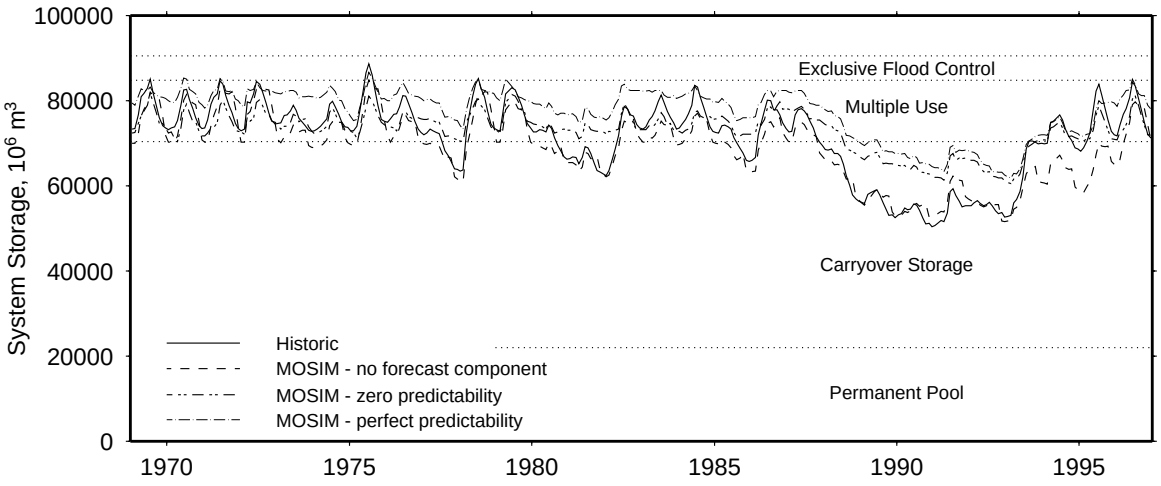

Figure 4.6 – Monthly historic and simulated main stem system storage, as in Figure 4.3, but including the system operation under the flexible rule curve adopted in this study to adapt operations to different levels of predictability. MOSIM – no forecast component corresponds to the MOSIM model plotted in Figure 4.3

With the addition of this capability of the system to respond to different levels of predictability, the system operation changes, as shown in Figure 4.6 for the cases of perfect and zero predictability. The greatest difference in operation is in dry years, where with predictability in the system is not drawn down as far as it was historically. It is also interesting to note that even the zero predictability case has considerably less drawdown of the system during the dry period of the late 1980s to early 1990s. This illustrates that since the synthetic forecast technique adds noise to the historic inflows, even a zero predictability scenario effectively incorporates some knowledge of future inflows, and does not represent a true “zero skill” forecast, which would assume climatological inflows.

RESULTS AND DISCUSSION

Current system configuration

As a bounding case, the annual system-wide hydropower benefits under a perfect forecast scenario (complete knowledge of future flows) are compared to those resulting from no predictability. The average annual hydropower benefits for the no predictability scenario were $530 million, while the perfect forecast scenario produced $540 million, representing an increase of 1.8%. This suggests a relative maximum potential benefit in the Missouri River basin, due to hydropower alone, with improved predictability that amounts to several million dollars but is small on the scale of the benefits already produced by the project.

This result is reasonable, given the scale of the existing project, where the total system storage (of the COE mainstem projects) is three times the annual inflow to the reservoirs. As illustrated in Figures 4.5, the greatest volume of water affected by the forecast in a month (that is, the maximum difference in slope between perfect and zero predictability), is approximately 900 x 10^6 m^3. This volume of water can be interpreted as an amount that can be stored under perfect forecast knowledge, while with zero predictability it would have to be released to leave room to store anticipated inflow (that would not ultimately occur). However, the extremely large size of the reservoirs relative to the inflows results in this volume representing an elevation difference, at Ft. Peck dam, of 1.0 m, or 1.5% of the total head available for hydropower generation at Ft. Peck. Similarly, the large reservoirs impounded by Garrison and Oahe dams relative to their inflows dampen the sensitivity to inflow forecasts, resulting in the relatively small range of benefits under perfect and no predictability forecasts.

To put this information in the context of past studies, we compiled the results from five previous studies that compared hydropower generation benefits under perfect forecast (or under optimal operation) and with zero forecast skill (or with little accounting for forecast knowledge). For each of these past studies, Figure 4.7 shows the ratio of system volume to annual inflow versus the percent difference in hydropower benefits with the best forecast as compared to least or no forecast skill. Although the value of forecast skill is a function of many factors such as the variability of inflows and demands, and the studies employ a variety of assumptions, Figure 4.7 shows that the ratio of system volume to average inflow limits the potential of a system to benefit

from forecast information. As an extreme case (large storage relative to mean flow), the Missouri River main stem falls within the trajectory seen from past studies, showing that 12-month forecasts in this study have a limited effect on this system, designed for multiple year storage.

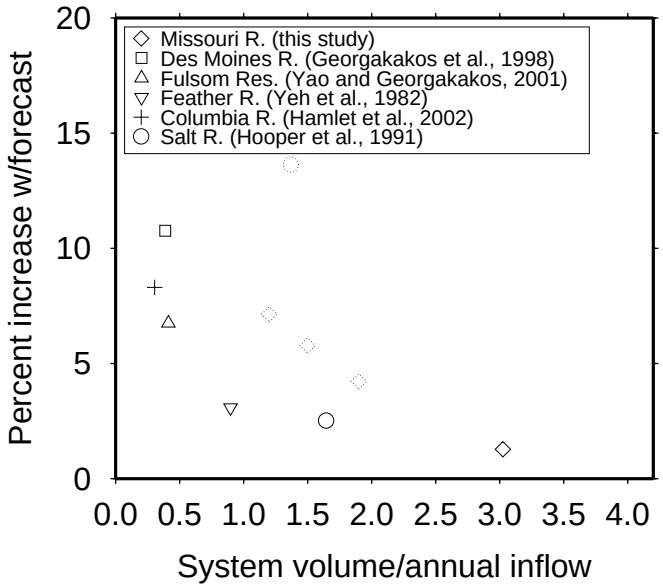

Figure 4.7 - Ratio of system volume to annual system inflow versus the percent difference between perfect and no forecast skill for past studies and the current study. Symbols drawn with dotted pen indicate sensitivity studies for reduced volume systems (see discussion in text).

Hooper et al. (1991) included a sensitivity study of the effect of reducing system storage volume on the benefits of forecast information. To simulate the effects of a volume reduction due to system modification, the system storage capacity was reduced by 17%, and the resulting difference between a perfect and zero forecast increased markedly to 13.6% (the reduced capacity Salt River system is shown in Figure 4.7 with a dotted pen). The Salt River system Hooper et al. analyzed may be more sensitive to changes in system storage than the Missouri River main stem system, because the Salt River system relies on costly groundwater pumping to achieve water supply requirements not met by surface runoff, and the pumping cost is included in their analysis. However, it does show that a reduction in total system capacity may result in greater forecast value. In the present study, a similar sensitivity study was performed for two purposes: 1) to identify a system capacity at which the value of forecast information provides a greater marginal increase in benefits, and 2) to examine the value of the climate, snow, and soil moisture information within the bounds of perfect and zero predictability.

Modified system configuration

Although the current storage capacity of the Missouri River main stem reservoirs is too large to show a substantial difference in hydropower benefits between different levels of predictability, for reasons discussed above, a smaller system in the same geographical setting could show greater sensitivity. To investigate this, the MOSIM model was altered by reducing the total capacities of the carryover storage and permanent pool zones of the three upstream reservoirs, resulting in a hypothetical system with smaller reservoir storage capacities that is more sensitive to changes in forecasted inflows. The three reduced Missouri system configurations are summarized in Table 4.6. The smaller system sizes result in a greater range of elevations for the multiple use zone (which retained its original size for all configurations), and the value of forecast information relative to no forecast knowledge likewise increases. The smallest system, with a volume/flow ratio of 1.2, showed a difference of 7.1% in hydropower benefits between the perfect and zero predictability alternatives, representing a difference of $25.7 million in annual average hydropower benefits.

Table 4.6 - - Data related to the sensitivity study with resizing of the main-stem Missouri River system reservoirs.

Total System Volume, 10^6 m^3	System Volume/Annual Flow at Gavins Pt.	Avg. Elevation Range in Multiple Use Zone, m	% Increase in Benefits with Perfect Forecast
90520	3.0	3.0	1.8
58240	1.9	5.4	4.2
45420	1.5	7.3	5.8
36450	1.2	15.2	7.1

For this study, this reduced main stem system was used in the analysis of the value of forecast information added by knowledge of the climate state and the initial state of snow water and soil moisture, as developed by Maurer and Lettenmaier (2002b). The three cases of incremental knowledge of climate and land surface state identified above were applied to this reduced main stem system. The total hydropower benefits of the project using these three cases, bounded by the hydropower benefits for perfect and zero predictability scenarios, are summarized in Table 4.7. Figure 4.8 shows the system reliability in meeting the minimum environmental flow releases for the Least Tern and Piping Plover habitat at Ft. Peck and Garrison dams. Figure 4.8 shows that the reliability of meeting these release targets is generally equal or better under greater predictability and higher benefit alternatives. In addition, the maximum winter releases are met 100% of the

time at these points, as are the navigation release targets at Gavins Point. This illustrates that the increase in benefits between these alternatives is not due to a reduction in reliability in meeting some other system benefit.

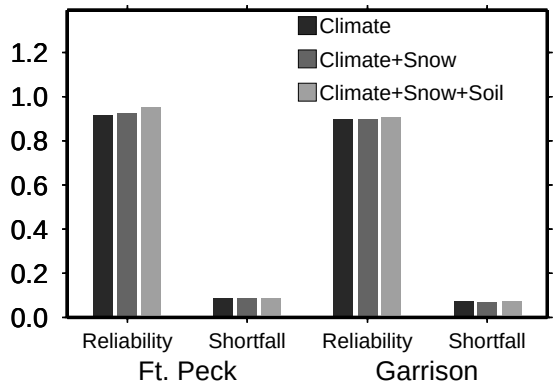

Figure 4.8 - Reliability of system for meeting environmental release targets at Ft. Peck and Garrison dams, measured as the fraction of time that the releases are met, and the average magnitude of each shortfall expressed as a fraction of the target release.

Table 4.7 shows that for this reduced configuration of the Missouri River main stem reservoir system, the total potential annual hydropower gain above zero predictability accounting for the climate state, with perfect knowledge of the snow water content and soil moisture, amounts to $6.8 million annually, which is 26% of the total difference between zero and perfect forecast skill. Using currently available knowledge of the climate signal, with no knowledge of snow or

Table 4.7 - Total system hydropower benefits for reduced-volume Missouri River main stem dams under different levels of predictive skill.

Scenario/Forecast Knowledge	Average Annual Hydropower Benefits, millions of dollars
Zero predictability	$359.8
Climate state	$363.2
Climate state and snow water content	$364.5
Climate, snow, and soil moisture	$366.6
Lag flow forecast	$363.5
Perfect forecast skill	$385.5

soil moisture states, provides $3.4 million in benefits above the no predictability case. The incremental benefit of perfectly knowing snow state throughout the basin, in excess of the benefit resulting from knowledge of climate state, is $1.3 million. Although soil moisture shows high predictability at lead times less than three months and has its highest correlations for

predictability of winter runoff, when runoff is lowest, the incremental benefit (above that already achieved with snow and climate knowledge) due to perfect knowledge of soil moisture state is $2.1 million. As noted in above, the predictability of summer runoff attributable to knowledge of snow water is high at Fort Peck, but lower at the more downstream projects, hence snow has an overall system impact less than that due to soil moisture.

Using the SOI and AO climate indicators, which are published monthly (and are therefore available at forecast time), the hydropower benefits obtained from 12 month forecasts, in excess of those for the no predictability scenario, are approximately equal to that which can be obtained using only past inflow observations (the "lag flow" forecast indicated in Table 4.7). When a perfect knowledge of the basin snow and soil moisture state at the time the forecast is made is added to knowledge of the climate indicators, the total increase in hydropower benefits (above a no predictability scenario) double.

It should be emphasized that these results apply to the entire (reduced volume) main stem system. Any component operated on its own, or other projects in the basin would have different sources and levels of predictability, and the dominance of these sources in producing hydropower benefits would likewise be different. Furthermore, as noted by Yao and Georgakakos (2001), the response of a water resources system to forecast information is highly dependent on the reservoir operating rules imposed. Hence, the conclusions from the present study, with system operations based on those used by the COE long term simulation model, would be expected to change under different operating rules.

The results in Table 4.7 are also dependent on the order in which the tiers of variables are introduced. As mentioned above, the best known variables are introduced first, hence any predictability associated with correlated variables is assigned to the better known variables. The implication of this on the results in Table 4.7 is that, for example, if it were assumed that soil moisture could be characterized using a hydrologic model to better accuracy than snow water content is observed, soil moisture would be introduced before snow in the development of the C_p values in Table 4.2. This would attribute a greater portion of the total variance explained to soil moisture (since soil moisture and snow water are correlated), and therefore a greater proportion of incremental benefits shown in Table 4.7 would be assigned to soil moisture.

Seasonal distribution of predictability

The seasonal distribution of the value of this predictability was investigated by generating forecasts using different levels of predictability (either a lag flow forecast, or some combination of knowledge of climate state, snow water content, and soil moisture) in one month, and no predictability in the remaining months. The month with predictive skill was stepped through the year, with the benefits determined for hydropower using the reduced volume system configuration. The resulting levels of benefits are shown in Figure 4.9, where for example "Jan" indicates the predictability level for January was set using the appropriate values for the level of knowledge indicated, and no predictability was assigned to all other months. The ordinate values indicate the average annual system (using the reduced system configuration) hydropower benefits above those obtained with no predictability.

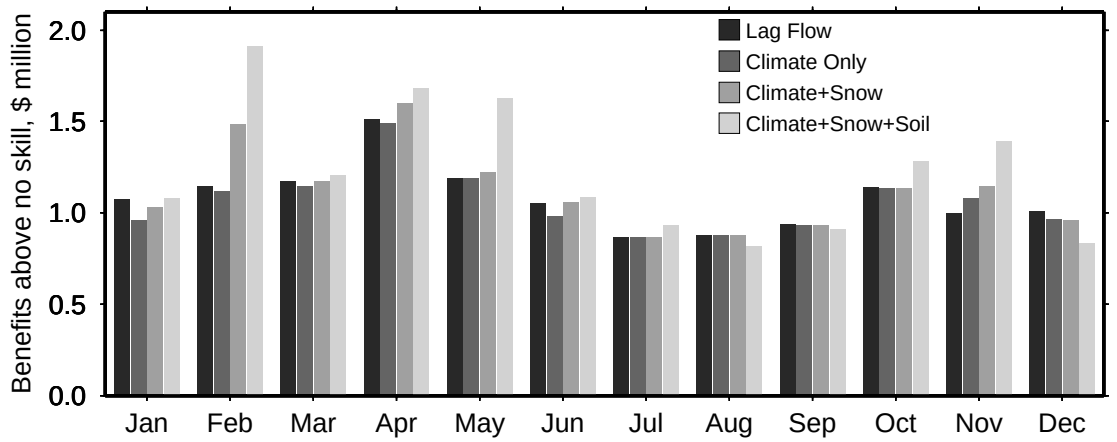

Figure 4.9 - Benefits above a zero predictability scenario with the specified level of predictability in the current month, and no predictability in other months.

Figure 4.9 shows several interesting features on the monthly scale. First, using this month-by-month technique, the benefits obtained form incorporating the known climate indicators (labeled "Climate Only" in Figure 4.9) in the prediction scheme are nearly identical to the benefits obtained using correlation relationships with historic observed flows ("Lag Flow"). The incremental benefits (above those already obtained using climate indicators) obtained with perfect knowledge of snow state throughout the basin has its major impact in February, when the high spring and summer flow volumes are highly correlated with the water stored in the snow pack. The benefits due to snow decrease sharply in March, however, since the March 1 target date of

the following year is the next opportunity for the system to adapt to forecasted inflows. This illustrates the interaction of benefits obtained by forecasts and the operating rules imposed on the system.

In general, the value of predictability in the spring, when interannual variability is greatest (Figure 4.2), is greater than during the remainder of the year. The late winter and spring, especially February and May, is also when the incremental benefits due to soil moisture knowledge, above those already obtained from knowledge of climate and snow, are greatest, illustrating the potential value of soil moisture knowledge in determining spring and summer inflows. Knowledge of soil moisture also provides incremental benefits during October and November, since the low winter inflows are dominated by soil moisture-driven base flow.

Using this technique to examine the month-by-month value of predictability has some counterintuitive results. One illustration of this is seen for December in Figure 4.9, where increasing information about the land surface moisture state in December (with no predictability in all other months) results in slight decreases in average annual benefits. This is explained by the use of the flexible rule curve to set the March 1 system evacuation target, and the non-linearity of monthly benefits. For example, a high level of knowledge about the upcoming flows in December might indicate that inflows will be low and releases can be limited. However, when the system returns to no predictability forecasts the following month and higher anticipated inflows, reservoir releases will increase in the following months of January and February. For lower predictability levels in December, the higher anticipated inflows would require higher reservoir releases in December, and subsequently potentially lower required releases in February. Any shift in releases from December to February with higher levels of predictability would result in lower hydropower benefits, as shown by the capacity values in Table 4.5.

CONCLUSIONS

The value of long-lead streamflow prediction skill added by knowledge of climate teleconnection information and land surface moisture state in the Missouri River basin on the main stem reservoir system was evaluated. The value was based on the hydropower generated by the main stem dams for a simulated period of 1898-1996 using a monthly simulation model, MOSIM,

developed for this study. Simulated forecasted flows were generated to represent the levels of predictability determined in a previous study.

The configuration of the Missouri River main stem reservoirs, which have a total storage capacity of three times the average annual discharge at the downstream end of the system, shows little sensitivity to streamflow prediction skill at long lead times (months to a year) – only a 1.8% difference in hydropower benefits between a zero and perfect predictability forecast. This is also reflected in past studies in other basins, where larger systems show smaller incremental benefits due to long-lead forecast skill.

To simulate the potential effects of predictability on a smaller system in the same geographical setting, a hypothetical Missouri River main stem system was developed with reduced storage equal to 1.2 times the annual flow volume. This system showed a larger difference between the zero and perfect forecast predictability case of 7.1%, and allowed the investigation of the levels of predictability due to climate and land surface state knowledge to be investigated. With the reduced main stem system, incorporating both a knowledge of the climate state as well as perfect knowledge of snow and soil moisture states in the forecast resulted in an increase of 1.9% in system hydropower benefits, representing $6.8 million annually. Of this $6.8 million total, use of currently available climate indicators provides the largest portion at $3.4 million, which is approximately the same as the value of predictability provided by historically observed inflows. Of the additional benefits above that already provided due to climate knowledge, soil moisture adds the greatest value, at $2.1 million. This provides an important context for operational implementation of hydrologic predictability, where for large water resources systems the benefits of added predictability may amount to modest sums, but represent a small percentage of additional benefits.

A monthly analysis indicates that, for the modified (reduced-volume) Missouri River main stem system configuration and operating rules considered in this study, including climate knowledge alone provides a level of benefits comparable to that obtainable using historic system inflow observations. Benefits above those obtainable using historic inflows can be obtained with the addition of knowledge of snow water content and soil moisture throughout the basin. Knowledge of soil moisture provides the bulk of these increased benefits, and has its greatest impact when knowledge is provided of soil moisture state in the spring and fall.

In the Missouri River basin, greater benefits due to runoff predictability may be realized in reservoir systems that are large enough to respond to long-lead forecast information (i.e. capable of storing several months of inflow) yet are small enough where the volume in flow affected by the forecast has an appreciable effect on the generated system benefits. Future research into the interaction of reservoir system size and predictability levels will help identify the areas where forecasts produced with additional knowledge of the climate and land surface state will be most beneficial.

CHAPTER V: CONCLUSIONS

"Life is a revolt against predictability."
Albert Camus

The motivation for this study was to investigate the opportunities for improving long-lead (monthly to seasonal) runoff prediction over large continental watersheds; and to evaluate the potential utility for water resources management. For the selected study area of the Mississippi River basin, the first task was to identify the magnitude, location, timing, and sources of runoff predictability. This required a comprehensive set of long-term (multi-decadal) records of spatially distributed soil moisture, snow water equivalent, and runoff. Such data are not available from observations, therefore a set of derived land surface moisture and energy states and fluxes was developed. The data set is based on gridded observed precipitation and temperature data, and parameterized radiative and other meteorological surface forcings that were used to drive a macroscale hydrologic model for the 50-year period 1950-2000. The simulated runoff is shown to match observations quite well over large river basins, which suggests that, over the long term, evapotransporation must also be realistic. Given the physically-based parameterizations in the model, we argue that over shorter timescales other terms in the surface water balance (e.g., soil moisture) are probably well represented, at least for the purposes of diagnostic studies. Furthermore, observed and modeled soil moisture change is shown to match quite closely over the state of Illinois, where long-term soil moisture observations are available. These characteristics give this data set promise for a variety of studies, especially where ground observations are lacking. For water and energy balance studies in particular, this derived data set is shown to be far superior to the land surface variables from coupled land-atmosphere reanalysis projects (e.g., Kalnay et al, 1996; Gibson et al., 1997), which have been the basis for a number of previous large scale studies.

The derived data set provided a unique source of hydrologically consistent, spatially distributed fields of land surface moisture and runoff that could be used to investigate the predictability of runoff due to initial land surface moisture conditions and climate state. Using this data set, the predictability of runoff throughout the Mississippi River basin was evaluated both spatially, and by season and prediction lead time. As surrogates for climate predictability, we used the Southern Oscillation Index (SOI) and an Arctic Oscillation (AO) index. The principal conclusions from this investigation were:

- Climatic indicators (SOI and AO) provided a small but significant source of predictability for DJF runoff for leads of one through three seasons that exceeded that due to the land surface state, especially in the eastern portions of the Mississippi River basin. Because these climate indicators are readily available, this represents a source of predictability that can be exploited operationally, as these indicators are available in near real-time.

- At the basin-wide level, for the predictors included, soil moisture (SM) is the dominant source of runoff predictability at lead 0 (which represents an average lead time of half a season, or 1.5 months) in all seasons.

- When the basin was divided at longitude 100 W into western and eastern portions, SM provided the dominant source of predictability at lead-0 in both regions, except in JJA in the western mountainous region, where snow water equivalent (SWE) was most important. For lead times of 1.5 months, then, a better determination of soil moisture state can provide valuable predictive capability of runoff throughout the basin.

- For areas west of longitude 100 W, the land surface state generally provides a stronger predictive capability than do climate indicators; whereas climate indicators are more important for eastern areas of the Mississippi basin at leads of one season or greater. Modest (although statistically significant) DJF runoff predictability exists at a lead time of 3 seasons due to both climate and SM, although much of this predictive capability is in areas producing little runoff, and is therefore of lessened practical importance. For JJA runoff in particular, locally significant runoff predictability, limited geographically to the western mountainous areas, at a lead of 2 seasons is coincident with high runoff producing areas.

This analysis of runoff predictability has the potential to be useful to water managers, especially in the western part of the Missouri River basin. To investigate the potential value of the these varying levels of runoff predictive skill added by knowledge of climate signals and land surface moisture state, the next phase of this study focused on the main stem reservoir system of the Missouri River basin, which comprises 44% of the Mississippi River basin area. As a highly managed system with a large reservoir storage capacity relative to system inflows, the Missouri River also is capable of responding to long-lead predictive information. The value of predictability under different scenarios was based on the hydropower generated by the main stem dams for a simulated period of 1898-1996 using a monthly simulation model, MOSIM, developed for this study. Simulated forecasted flows were generated to represent the levels of predictability determined in a previous study.

- The Missouri River main stem reservoirs, which have a total storage capacity of about three times the average annual inflow to the system, shows little sensitivity to streamflow prediction skill at long lead times (months to a year) – only a 1.8% difference in hydropower benefits between forecasts produced under perfect and zero predictability scenarios. A review of previous studies reveals a consistent relationship between economic (hydropower) benefits gained by increased predictability and system volume (normalized by average annual system inflow). This provided the motivation for investigating the potential effects of the predictability levels on a smaller reservoir system in the same geographical setting.

A hypothetical Missouri River main stem system was developed with reduced storage equal to 1.2 times the mean annual flow volume. Because the existing main stem reservoir system is capable of storing several years of inflow, its sensitivity to forecasts with a 12 month horizon is limited. The use of the hypothetical reduced-volume system allowed the investigation of potential value of 12 month forecast information to a smaller reservoir system. The reduced-volume system showed a larger difference between the zero and perfect forecast skill case of 7.1%, and allowed the investigation of the levels of predictability due to climate and land surface state knowledge to be investigated.

- With the reduced-volume main stem system, incorporating a perfect knowledge of basin initial conditions (i.e., both a knowledge of the climate state as well as perfect knowledge

of snow and soil moisture states) in the forecast resulted in an increase of 1.9% in system hydropower benefits, representing $6.8 million annually.

- Of this $6.8 million total, use of currently available climate indicators provides the largest portion at $3.4 million, which is approximately the same as the value of predictability provided by historically observed inflows.

- Of the additional benefits above those already provided due to climate knowledge, soil moisture information adds the greatest value, at $2.1 million.

This study provides an important context for operational implementation of hydrologic predictability, where for large water resources systems the benefits of added predictability may be modest, but represent a small percentage of additional benefits. In the Missouri River basin, greater benefits may be realized in smaller reservoir systems that are large enough to respond to long lead forecast information (i.e. capable of storing several months of inflow) yet are small enough that the volume in flow affected by the forecast has an appreciable effect on the generated system benefits. Future research into the interaction of reservoir system size and predictability levels will help identify the areas where forecasts produced with additional knowledge of the climate and land surface state will be most beneficial.

BIBLIOGRAPHY

Abdulla, F.A., D.P. Lettenmaier, E.F. Wood, and J.A. Smith, 1996, Application of a macroscale hydrologic model to estimate the water balance of the Arkansas-Red River basin, *J. Geophys. Res.,* 101 (D3), 7449-7459.

Augustine, J.A., J.J. DeLuisi, and C.N. Long, 2000, SURFRAD – A national surface radiation budget network for atmospheric research, *Bull. Amer. Meteor. Soc.,* 81, 2341-2357.

Baldwin, C.K., 2001, Seasonal streamflow forecasting using climate information, Proceedings of the 69th Western Snow Conference, Sun Valley, ID, April 16-19, 2001, 95-98.

Baldwin, M.P. and T.J. Dunkerton, 2001, Stratospheric harbingers of anomalous weather regimes, *Science* 294, 581-584

Barnston, A.G., M.H. Glantz, and Y. He, 1999, Predictive skill of statistical and dynamical climate models in SST forecasts during the 1997-98 El Niño episode and the 1998 La Niña onset, *Bull. American, Meterol. Soc.* 80, 217-243.

Barnston, A.G., 1994, Linear statistical short-term climate predictive skill in the northern hemisphere, *J. Climate* 7, 1513-1564.

Beard, D.P., 1994, Bureau of Reclamation revamps efforts to help fish, *Fisheries* 19, 6-7.

Beljaars, A.C., P. Viterbo, M.J. Miller, and A.K. Betts, 1996, The anomalous rainfall over the United States during July 1993: Sensitivity to land surface parameterization and soil moisture anomalies, *Mon. Wea. Rev.,* 124, 362-383.

Betts, A.K. and J.H. Ball, 1998, FIFE surface climate and site-averaged dataset 1987-89, *J. Atmos. Sc*i., 55, 1091-1108.

Betts, A.K., J.H. Ball, A.C.M. Beljaars, M.J. Miller, and P.A. Viterbo, 1996a, The land surface-atmosphere interaction: A review based on observational and global modeling perspectives, *J. Geophys. Res.,* 101 (D3), 7209-7225.

Betts, A.K., S.-Y. Hong, and H.-L. Pan, 1996b, Comparison of NCEP-NCAR reanalysis with 1987 FIFE data*, Mon. Wea. Rev*., 124, 1480-1498.

Brubaker, K.L., D. Entekhabi, and P.S. Eagleson, 1993, Estimation of continental precipitation recycling, *J. Climate,* 6, 1077-1089.

Calder, I.R., 1993, Hydrologic effects of land-use change, in *Handbook of Hydrology*, chap. 13, edited by D.R. Maidment, MsGraw-Hill, New York.Carroll, S.S., T.R. Carroll, and R.W. Poston, 1999, Spatial modeling and prediction of snow water equivalent using ground-based, airborne, and satellite snow data, *J. Geophys. Res.* 104, 19623-19629.

Carroll, S.S., T.R. Carroll, and R.W. Poston, 1999, Spatial modeling and prediction of snow water equivalent using ground-based, airborne, and satellite snow data, *J. Geophys. Res.* 104, 19623-19629.

Castruccio, P.A., H.L. Loats, D. Lloyd, and P.A.B. Newman, 1980, Cost/benefit analysis in the operational application of satellite snowcover operations, In: Operational Applications of Snowcover Operations, A. Rango and R. Peterson, Eds., NASA Conference Publication No. 2116

Cayan, D.R., K.T. Redmond and L.G. Riddle, 1999, ENSO and hydrologic extremes in the western United States, *J. Climate* 12, 2881-2893.

Cherkauer, K.A., 2001, Understanding the hydrologic effects of frozen soil, Water Resources Series Technical Report No. 167, University of Washington, Seattle, WA, September, 2001.

Cherkauer, K. A., L. C. Bowling and D. P. Lettenmaier, 2002, Variable Infiltration Capacity (VIC) Cold Land Process Model Updates, *Global and Planetary Change* (in review).

Church, J.E., 1937, The human side of snow, *Scientific Monthly* 44, 137-149.

Coe, M.T., 2000, Modeling terrestrial hydrological systems at the continental scale: testing the accuracy of an atmospheric GCM, *J. Climate,* 13, 686-704.

Cosby, B.J., G.M. Hornberger, R.B. Clapp, and T.R. Ginn, 1984, A statistical exploration of the relationships of soil moisture characteristics to the physical properties of soils, *Water Resour. Res*., 20, 682-690.

Daly, C., G.H. Taylor, and W.P. Gibson, 1997, The PRISM approach to mapping precipitation and temperature, paper presented at 10th Conference on Applied Climatology, Amer. Meteor. Soc., Reno, Nev., Oct. 20-24.

Daly, C., R.P. Neilson, and D.L. Phillips, 1994, A statistical-topographic model for mapping climatological precipitation over mountainous terrain, *J. Appl. Meteor.,* 33, 140-158.

Datta, B. and S.J. Burges, 1984, Short-term, single, multi-purpose reservoir operation: importance of loss functions and forecast errors, *Water Resources Research* 20, 1167-1176.

DeFries, R.S. and J.R.G. Townshend, 1994, NDVI-derived land cover classification at global scales, *Int. J. Remote Sens.,* 15, 3567-3586.

Dirmeyer, P. A., 1995, Problems in initializing soil wetness, *Bull. Am. Meteorol. Soc.,* 76(11), 2234-2240.

Dracup, J.A. and E. Kahya, 1994, The relationships between U.S. streamflow and La Niña events, Water Resources Research 30, 2133-2141.

Duan, Q.Y., J.C. Schaake, and V.I. Koren, 1996, FIFE 1987 water budget analysis, *J. Geophys. Res*., 101 (D3), 7197-7207.

Ducoudré, N.I., K. Laval, and A. Perrier, 1993, SECHIBA, a new set of parameterizations of the hydrologic exchanges at the land-atmosphere interface within the LMD atmospheric general circulation model, *J. Climate,* 6, 248-273.

Ebisuzaki, W., M. Kanamitsu, J. Potter, and M. Fiorino, 1998, An overview of Reanalysis-2, paper presented at 23rd Climate Diagnostics and Prediction Workshop, National Oceanic and Atmospheric Administration, Climate Prediction Center, Miami, Fla., Oct. 26-30.

Environment Canada, 1999, Canadian daily climate data on CD-ROM. Environment Canada, Meteorological Service of Canada, Downsview, Ontario.

FAO, 1998, Digital soil map of the world and derived soil properties, Food and Agriculture Organization, Land and Water Digital Media Series No. 1.

Fedorov, A.V., 2002, The response of the coupled tropical ocean-atmosphere to westerly wind bursts, *Q. J. R. Meteor. Soc.* 128, 1-23.

Fennessy, M.J. and J. Shukla, 2000, Seasonal prediction over North America with a regional model nested in a global model, *J. Climate* 13, 2605-2627.

Garen, D.C., 1998, ENSO indicators and long-range climate forecasts: usage in seasonal streamflow volume forecasting in the western United States, *EOS, Transactions*, 79, p. F325.

Garen, D.C., 1992, Improved techniques in regression-based streamflow volume forecasting, *J. Water Resources Planning and Management* 118, 654-670.

Gates, L.W., 1992, AMIP: The atmospheric model intercomparison project, *Bull. Amer. Meteor. Soc.,* 73, 1962-1970.

Gates, L.W., et al. 1999, An overview of the results of the atmospheric model intercomparison project (AMIP I), *Bull. Amer. Meteor. Soc.,* 80, 29-55.

Georgakakos, K.P., A.P. Georgakakos, and N.E. Graham, 1998, Assessment of benefits of climate forecasts for reservoir management in the GCIP region, *Gewex News* 8(3), 5-7, August 1998.

Gershunov, A., 1998, ENSO influence on intraseasonal extreme rainfall and temperature frequencies in the contiguous United States: Implications for long-range predictability, *J. Climate* 11, 3192-3203.

Gibson, J.K., P. Kallberg, S. Uppala, A. Hernandez, A. Nomura, and E. Serrano, 1997, *ERA Description*, *Reanalysis Proj. Rep. Ser.*, vol. 1, Eur. Cent. for Medium-Range Weather Forecasts, Reading, England.

Goddard, L. S.J. Mason, S.E. Zebiak, C.F. Ropelewski, R. Basher and M.A. Kane, 2001, Current approaches to seasonal-to-interannual climate predictions, *Int. J. Climatology* 21, 1111-1152.

Goodison, B.E., P.Y.T. Louie and D. Yang, 1998, WMO Solid precipitation measurement intercomparison, Instruments and Observing Methods Report No. 67 (WMO/TD 872), World Meteorological Organization, Geneva.

Goodison, B.E. and A.E. Walker. 1994. Canadian development and use of snow cover information from passive microwave satellite data. In *Passive remote sensing of land-atmosphere interactions*. Choudhury, B.J., Y.H. Kerr, E.G. Njoku and P. Pampaloni (eds.), ESA/NASA International Workshop, Utrecht, The Netherlands: 245-262.

Groisman, P.Y. and D.R. Legates, 1994, The accuracy of United States precipitation data, *Bull. American Meteor. Soc.* 75, 215-227.

Hall, D.K., G.A. Riggs, V.V. Salomonson, N. DiGiromamo, and K.J. Bayr, 2001, MODIS snow cover products, *Remote Sensing of Environment* (in press).

Hamlet, A.F. and D.P. Lettenmaier, 1999, Columbia River streamflow forecasting based on ENSO and PDO climate signals, *J. Water Resour. Planning and Management* 125, 333-341.

Hamlet, A.H., D. Huppert and D.P. Lettenmaier, 2002, Economic value of long-lead streamflow forecasts for Columbia River hydropower, *J. Water Resour. Planning and Management* 128, 91-101.

Hansen, M.C., R.S. DeFries, J.R.G. Townshend, and R. Sohlberg, 2000, Global land cover classification at 1 km spatial resolution using a classification tree approach, *Int. J. Remote Sens.,* 21, 1331-1364.

Higgins, R.W., A. Leetmaa, Y. Xue, and A. Barnston, 2000, Dominant factors influencing the seasonal predictability of U.S. precipitation and surface air temperature, *J. Climate* 13, 3994-4017.

Higgins, R.W., K.C. Mo, and S.D. Schubert, 1996, The moisture budget of the central United States as evaluated in the NCEP/NCAR and the NASA/DAO reanalyses, *Mon. Wea. Rev*., 124, 939-963.

Hollinger, S.E., and S.A. Isard, 1994, A soil moisture climatology of Illinois, *J. Climate*, 7, 822-833.

Hooper, E.R., A.P. Georgakakos, and D.P. Lettenmaier, 1991, Optimal stochastic operation of Salt River Project, Arizona, *J. Water Resources Planning and Management* 117, 566-587.

Hornberger, G.M. et al., 2001, A plan for a new science initiative on the global water cycle, U.S. Global Change Research Program, Washington, D.C.

Hotchkiss, R.H., S.F. Jorgensen, M.C. Stone, and T.A. Fontaine, 2000, Regulated river modeling for climate change impact assessment: the Missouri River, *J. American Water Resources Association* 36, 375-386.

Hu, Q. and S. Feng, 2001, Variations of teleconnection of ENSO and interannual variation in summer rainfall in the central United States, *J. Climate* 14, 2469-2480.

Huang, J., H.M. van den Dool, and K.P. Georgakakos, 1996, Analysis of model-calculated soil moisture over the United States (1931-1993) and applications to long-range temperature forecasts, *J. Climate,* 9, 1350-1362.

Huffman, G.J., R.F. Adler, M.M. Morrissey, S. Curtis, R. Joyce, B. McGavock, and J. Susskind, 2001, Global precipitation at one-degree daily resolution from multi-satellite observations, *J. Hydrometeor*., 2, 36-50.

Imagine That, Inc., 2001, Extend professional simulation tool, version 5, Imagine That, Inc., San Jose, California.

Intergovernmental Panel on Climate Change, 2001, Climate change 2001: Impacts, adaptation, and vulnerability, Cambridge University Press, Cambridge, UK.

Jackson, R.B.., J. Canadell, J.R. Ehringer, H.A. Mooney, O.E. Sala and E.D. Schulze, 1996, A global analysis of root distributions for terrestrial biomes, *Oecologia,* 108, 389-411.

Janowiak, J.E., A. Gruber, C.R. Kondragunta, R.E. Livezy, and G.J. Huffman, 1998, A comparison of the NCEP NCAR reanalysis precipitation and the GPCP rain gauge satellite combined dataset with observational error considerations, *J. Climate*, 11, 2960-2979.

Jorgensen, S.F., 1996, Hydrologic modeling of Missouri River reservoirs in a climate model, M.S. thesis, University of Nebraska, Lincoln, Nebraska, December 1996.

Kahya, E. and J.A. Dracup, 1993, U.S. streamflow patterns in relation to El Niño/Southern Oscillation, Water Resources Research 29, 2491-2503.

Kalnay, E., et al., 1996, The NCEP/NCAR 40-year reanalysis project, *Bull. Amer. Meteor. Soc.,* 77, 437-471.

Kanamitsu, M., W. Ebisuzaki, J. Woolen, J. Potter, and M. Fiorino, 2000, An overview of NCEP/DOE Reanalysis-2, in Proceedings, Second WCRP International Conference on Reanalyses, *Rep. WCRP-109*, World Meteorol. Org., Geneva.

Kelly, R.E.J., A.T.C. Chang, J.L. Foster, and D.K. Hai, 2001, Development of a passive microwave global snow monitoring algorithm for the Advanced Microwave Scanning Radiometer-EOS, Proceedings IEEE 2001 International Geoscience and Remote Sensing Symposium, Scanning the present and reolving the future, IEEE, Piscataway, NJ.

Kerr, Y.H., P. Waldteufel, J.P. Wigneron, J. Martinuzzi, J. Font, and M. Berger, 2001, Soil moisture retrieval from space: the soil moisture and ocean salinity (SMOS) mission, *IEEE Trans. Geosci. and Remote Sens.* 39, 1729-1735.

Kimball, J.S., S.W. Running, and R. Nemani, 1997, An improved method for estimating surface humidity from daily minimum temperature, *Agric. For. Meteor.*, 85, 87-98.

Knaff, J.A. and C.W. Landsea, 1997, An El Niño-Southern Oscillation climatology and persistence (CLIPER) forecasting scheme, *Weather Forecasting* 12, 633-652.

Koike, T., E. Njoku, T.J. Jackson, and S. Paloscia, 2000, Soil moisture algorithm development and validation for the ADEOS-II/AMSR, Proceedings IEEE 2000 International Geoscience and Remote

Sensing Symposium, Taking the pulse of the planet: the role of remote sensing in managing the environment, IEEE, Piscataway, NJ.

Koster, R.D., T. Oki, and M.J. Suarez, 1999, The off-line validation of land surface models: Assessing success at the annual timescale*, J. Meteor. Soc. Jpn.*, 77 (1B), 257-263.

Koster, R.D., M.J. Suarez, and M. Heiser, 2000, Variance and predictability of precipitation at seasonal-to-interannual timescales, *J. Hydrometeorol*., 1, 26-46.

Kumar, A. and M.P. Hoerling, 1998, Annual cycle of pacific-north American seasonal predictability associated with different phases of ENSO, *J. Climate* 11, 3295-3308.

Kunkel, K.E. and J.R. Angel, 1999, Relationship of ENSO to snowfall and related cyclone activity in the contiguous United States, *J. Geophys. Res.* 104, 19,425-19,434.

Landsea, C.W. and J.A. Knaff, 2000, How much skill was there in forecasting the very strong 1997-98 El Niño?, *Bull. American Meteorol. Soc.* 81, 2107-2119.

Lenters, J.D., M.T. Coe, and J.A. Foley, 2000, Surface water balance of the continental United States, 1963-1995: Regional evaluation of a terrestrial biosphere model and the NCEP/NCAR reanalysis, *J. Geophys. Res.,* 105 (D17), 22,393-22,425.

Lettenmaier, D.P., 1984, Synthetic streamflow forecast generation, *ASCE Journal of Hydraulic Engineering* 110, 277-289.

Liang, X., D.P. Lettenmaier, E. Wood, and S.J. Burges, 1994, A simple hydrologically based model of land surface water and energy fluxes for general circulation models, *J. Geophys. Res*., 99 (D7), 14,415-14,428.

Liang, X., D. P. Lettenmaier, and E. F. Wood, 1996, One-dimensional statistical dynamic representation of subgrid spatial variability of precipitation in the two-layer variable infiltration capacity model, *J. Geophys. Res.,* 101 (D16), 21,403-21,422.

Lin and Derome, 1998, A three-year lagged correlation between the North Atlantic oscillation and winter conditions over the north pacific and north America, *Geophys. Research. Letters* 25. 2829-2832.

Linsley, R.K. and W.C. Ackerman, 1942, Method of predicting the runoff from rainfall, *Transactions American Society of Civil Engineers* 107, 825-846.

Livezey, R.E. and W.Y. Chen, 1983, Statistical field significance and its determination by Monte Carlo techniques, *Monthly Weather Review* 111, 46-59.

Livezey, R.E. and T.M. Smith, 1999, Covariability of aspects of North American climate with global sea surface temperatures on interannual to interdecadal timescales, *J. Climate* 12, 289-302.

Lohmann, D., R. Nolte-Holube, and E. Raschke, 1996, A large-scale horizontal routing model to be coupled to land surface parameterization schemes, *Tellus,* 48A, 708-721.

Lohmann, D., et al., 1998a, The project for intercomparison of land-surface parameterization schemes (PILPS) phase 2(c) Red-Arkansas basin experiment, 3, Spatial and temporal analysis of water fluxes, *Global Planet. Change,* 19, 161-179.

Lohmann, D., E. Raschke, B. Nijssen, and D.P. Lettenmaier, 1998b, Regional scale hydrology, II, Application of the VIC-2L model to the Weser River, Germany, *Hydrol. Sci. J*., 43, 131-141.

Lund, J.R. and I. Ferreira, 1996, Operating rule optimization for Missouri river reservoir system, *J. Water Resources Planning and Management* 122, 287-295.

Ma, X.L., Wan, Z., C.C. Moeller, W.P. Menzel, and L.E. Gumley, 2002, Simultaneous retrieval of atmospheric profiles, land-surface temperature, and surface emissivity from moderate-resolution imaging spectroradiometer thermal infrared data: extension of a two0step algorithm, *Applied Optics* 41, 909-24.

Mahrt, L., and H. Pan, 1984, A two-layer model of soil hydrology, *Bound.-Layer Meteor*., 29, 1-20.

Manabe, S., 1969, Climate and the ocean circulation: I. The atmospheric circulation and the hydrology of the earth's surface, *Mon. Wea. Rev.* 97, 739-774.

Mantua, N.J., S.R. Hare, Y. Zhang, J.M. Wallace, R.C. Francis, 1997, A Pacific interdecadal oscillation with impacts on salmon production, *Bull. Amer. Meteor. Soc.* 78, 1069-1079.

Marston, E., 1987, The west's water-crats and dam-icans, In: Western Water Made Simple, Island Press, Washington, D.C., 237 pp.

Maurer, E.P., A.W. Wood, J.C. Adam, D.P. Lettenmaier, and B. Nijssen, 2002, A Long-Term Hydrologically-Based Data Set of Land Surface Fluxes and States for the Continental United States, *J. Climate* (in press).

Maurer, E.P. and D.P. Lettenmaier, 2002a, Predictability of seasonal runoff in the Mississippi River basin, *J. Geophys. Res.* (in press).

Maurer, E.P. and D.P. Lettenmaier, 2002b, Potential effects of long-lead hydrologic predictability on Missouri River main-stem reservoirs *J. Climate.* (in review).

Maurer, E.P., G.M. O'Donnell, D.P. Lettenmaier, and J.O. Roads, 2001, Evaluation of the Land Surface Water Budget in NCEP/NCAR and NCEP/DOE Reanalyses using an Off-line Hydrologic Model. *J. Geophys. Res.,*106 (D16), 17,841-17,862

Maurer, E.P., B. Nijssen, D.P. Lettenmaier, 2000, Use of Reanalysis Land Surface Water Budget Variables in Hydrologic Studies. *GEWEX News*, 10 (4) pp. 6-8.

McCabe G.J. and M.D. Dettinger, 1999, Decadal variations in the strength of ENSO teleconnections with precipitation in the western U.S., *Intl. J. of Climatology*, 19, 1399-1410.

Metcalfe, J.R., B. Routledge and K. Devine, 1997, Rainfall measurement in Canada: changing observational methods and archive adjustment procedures. *J.Climate,* 10, 92-101.

Mileti, D.S., 1999, Disasters by design: a reassessment of natural hazards in the United States, John Henry Press, Washington D.C.

Miller, D.A., and R.A. White, 1998, A conterminous United States multi-layer soil characteristics data set for regional climate and hydrology modeling, *Earth Interactions,* 2, 1-15.

Mitchell, K., et al., 1999, The GCIP Land Data Assimilation (LDAS) Project – Now underway, *GEWEX News,* 9 (4), 3-6.

Myneni, R.B., R.R. Nemani. and S.W. Running, 1997, Estimation of global leaf area index and absorbed PAR using radiative transfer models, *IEEE Trans. Geosci. Remote Sens.*, 35, 1380-1393.

Namias, J., 1952, The annual course of month-to-month persistence in climatic anomalies, *Bull. Amer. Meteor. Soc*., 33, 279-285.

Namias, J., 1962, Influences of abnormal heat sources and sinks on atmospheric behavior*, Proc. of the International Symposium on Numerical Weather Prediction*, Meteorol. Soc. Japan, 615-627.

National Assessment Synthesis Team, 2001, Climate change impacts on the United States: The potential consequences of climate variability and change, Cambridge University Press, Cambridge, UK, 620pp.

National Research Council, 2002a, Predictability and limits-to-prediction in hydrologic systems, National Academy Press, Washington, D.C.

National Research Council, 2002b, The Missouri river ecosystem: exploring the prospects for recovery, Water Science and Technology Board, Division on Earth and Life Sciences, Washington, D.C.

National Research Council, 2001, Envisioning the agenda for water resources research in the twenty-first century, Water Science and Technology Board, Washington, D.C., 61 pp.

National Snow and Ice Data Center, 1996, Northern Hemisphere Weekly Snow Cover and Sea Ice Extent, vol. 1.0 and 2.0 (CD-ROM), Cooperative Institute for Research in Environmental studies, University of Colorado, Boulder, CO, USA.

National Water And Climate Center, 1998, The NRCS water supply forecasting system, U.S. Department of Agriculture, National Resources Conservation Service, NWCC Briefing Paper, June 1998.

Nijssen, B., D.P. Lettenmaier, X. Liang, S.W. Wetzel, and E. Wood, 1997, Streamflow simulation for continental-scale basins, *Water Resour. Res*., 33, 711-724.

Nijssen, B., G.M. O'Donnell, D.P Lettenmaier, D. Lohmann, and E.F. Wood, 2001, Predicting the discharge of global rivers, *J. Climate,* 14, 3307-3323.

Njoku, E.G. and L. Li, 1999, Retrieval of land surface parameters using passive microwave measurements at 6-18 GHz*, IEEE Trans. Geosci. and Remote Sens*. 37, 79-93.

Oglesby, R.J., S. Marshall, D.J. Erikson, J.O. Roads and F.R. Robertson, 2002, Thresholds in atmosphere-soil moisture interactions: results from climate model studies, *J. Geophys. Res.* 107, 10.1029/2001JD001045.

Pauwels, V.R.N., R. Hoeben, N.E.C. Verhoest, and F.P. De Troch, 2001, The importance of spatial patterns of remotely sensed soil moisture in the improvement of discharge predictions for small-scale basins through data assimilation, *J. Hydrology-Amst.* 251, 88-102.

Philander, S.G., 1999, El Niño and La Niña predictable climate fluctuations, *Rep. Prog. Phys.* 62, 123-142.

Pielke, R.A. and M.W. Downton, 2000, Precipitation and damaging floods: trends in the United States, 1932-97, *J. Climate* 13, 3625-3637.

Pitman, et al., 1999, Key results and implications from phase 1(c) of the project for intercomparison of land-surface parameterization schemes, *Climate Dyn.,* 15, 673-684.

Plummer J.L., 1994, Western water resources: The desert is blooming, but will it continue?, *Water Resources Bulletin* 30, 595-603.

Polcher, J., L. Bowling and D. Lettenmaier, 2001, First use of ALMA in PILPS 2e, *GEWEX News,* 11 (3), 11-14.

Potts, H.L., 1937, Snow-surveys and runoff-forecasting from photographs, *Trans. Amer. Geophys. Union*, Reports and Papers, Hydrology—1937, 658-660.

Rango, A. and J. Martinec. 1979. Application of a snowmelt-runoff model using Landsat data. *Nordic Hydrology* 10: 225-238.

Rango, A., A.E. Walker and B.E. Goodison. 2000. Snow and ice. In *Remote sensing in hydrology and water management*. Schultz, G.A. and E.T Engman (eds.). Springer-Verlag; 239-262.

Rasmussen, E.M. and J.M. Wallace, 1983, Meteorological aspects of the El Niño/Southern Oscillation, *Science* 222, 1195-1202.

Rawls, W.J., D. Gimenez, and R. Grossman, 1998, Use of soil texture, bulk density, and slope of the water retention curve to predict saturated hydraulic conductivity, *Trans. ASAE*, 41 (4), 983-988.

Rawls, W.J., L.R. Ahuja, D.L. Brakensiek, and A. Shirmohammadi, 1993, Infiltration and soil water movement, in *Handbook of Hydrology*, edited by D. Maidment, pp. 5.1-5.51, McGraw-Hill, New York.

Reisner, M., 1986, *Cadillac Desert*, Viking Penguin, Inc., New York, 514 pp.

Reisner, M., and S. Bates, 1990, *Overtapped Oasis: Reform or Revolution for Western Water*, Island Press, Washington, D.C., 196 pp.

Reynolds, C.A., T.J. Jackson, and W.J. Rawls, 2000, Estimating soil water-holding capacities by linking the Food and Agriculture Organization soil map of the world with global pedon databases and continuous pedotransfer functions, *Water Resour. Res.,* 36, 3653-3662.

Riebsame, W.E., S.A. Chagnon, and T.R. Karl, 1991, Drought and natural resources management in the United States: impacts and implications of the 1987-89 drought, Westview Press, Boulder, Colorado.

Roads, J., and A. Betts, 2000, NCEP/NCAR and ECMWF reanalysis surface water and energy budgets for the Mississippi River basin, *J. Hydrometeorol*., 1, 88-94.

Robock, A., C.A. Schlosser, K.Y. Vinnikov, N.A. Speranskaya, J.K. Entin, and S. Qiu, 1998, Evaluation of the AMIP soil moisture simulations, *Global Planet. Change,* 19, 181-208.

Robock, A., K.Y. Vinnikov, G. Srinivasan, J.K. Entkin, S.E. Hollinger, N.A. Speranskaya, S. Liu, and A. Namkhai, 2000, The global soil moisture data bank, *Bull. Amer. Meteor. Soc*., 81, 1281-1299.

Rohli, R.V., A.J. Vega, M.R. Binkley, S.D. Britton, H.E. Heckman, J.M. Jenkins, Y. Ono, and D.E. Sheeler, 1999, Surface and 700 hPa atmospheric circulation patterns for the Great Lakes basin and eastern North America and relationship to atmospheric telecommunications, *Journal of Great Lakes Research* 25, 45-60.

Ropelewski, C.F. and P.D. Jones, 1987, An extension of the Tahiti-Darwin Southern Oscillation Index, *Monthly Weather Review* 115, 2161-2165.

Schaake, J.C., Q. Duan, K.E. Mitchell, P.R. Houser, E.F. Wood, D.P. Lettenmaier, B. Cosgrove, D. Lohmann, R. Pinker, A. Roback, J. Sheffield, and D. Tarpley, 2002, Another statistical look at LDAS soil moisture fields, Proceedings 16th Conference on Hydrology, American Meteorological Society, January 13-17, 2002, Orlando, FL.

Shepard, D.S., 1984, Computer mapping: The SYMAP interpolation algorithm, in *Spatial Statistics and Models*, edited by G.L. Gaile and C.J. Willmott, pp. 133-145, D. Reidel, Norwell, Mass.

Sellers, P.J., F.G. Hall, G. Asrar, D.E. Strebel, and R.E. Murphy, 1992, An overview of the first international satellite land surface climatology project (ISLSCP) field experiment (FIFE), *J. Geophys. Res*. 97, 18,345-18,371.

Servicio Meteorológico Nacional, 2000, Dat322 v.1.0 (CD-ROM), Instituto Mexicano de Tecnología del Agua, Comisión Nacional del Agua, Morelos, México.

Shi, J. and J. Dozier. 2000. Estimation of snow water equivalence using SIR-C/X-SAR. I. Inferring snow density and subsurface properties. *IEEE Trans. on Geosci. and Remote Sensing* 38: 2465-2473.

Shukla, J. 1998, Predictability in the midst of chaos: a scientific basis for climate forecasting, *Science* 282, 728-731.

Soil Conservation Service, 1988, Snow surveys and water supply forecasting, U.S. Department of Agriculture, Soil Conservation Service Agricultural Information Bulletin 536, June 1988.

Solley, W.B., R.R. Pierce, and H.A. Perlman, 1998, Estimated Use of Water in the United States in 1995, U.S. Geological Survey Circular 1200, Denver, CO.

Taylor, K.E., 2001, Summarizing multiple aspects of model performance in a single diagram, *J. Geophys. Res.* 106, 7183-7192.

Thompson, D.W.J. and J.M. Wallace, 1998, The Arctic Oscillation signature in the wintertime geopotential height and temperature fields. *Geophys. Res. Lett.,* 25, No. 9, 1297-1300.

Thompson, D.W.J. and J.M. Wallace, 2000, Annular modes in the extratropical circulation. Part I: Month-to-month variability. *J. Climate* 13, 1000-1016.

Thornton, P.E., and S.W. Running, 1999, An improved algorithm for estimating incident daily solar radiation from measurements of temperature, humidity, and precipitation, *Agric. For. Meteor.,* 93, 211-228.

Trenberth, K.E., 1997, The definition of El Niño, *Bull. of the American Meteorological Society* 78, 2771-2777.

Trenberth, K.E. and C.J. Guillemot, 1998, Evaluation of the atmospheric moisture and hydrological cycle in the NCEP/NCAR reanalysis, *Climate Dyn.,* 14, 213-231.

Twedt, T.M., J.C. Schaake, and E.L. Peck, 1977, National Weather Service extended streamflow prediction, Proc. of the 45th Annual Meeting of the Western Snow Conference, April 18-21, 1977, Albuquerque, NM, 52-57.

U.S Army Corps of Engineers, 1979, Missouri River main stem reservoir system reservoir regulation manual: Vol. 1, master manual, Missouri River Division, Omaha, Nebraska.

U.S Army Corps of Engineers, 1991, Missouri River system analysis model – phase I, Hydrologic Engineering Center, Davis, California, February, 1991.

U.S Army Corps of Engineers, 1994a, Missouri River master water control manual review and update, Volume 2: reservoir regulation studies, long range study model, Missouri River Division, July 1994.

U.S Army Corps of Engineers, 1994b, Missouri River master water control manual review and update, Volume 6D: economic studies, Missouri River Division, July 1994.

U.S Army Corps of Engineers, 1998, Missouri River main stem reservoirs: system description and operation, Northwestern Division, Missouri River Region, Reservoir Control Center, Fall 1998.

U.S Army Corps of Engineers, 1999, Missouri River main stem reservoirs hydrologic statistics, RCC Technical Report F-99, Missouri River Region, Reservoir Control Center.

U.S Army Corps of Engineers, 2001, Missouri River master water control manual review and update, revised draft environmental impact statement, Northwestern Division, Omaha, Nebraska, August 2001.

U.S. Census Bureau, 2000, National population projection summary file NP-T1, annual projections of the total resident population as of July 1: 1999-2100, Populations Projection Program, Washington, D.C.

U.S. Department of Agriculture, 1997, Census of agriculture – United States data, National Agricultural Statistics Service, Washington, D.C.

Vörösmarty, C.J., P. Green, J. Salisbury, and R.B. Lammers, 2000, Global Water Resources: Vulnerability from Climate Change and Population Growth, *Science* 289, 284-288.

Walker, J.P. and P.R. Houser, 2001, A methodology for initializing soil moisture in a global climate model: assimilation of near surface soil moisture observations, *J. Geophys Res.* 106, 11761-74.

Wang, H., M. Ting, and M. Ji, 1999, Prediction of seasonal mean United States precipitation based on El Niño seas surface temperatures, *Geophys. Research Letters* 26, 1341-1344.

Western Water Policy Review Advisory Commission, 1998. Water in the West: The Challenge for the Next Century, Washington, D.C., June 1998.

Widmann, M., and C.S. Bretherton, 2000, Validation of mesoscale precipitation in the NCEP reanalysis using a new grid-cell data set for the northwestern United States*, J. Climate*, 13, 1936–1950.

Wolter, K., R.M.. Dole, and C.A. Smith, 1999, Short-term climate extremes over the continental United States and ENSO. Part I: seasonal temperatures, *J. Climate* 12, 3255-3272.

Wood, A.W., E.P. Maurer, A. Kumar, and D.P. Lettenmaier, 2002, Long range experimental hydrologic forecasting for the eastern U.S., *J. Geophys. Res.* (in press).

Wood, E.F., M. Sivapalan, K. Beven, and L. Band, 1988, Effects of spatial variability and scale with implications to hydrologic modeling, *J. Hydrol*., 102, 29-47.

Wood, E.F., D. Lettenmaier, X. Liang, B. Nijssen, and S.W. Wetzel, 1997, Hydrological modeling of continental-scale basins, *Annu. Rev. Earth Planet. Sci*., 25, 279-300.

World Meteorological Organization (WMO), 1992, Scientific plan for the GEWEX Continental-scale International Project (GCIP), WCRP-67 WMO/TD-No. 61, WMO Geneva, 65 pp.

Xie, P., and P.A. Arkin, 1997, Global precipitation: A 17-year monthly analysis based on gauge observations, satellite estimates, and numerical model outputs, *Bull. Amer. Meteor. Soc*., 78, 2539-2558.

Yao, H. and A. Georgakakos, 2001, Assessment of Folsom Lake response to historical and potential future climate scenarios 2. reservoir management, *J. Hydrology* 249, 176-196.

Yeh, W. W-G., L. Becker, and R. Zettlemoyer, 1982, Worth of inflow forecast for reservoir operation, *J. Water Resources Planning and Mgmt.* 108, 257-269.

Ziegler, A.D., J. Sheffield, E.F. Wood, E.P. Maurer, B. Nijssen, and D.P. Lettenmaier, 2001, Detection of an acceleration in the global water cycle: The potential role of FRIEND, International Association of Hydrological Sciences (IAHS) Redbook publication 274, 51-57.

APPENDIX: DEVELOPMENT OF FORECAST RESERVOIR INFLOWS

Lettenmaier (1984) defined an index of forecast skill, the coefficient of prediction, as:

$$C_p = 1 - \frac{E\left(\tilde{X}_t - X_t\right)^2}{\sigma_t^2} \qquad \text{(A-3)}$$

where $\tilde{X}_t$ is the forecasted flow at time t, X_t denotes the recorded flow, and σ_t is the standard deviation of the recorded flows in period t. For the predictabilities determined by Maurer and Lettenmaier (2002) using multiple linear regression techniques, C_p is numerically equal to the square of the correlation coefficient, i.e. the fraction of the runoff variance explained by the predictors.

For a given level of forecast skill, forecasted flows are developed from the "recorded" flows as follows. As represented by Lettenmaier (1984), forecast flows are equal to recorded flows plus an additive error component:

$$\tilde{X}_t = X_t + \varepsilon_t \qquad \text{(A-4)}$$

where ε_t is an error term that grows as the forecasts contain less skill. The forecast error is a function of the forecast accuracy, with zero error associated with a perfect forecast and the maximum error associated with no forecast skill. In order to generate errors for different scenarios of forecast skill, the following methodology was used.

The error term, ε_t, is normally distributed with a mean of zero and a variance computed by:

$$\sigma_\varepsilon^{\,2} = (1 - C_p)\sigma_t^{\,2} \qquad \text{(A-5)}$$

where σ_t is the standard deviation of the recorded flows in period t; in this case t represents months, so σ_t is the standard deviation of the set of flows for month t. In Lettenmaier (1984) the ε_t is assumed to have a lag-1 (using daily data) Markov correlation structure. The effective lag-1

correlation coefficient, ρ, of the recorded flow is derived such that the established value of C_p is reproduced. The lag-1 forecast error correlation, ρ_ε is estimated, which is a function ρ and the length of the forecast and observation periods. As illustrated in the implementation of this technique by Datta and Burges (1984), as well as in the example in Lettenmaier (1984), even very large values of C_p and ρ produce relative low correlation values of ρ_ε. In this implementation, ρ_ε was estimated at below 0.1 for the range of C_p values reported by Maurer and Lettenmaier (2002), and would therefore have a negligible effect on the estimated forecast values. Hence, the forecast errors were assumed uncorrelated for this study. With these assumptions, this method reduces to that used by Yeh et al. (1982) for stochastic flow generation.